Three years of Ulysses dust data: 2005 to 2007

H. Krüger[a,b,1], V. Dikarev[c], B. Anweiler[b], S. F. Dermott[d], A. L. Graps[e], E. Grün[b,f], B. A. Gustafson[d], D. P. Hamilton[g], M. S. Hanner[h], M. Horányi[f], J. Kissel[a], D. Linkert[b], G. Linkert[b], I. Mann[i], J. A. M. McDonnell[j], G. E. Morfill[k], C. Polanskey[l], G. Schwehm[m] and R. Srama[b,n]

a) Max-Planck-Institut für Sonnensystemforschung, 37191 Katlenburg-Lindau, Germany
b) Max-Planck-Institut für Kernphysik, 69029 Heidelberg, Germany
c) Fakultät für Physik, Universität Bielefeld, Postfach 100131, 33501 Bielefeld, Germany
d) University of Florida, 211 SSRB, Campus, Gainesville, FL 32609, USA
e) Department of Space Studies, Southwest Research Institute, 1050 Walnut Street Suite 300, Boulder, Colorado, 80302, USA
f) Laboratory for Atmospheric and Space Physics, Univ. of Colorado, Boulder, CO 80309, USA
g) University of Maryland, College Park, MD 20742-2421, USA
h) Astronomy Dept. 619 LGRT, University of Massachusetts, Amherst MA 01003, USA
i) School of Science and Engineering, Kindai University, Kowakae 3-4-1, Higashi-Osaka, Osaka, 577-8502, Japan
j) Planetary and Space Science Research Institute, The Open University, Milton Keynes, MK7 6AA, UK
k) Max-Planck-Institut für Extraterrestrische Physik, 85748 Garching, Germany
l) Jet Propulsion Laboratory, Pasadena, California 91109, USA
m) ESAC, PO Box 78, 28691 Villanueva de la Cañada, Spain
n) Universität Stuttgart, Institut für Raumfahrtsysteme, Pfaffenwaldring 31, 70569 Stuttgart, Germany

Abstract

The Ulysses spacecraft has been orbiting the Sun on a highly inclined ellipse ($i = 79^\circ$, perihelion distance 1.3 AU, aphelion distance 5.4 AU) since it encountered Jupiter in February 1992. Since then it made almost three revolutions about the Sun. Here we report on the final three years of data taken by the on-board dust detector. During this time, the dust detector recorded 609 dust impacts of particles with masses $10^{-16}\,\mathrm{g} \leq m \leq 10^{-7}\,\mathrm{g}$, bringing the mission total to 6719 dust data sets. The impact rate varied from a low value of 0.3 per day at high ecliptic latitudes to 1.5 per day in the inner solar system. The impact direction of the majority of impacts between 2005 and 2007 is compatible with particles of interstellar origin, the rest are most likely interplanetary particles. We compare the interstellar dust measurements from 2005/2006 with the data obtained during earlier periods (1993/1994) and (1999/2000) when Ulysses was traversing the same spatial region at southern ecliptic latitudes but the solar cycle was at a different phase. During these three intervals the impact rate of interstellar grains varied by more than a factor of two. Furthermore, in the two earlier periods the grain

[1] *Correspondence to:* Harald Krüger, krueger@mps.mpg.de

impact direction was in agreement with the flow direction of the interstellar helium while in 2005/2006 we observed a shift in the approach direction of the grains by approximately 30° away from the ecliptic plane. The reason for this shift remains unclear but may be connected with the configuration of the interplanetary magnetic field during solar maximum. We also find that the dust measurements are in agreement with the interplanetary flux model of Staubach et al. (1997) which was developed to fit a 5-year span of Ulysses data.

1 Introduction

Ulysses was the only space mission so far that left the ecliptic plane and flew over the poles of the Sun. The spacecraft was launched in 1990 and was very successfully operated until 30 June 2009, although individual instruments had to be turned off to conserve power. Its orbital plane was almost perpendicular to the ecliptic plane (79° inclination) with an aphelion at Jupiter. This special orbit orientation allowed Ulysses to unambiguously detect interstellar dust grains entering the heliosphere because the spacecraft's orbital plane was almost perpendicular to the flow direction of the interstellar dust. Ulysses had a highly sensitive impact ionisation dust detector on board which measured impacts of micrometre and sub-micrometre dust grains. The detector was practically identical with the dust instrument which flew on board the Galileo spaceprobe. Both instruments were described in previous publications by Grün et al. (1992a,b, 1995c).

1.1 Summary of results from the Ulysses dust investigations

Comprehensive reviews of the scientific achievements of the Ulysses mission including results from the dust investigation were given by Balogh et al. (2001) and Grün et al. (2001). References to other works related to Ulysses and Galileo measurements on dust in the planetary system were also given by Grün et al. (1995a,b); Krüger et al. (1999a,b, 2001a,b, 2006b,a); Krüger and Grün (2009). Some mission highlights are also summarized in Table 1.

Various dust populations were investigated with the Ulysses and Galileo dust experiments in interplanetary space: the interplanetary dust complex including β-meteoroids (i.e. dust particles which leave the solar system on unbound orbits due to acceleration by radiation pressure), interstellar grains sweeping through the heliosphere, and dust stream particles expelled from the jovian system by electromagnetic forces, to name only the most significant dust types detected with Ulysses which have been analysed so far. In the following, we summarise the most significant achievements of the Ulysses dust measurements.

Ulysses and Galileo dust measurements were used to study the 3-dimensional structure of the interplanetary dust complex and its relation to the underlying populations of parent bodies like asteroids and comets (Divine, 1993; Grün et al., 1997; Staubach et al., 1997). Studies of asteroidal dust released from the IRAS dust bands show that they are not efficient

enough dust sources to maintain the observed interplanetary dust cloud (Mann et al., 1996). The state of the inner solar system dust cloud within approximately 1 AU from the Sun including dust destruction and ion formation processes in relation to so-called solar wind pickup ions detected by the Solar Wind Ion Composition Spectrometer (SWICS) onboard Ulysses was investigated (Mann et al., 2004; Mann and Czechowski, 2005). An improved physical model was developed for the interplanetary meteoroid environment (Dikarev et al., 2001, 2002, 2005) which uses long-term particle dynamics to define individual interplanetary dust populations. The Ulysses and Galileo in-situ dust data are an important data set for the validation of this model. The properties of β-meteoroids were also studied with the Ulysses data set (Wehry and Mann, 1999; Wehry et al., 2004). Finally, the potential connection of cometary dust trails and enhancements of the interplanetary magnetic field as measured by Ulysses was discussed by Jones and Balogh (2003).

During its first flyby at Jupiter in 1992, the Ulysses dust instrument discovered burst-like intermittent streams of tiny dust grains in interplanetary space (Grün et al., 1993) which had been emitted from the jovian system (Hamilton and Burns, 1993; Horányi et al., 1993; Zook et al., 1996). This discovery was completely unexpected as no periodic phenomenon for tiny dust grains in interplanetary space was previously known. These grains strongly interacted with the interplanetary and the jovian magnetic fields (Horányi et al., 1997; Grün et al., 1998) and the majority of them originated from Jupiter's moon Io (Graps et al., 2000). In February 2004 Ulysses had its second Jupiter flyby (at 0.8 AU distance from the planet) and again measured the jovian dust streams (Krüger et al., 2005a, 2006c; Flandes and Krüger, 2007; Flandes et al., 2009).

Another important discovery made with Ulysses were interstellar dust particles sweeping through the heliosphere (Grün et al., 1993). The grains which originated from the very local interstellar environment of our solar system were identified by their impact direction and impact velocities, the latter being compatible with particles moving on hyperbolic heliocentric trajectories (Grün et al., 1994). Their dynamics depends on the grain size and is strongly affected by the interaction with the interplanetary magnetic field and by solar radiation pressure (Landgraf et al., 1999; Landgraf, 2000; Mann and Kimura, 2000; Czechowski and Mann, 2003b,a; Landgraf et al., 2003). As a result, the size distribution and fluxes of grains measured inside the heliosphere are strongly modified. Studies of the dust impacts detected with both Ulysses and Galileo showed that the intrinsic size distribution of interstellar grains in the local interstellar environment of our solar system extends to grain sizes larger than those detectable by astronomical observations (Frisch et al., 1999; Frisch and Slavin, 2003; Landgraf et al., 2000; Grün and Landgraf, 2000). Observations of radar meteors entering the Earth's atmosphere at high speeds also indicate the existence of even larger interstellar grains (Taylor et al., 1996; Baggaley and Neslušan, 2002).

The Ulysses and Galileo interstellar dust measurements showed that the dust-to-gas mass ratio in the local interstellar cloud is higher than the standard interstellar value derived from cosmic abundances (Landgraf, 1998; Frisch et al., 1999). This implied the existence of inhomogeneities in the diffuse interstellar medium on relatively small length scales. In

2005/2006 the Ulysses measurements showed a 30° shift in the impact direction of interstellar grains with respect to the interstellar helium flow (Krüger et al., 2007). The reason of this shift is presently unclear. Finally, it turned out that the dust sensor side walls have a similar sensitivity to dust impacts as the detector target itself (Altobelli et al., 2004; Willis et al., 2005). This shows that earlier investigations which neglected the contributions of the side wall overestimated the interstellar dust flux by about 20%. Since the contribution of the sensor side wall increases the effective dust instrument field-of-view, the velocity dispersion of the observed interstellar dust stream turned out to be smaller by about 30% than previously thought (Altobelli et al., 2004).

Due to its unique highly inclined heliocentric trajectory Ulysses was able to monitor interstellar dust at high ecliptic latitudes between 3 and 5 AU. Dust measurements between 0.3 and 3 AU in the ecliptic plane exist also from Helios, Galileo and Cassini. This data shows evidence for distance-dependent alteration of the interstellar dust stream caused by radiation pressure, gravitional focussing and electromagnetic interaction of the grains with the time-varying interplanetary magnetic field (Altobelli et al., 2003, 2005b,a).

1.2 The Ulysses and Galileo dust data papers

The Ulysses dust detector obtained dust data for more than 17 years, making it the longest continually-operating spacebourne dust detector to date. With the publication of this paper, the full Ulysses data set, along with 13 years of Galileo data, will be fully described in the scientific literature. The reduction process of Ulysses and Galileo dust data was described by Grün et al. (1995c, hereafter Paper I). In the odd-numbered Papers III, V, VII and IX (Grün et al., 1995a; Krüger et al., 1999b, 2001b, 2006a) we presented the Ulysses data set spanning the time period from launch in October 1990 to December 2004. The companion even-numbered Papers II, IV, VI and VIII (Grün et al., 1995b; Krüger et al., 1999a, 2001a, 2006b) discussed the ten years of Galileo data from October 1989 to December 1999. The current paper (Paper XI) extends the Ulysses data set from January 2005 until the Ulysses dust measurements ceased in November 2007, and a companion paper (Krüger et al., 2010, Paper X) presents Galileo's final measurements at Jupiter from 2000 to 2003. A summary of the temporal and spatial coverage of our Ulysses data papers is given in Table 1.

The main data products are a table of the impact rate of all impacts determined from the particle accumulators and a table of both raw and reduced data of all dust impacts for which the full data set of measured impact parameters was transmitted to Earth. The information presented in these papers is similar to data which we have submitted to the various data archiving centres (Planetary Data System, NSSDC, Ulysses Data Centre). Electronic access to the data is also possible via the world wide web: http://www.mpi-hd.mpg.de/dustgroup/.

This paper is organised like our earlier Papers III, V, VII and IX. We begin with an overview of important events of the Ulysses mission between 2005 and 2007 (Section 2). Sections 3 and 4 describe and analyse the Ulysses dust data set for this period. In Section 5 we discuss the dust data set from the entire Ulysses mission, we analyse in particular the interstellar dust measurements obtained in the 2005 to 2007 interval, and we compare these results to

previous ones. In Section 6 we summarise our conclusions.

2 Mission and instrument operation

2.1 Ulysses mission and dust instrument characteristics

The Ulysses spacecraft was launched on 6 October 1990. A swing-by manoeuvre at Jupiter in February 1992 rotated the orbital plane 79° relative to the ecliptic plane. On the resulting trajectory (Figure 1) Ulysses finished two full revolutions about the Sun. Passages over the south pole of the Sun occurred in October 1994, November 2000 and February 2007, passages through the ecliptic plane at a perihelion distance of 1.3 AU occurred in March 1995, May 2001 and August 2007, and passes over the Sun's north pole were in August 1995, October 2001 and January 2008. In April 1998 and July 2004 the spacecraft crossed the ecliptic plane at an aphelion distance of 5.4 AU. Orbital elements for the out-of-ecliptic part of the Ulysses trajectory are given in Paper VII. Figure 1 shows that during most of the time interval considered in this paper Ulysses was at southern ecliptic latitudes.

Ulysses is a spinning spacecraft, and the dust sensor orientation at the time of a dust particle impact is recorded, allowing for an independent determination of the grain impact direction. Ulysses spins at five revolutions per minute about the centre line of its high gain antenna which normally points at Earth. Figure 2 shows the deviation of the spin axis from the Earth direction for the period 2005 to 2007. Most of the time the spin axis pointing was within 1° of the nominal Earth direction, similar to the mission before 2005. This small deviation is usually negligible for the analysis of measurements with the dust detector. The Ulysses spacecraft and mission are explained in more detail by Wenzel et al. (1992). Details about the data transmission to Earth can also be found in Paper III.

The Ulysses dust detector (GRU) has a 140° wide field of view and is mounted at the spacecraft nearly at right angles (85°) to the antenna axis (spacecraft spin axis). Due to this mounting geometry, the dust sensor is most sensitive to particles approaching from the plane perpendicular to the spacecraft-Earth direction. The impact direction of dust particles is measured by the rotation angle which is the sensor viewing direction at the time of a dust impact. During one spin revolution of the spacecraft the rotation angle scans through a complete circle of 360°. Zero degrees rotation angle is defined to be the direction closest to ecliptic north. At high ecliptic latitudes, however, the sensor pointing at 0° rotation angle significantly deviates from the actual north direction. During the passages over the Sun's polar regions the sensor always scans through a plane tilted by about 30° from the ecliptic plane and all rotation angles lie close to the ecliptic plane (cf. Figure 4 in Grün et al., 1997). A sketch of the viewing geometry around aphelion passage can be found in Grün et al. (1993).

The available electrical power on board Ulysses became an issue beginning in 2001 due to decreasing power generation of the radioisotope batteries (RTGs). Some instrument heaters on board had to be switched off to save power which in turn also reduced the on

board temperature. Later, in 2002, power consumption could not be sufficiently reduced anymore by simply switching off heaters, and a cycling instrument operation scheme had to be implemented: one or more of the scientific instruments had to be switched off at a time. In the 2005 to 2007 interval considered in this paper the dust instrument was switched off during a total time period of about seven months, separated into three individual time periods (see Sect. 2.2). After 30 November 2007 the dust instrument remained switched off permanently. It was planned to switch the dust instrument on in January 2008 again, but due to a failure on board the spacecraft, this did not happen. Hence, no dust data were obtained after 30 November 2007 although operation of the Ulysses spacecraft continued until 30 June 2009.

2.2 Dust instrument operation

Table 2 gives significant mission and dust instrument events from 2005 to 2007. Earlier events are only listed if especially significant. A comprehensive list of events from launch until the end of 2004 was given in Papers III, V, VII and IX.

During the earlier Ulysses mission phases until 2000, several spacecraft anomalies occurred during which all scientific instruments on board were switched off automatically (Disconnection of all Non-Essential Loads – DNELs for short). No such anomaly occurred in the 2005 to 2007 interval. The dust instrument was switched off between 28 September 2006 and 9 March 2007, from 2 April 2007 to 30 April 2007 and after 30 November 2007 (*cf.* Table 1), respectively, because there was not enough electical power generated by the RTGs anymore to operate all instruments simultaneously.

The dust instrument has two heaters to allow for a relatively stable operating temperature within the sensor. By heating one of the two or both heaters, three different heating power levels can be achieved (0.4 W, 0.8 W or 1.2 W; for comparison, the total power consumption of the instrument without heaters is 2.2 W). Sensor heating was necessary when the spacecraft was outside about 2 AU because relatively little radiation was received from the Sun.

Before 2001 one or both heaters were switched on beyond 2 AU, except close to the Sun when both were switched off. Since November 2001 the maximum allowed heating power for nominal dust instrument operation has been limited to 0.8 W to save power on board Ulysses. This reduced the sensor temperature by about 10° C as compared to the configuration with 1.2 W heating power at similar heliocentric distance. The full heating power was only allowed for short periods before instrument switch on to avoid damage of the electronics. In 2005 and 2006 the instrument was operated with 0.8 W heating power, and in 2007 the heating power was set to 0.4 W, except during switch-ons when it was raised to 1.2 W.

Table 2 lists the total powers consumed by the heaters. From 2005 to 2007 the temperature of the dust sensor was between -37° C and $+16^\circ$ C. The lower limit for the specified operational range is -30° C. No major effect of the reduced temperature was recognised (for an

anomalous temperature-related flipping in the housekeeping value of the channeltron high voltage in 2004 see Paper IX).

No reprogramming of the Ulysses dust instrument occurred in the 2005 to 2007 interval. In the earlier mission the instrument was reprogrammed three times and the reader is referred to Papers V and IX for details. In particular, a new classification scheme for impact events was implemented in April 2002 which is the same as the one installed in the Galileo instrument in July 1994 (Paper IV).

2.3 Instrument sensitivity and noise

Analysis of the in-orbit noise characteristics of the dust instrument (Paper III) led to a relatively noise-free configuration with which the instrument was normally operated until August 2000: channeltron voltage 1140 V (HV = 3); event definition status such that either the channeltron or the ion-collector channel could, independent of each other, start a measurement cycle (EVD = C, I); detection thresholds for ion-collector, channeltron and electron-channel set to the lowest levels and the detection threshold for the entrance grid set to the first digital step (SSEN = 0, 0, 0, 1). See Paper I for a description of these terms.

During the entire Ulysses mission dedicated noise tests were performed at monthly intervals in order to monitor instrument health and noise characteristics. During all these tests the operational settings were changed in four steps at one-hour intervals, starting from the nominal configuration described above: a) set the event definition status such that the channelton, the ion collector and the electron-channel can initiate a measurement cycle (EVD = C, I, E); b) set the thresholds for all channels to their lowest levels (SSEN = 0, 0, 0, 0); c) reset the event definition status to its nominal configuration (EVD = C, I) and increase the channeltron high voltage by one step with respect to the nominal configuration; d) reset the instrument to its nominal configuration (i.e. reduce the channeltron high voltage by one step and set the detection thresholds to SSEN = 0, 0, 0, 1).

The noise tests performed in the earlier mission before 2000 revealed a long-term drop in the noise sensitivity of the instrument which was most likely caused by a reduction in the channeltron amplification due to electronics degradation (Paper IX and Krüger et al., 2005b). To counterbalance the reduced amplification we increased the channeltron high voltage by one digital step in August 2000 (HV = 4, 1250 V) which raised the instrument sensitivity close to its original value from the earlier mission again (Paper IX). Although the aging of the channeltron led to a drop in the number of class 3 impacts, the dust impacts which have caused these events should have shown up in lower quality classes. The noise response of the Ulysses dust detector was monitored since then and no significant drop in the sensitivity was recognized. In the time interval considered here HV=4, EVD=C,I, SSEN=0001 was the nominal configuration of the dust instrument (during noise tests the channeltron voltage was always raised by one digital step, i.e. to HV = 5, 1370 V).

Figure 3 shows the noise rate of the dust instrument for the 2005 to 2007 period. The upper panel shows the daily maxima of the noise rate. In the earlier mission before November 2001 the daily maxima were dominated by noise due to interference with the sounder of

the Unified RAdio and Plasma wave instrument (URAP) on board Ulysses (Stone et al., 1992). Since November 2001 the sounder was switched off permanently for power saving and no sounder noise occurred anymore (see Papers III, V, VII and IX for details of the sounder operation and sounder-related noise). Individual sharp spikes in the upper panel of Figure 3 are caused by noise tests which occurred at approximately monthly intervals, They are best seen in 2007 when Ulysses was close to the Sun which is known to be a strong source of noise.

The bottom panel of Figure 3 shows the daily averages in the noise rate. The average was about 10 events per day at random times and it shows that dead time is negligible. These noise rates are very similar to those measured since August 2000 (Paper IX) when the instrument was operated with the same channeltron voltage as in the 2005-07 interval, implying that no significant channeltron degradation has occurred since 2000.

3 Impact events

The dust instrument classifies all impact events into four classes and six ion charge amplitude ranges which leads to 24 individual categories, with one accumulator belonging to one individual category. Class 3, our highest class, are real dust impacts and class 0 are mostly noise events. Depending upon the noise of the charge measurements, classes 1 and 2 can be true dust impacts or noise events. Two classification schemes were used in the Ulysses dust instrument: since 26 March 2002, when the dust instrument was reprogrammed, the classification scheme has been the same as the one used in the Galileo instrument (described in Paper IV). A different scheme was used before which is described in Paper I.

Between 1 January 2005 and 30 November 2007 the complete data sets (sensor orientation, charge amplitudes, charge rise times, etc.) of 6970 events including 609 dust impacts were transmitted to Earth. Table 3 lists the number of all dust impacts counted with the 24 accumulators of the instrument. 'AC*xy*' refers to class number '*x*' and amplitude range '*y*' (for a detailed description of the accumulator categories see Paper I). As discussed in the previous section, most noise events were recorded during the time periods when the dust instrument was configured to its high sensitive state for noise tests. During these periods many events were only counted by one of the 24 accumulators because their full information was overwritten before the data could be transmitted to Earth. Since the dust impact rate was low during times outside these periods, it is expected that only the data sets of very few true dust impacts were lost.

Table 4 lists all 609 particles detected between January 2005 and November 2007 for which the complete information exists. Note that approximately 45 jovian stream particles were detected in six dust streams in 2005 (AR1, Krüger et al., 2006c) which are about 10 nm in size and their velocities exceed $200\,\mathrm{km\,s^{-1}}$ (Zook et al., 1996). Their mass and speed calibration is unreliable because their masses and speeds are outside of the calibration range of the dust instrument.

In Table 4 dust particles are identified by their sequence number and their impact time.

The event category – class (CLN) and amplitude range (AR) – are given. Raw data as transmitted to Earth are displayed in the next columns: sector value (SEC) which is the spacecraft spin orientation at the time of impact, impact charge numbers (IA, EA, CA) and rise times (IT, ET), time difference and coincidence of electron and ion signals (EIT, EIC), coincidence of ion and channeltron signal (IIC), charge reading at the entrance grid (PA) and time (PET) between this signal and the impact. Then the instrument configuration is given: event definition (EVD), charge sensing thresholds (ICP, ECP, CCP, PCP) and channeltron high voltage step (HV). See Paper I for further explanation of the instrument parameters.

The next four columns in Table 4 give information about Ulysses' orbit: heliocentric distance (R), ecliptic longitude and latitude (LON, LAT) and distance from Jupiter (D_{Jup}, in astronomical units). The next column gives the rotation angle (ROT) as described in Section 2. Then follows the pointing direction of the dust instrument at the time of particle impact in ecliptic longitude and latitude (S_{LON}, S_{LAT}). Mean impact velocity (v, in $\mathrm{km\,s^{-1}}$) and velocity error factor (VEF, i.e. multiply or divide stated velocity by VEF to obtain upper or lower limits) as well as mean particle mass (m, in grams) and mass error factor (MEF) are given in the last columns. For VEF > 6, both velocity and mass values should be discarded. This occurs for 72 impacts. No intrinsic dust charge values are given (see Svestka et al., 1996, for a detailed analysis). Recently, reliable charge measurements for interplanetary dust grains were reported for the Cassini dust detector (Kempf et al., 2004). These measurements may lead to an improved understanding of the charge measurements of Ulysses and Galileo in the future.

4 Analysis

The most important impact parameter determined by the dust instrument is the positive charge measured on the ion collector, Q_{I}, because it is relatively insensitive to noise. Figure 4 shows the distribution of Q_{I} for all dust particles detected from 2005 to 2007. Ion impact charges have been detected over the entire range of six orders of magnitude in impact charge that the dust instrument can measure. One impact is close to the saturation limit of $\sim 10^{-8}\,\mathrm{C}$ and may thus constitute a lower limit of the actual impact charge. The impact charge distribution of the big particles ($Q_{\mathrm{I}} > 10^{-13}\,\mathrm{C}$) follows a power law distribution with index -0.45 and is shown as a dashed line. This value is very similar to earlier Ulysses measurements of 2000 to 2004 (-0.40; cf. Paper IX).

In the earlier 1993 to 2004 data set (Papers V, VII and IX) the impact charge distribution was reminiscent of three individual populations: small particles with impact charges $Q_{\mathrm{I}} < 10^{-13}\,\mathrm{C}$ (AR1), intermediate size particles with $10^{-13}\,\mathrm{C} \leq Q_{\mathrm{I}} \leq 10^{-11}\,\mathrm{C}$ (AR2 and AR3) and big particles with $Q_{\mathrm{I}} > 10^{-11}\,\mathrm{C}$ (AR4 to AR6). This is also visible in the present data set, although less pronounced. The intermediate particles are mostly of interstellar origin and the big particles are attributed to interplanetary grains (Grün et al., 1997, see also Section 5). The small particle impacts (AR1) detected over the polar regions of the

Sun are candidates for being interplanetary β-meteoroids (Hamilton et al., 1996; Wehry and Mann, 1999; Wehry et al., 2004).

It should be noted that the charge distribution shown in Figure 4 is very similar to the one measured with Galileo in interplanetary space between 1993 and 1995 (i.e. between 1 and 5 AU; Paper IV). In particular, the power law index of -0.43 for the big particles was practically identical. This indicates that both dust instruments basically detected the same dust populations in interplanetary space and that their responses to dust impacts are very similar. The only significant difference is a dip in the Ulysses charge distribution at $2 \cdot 10^{-10}$ C (Figure 4) which is also evident in all earlier Ulysses data (Papers III, V, VII and IX). In particular, it is visible in both the ecliptic and out-of-ecliptic phases of Ulysses which indicates that it is not sensitive to the impact speed or the dust population of the grains. A small but much weaker dip is also seen in some but not all Galileo data sets. We therefore conclude that the dip is most likely due to an artefact in the Ulysses instrument electronics in AR5.

The ratio of the channeltron charge Q_C and the ion collector charge Q_I is a measure of the channeltron amplification A, which in turn is an important parameter for dust impact identification (Paper I). In Figure 5 we show the charge ratio Q_C/Q_I as a function of Q_I for the 2005 to 2007 dust impacts with the channeltron high voltage set to 1250 V (HV = 4). This diagram is directly comparable with similar diagrams in the previous Papers III, V and VII for HV = 3 and Paper IX for HV = 4, respectively.

The mean amplification determined from particles with $10^{-12}\,\mathrm{C} \leq Q_I \leq 10^{-11}\,\mathrm{C}$ and HV = 4 in the 2005 to 2007 interval is $A \simeq 1.57$. This value is somewhat lower than the values derived from the first five years of the mission (1990 to 1995; Papers III and V) and comparable to the more recent determinations (1996 to 2004; Papers VII and IX). It indicates that a sufficiently high channeltron amplification and stable instrument operation could be maintained with this higher voltage (HV = 4) since 2000. It shows in particular that the channeltron degradation could be mostly counterbalanced by increasing the high voltage by one digital step. Much more severe electronics degradation was found for the Galileo dust detector during Galileo's orbital tour in the jovian system. It was likely related to the harsh radiation environment in the magnetosphere of the giant planet (Krüger et al., 2005b).

In Figure 6 we show the masses and velocities of all dust particles detected between 2005 and 2007. As in the earlier periods before 2005, velocities occur over the entire calibrated range from 2 to 70 km s^{-1}. The masses vary over almost nine orders of magnitude from $\sim 10^{-7}$ g to 10^{-16} g. The mean errors are a factor of 2 for the velocity and a factor of 10 for the mass. The clustering of the velocity values is due to discrete steps in the rise time measurement but this quantisation is much smaller than the velocity uncertainty. For many particles in the lowest two amplitude ranges (AR1 and AR2) the velocity had to be computed from the ion charge signal alone which leads to the vertical striping in the lower mass range in Figure 6 (most prominent above 10 km s^{-1}). In the higher amplitude ranges the velocity could normally be calculated from both the target and the ion charge signal, resulting in a more continuous distribution in the mass-velocity plane. Impact velocities

below about $3\,\mathrm{km\,s^{-1}}$ should be treated with caution because anomalous impacts onto the sensor grids or structures other than the target generally lead to prolonged rise times and hence to unnaturally low impact velocities.

5 Discussion

In Figure 7 we show the dust impact rate detected in various amplitude ranges together with the total impact rate summed over all amplitude ranges. The highest overall impact rate was recorded in 2007 when Ulysses was in the inner solar system and relatively close to the ecliptic plane. It coincides with a peak in the rate of bigger particles in the three highest ion amplitude ranges (AR4 – AR6). These impacts are attributed to interplanetary particles on low inclination orbits (Grün et al., 1997). The majority of them are the impacts with $Q_{\mathrm{I}} > 10^{-10}$ C shown in Figure 4. The impact rate of intermediate sized particles in AR2 and AR3 showed relatively little variation. This size range is dominated by interstellar impactors. The details of the various dust populations are discussed further below.

Figure 8 shows the sensor orientation at the time of a particle impact (rotation angle). The big particles (diamonds, impact charge $Q_{\mathrm{I}} \geq 8 \cdot 10^{-14}$ C which roughly corresponds to AR2-6) are concentrated towards the upstream direction of interstellar helium (cf. Figure 10, bottom panel; Witte et al., 1996; Witte, 2004; Witte et al., 2004). They have been detected with a relatively constant rate during the entire three-year period (Figure 7). The particles with the highest ion amplitude ranges (AR4 to AR6) are not distinguished in this diagram because they cannot be separated from interstellar particles by directional arguments alone. They have to be distinguished by other means (e. g. mass and speed). In addition, their total number is so small that they constitute only a small "contamination" of the interstellar particles in Figure 8. In the ecliptic plane at 1.3 AU, however, interplanetary particle flux dominates over interstellar flux by a factor of about 3 (in number).

5.1 Interstellar dust

Interstellar particles move on hyperbolic trajectories through the solar system and approach Ulysses from the same direction as the interstellar gas (Grün et al., 1994; Baguhl et al., 1995a; Witte et al., 1996; Witte, 2004; Witte et al., 2004). They can therefore be identified by their impact direction and their impact speed. Earlier investigations showed that in the Ulysses and Galileo dust data sets the interstellar impactors are mostly found in amplitude ranges AR2 and AR3.

In the earlier mission from 1993 to 2004 the impact rate of interstellar grains (as derived from the AR2 and AR3 accumulators) varied by about a factor of 2.5: between 1993 and 1995 the rate was $\sim 2 \cdot 10^{-6}\,\mathrm{s^{-1}}$ (Paper V) while in the 1996 to 1999 interval it dropped to $\sim 8 \cdot 10^{-7}\,\mathrm{s^{-1}}$ (Paper VII) and from 2000 to 2004 the average impact rate was again $\sim 2 \cdot 10^{-6}\,\mathrm{s^{-1}}$ (Paper IX). In 2005/2006 the average impact rate of interstellar impactors was somewhat higher: $\sim 3 \cdot 10^{-6}\,\mathrm{s^{-1}}$ (bottom panel of Figure 7). In 2007, when Ulysses

was in the inner solar system again, the impact rate derived from AR2 and AR3 was still higher. Here, however, the impact rate is not due to interstellar particles alone because of a strong contribution from interplanetary impactors.

The dashed curve in Figure 7 (bottom panel) shows the expected impact rate of interstellar particles assuming that they approach from the direction of interstellar helium (Witte et al., 1996; Witte, 2004; Witte et al., 2004) and that they move through the solar system on straight trajectories with a relative velocity of 26 km s^{-1}. This assumption means dynamically that radiation pressure cancels gravity for these particles ($\beta = 1$) and that their Larmor radii are large compared with the dimension of the solar system. Both assumptions are reasonable for particles with masses between 10^{-13} and 10^{-12} g which is the dominant size range measured for interstellar grains (Grün et al., 1997). The variation predicted by the model is caused by changes in the instrument's viewing direction with respect to the approach direction of the particles and changes in the relative velocity between the spacecraft and the particles. The dust particle flux is independent of heliocentric distance in this simple model, which gives relatively good agreement with the observed impact rate.

Ulysses has monitored the interstellar dust flow through the solar system for more than 15 years. This time period covers more than two and a half revolutions of the spacecraft about the Sun through more than 2/3 of a complete 22-year solar cycle. Thus, Ulysses measured interstellar dust during solar minimum and solar maximum conditions of the interplanetary magnetic field (IMF). The interstellar dust flux modulation due to grain interaction with the magnetic field during solar minimum could be well explained (Landgraf, 1998, 2000; Landgraf et al., 2003). By taking into account the sensor side wall in the instrument field of view we could recently improve the flux determination (Altobelli et al., 2004).

Ulysses provides the unique opportunity to compare repeated dust measurements at the same locations in the solar system for different phases of the solar cycle and the interplanetary magnetic field. In Figure 9 we show the approach direction of interstellar grains for three selected periods when Ulysses was between approximately -8 and -56° ecliptic latitude during approach to the inner solar system. During these three intervals the dust detection geometry as indicated by the contour lines was very similar so that we can compare them directly. At least three differences are obvious between the three panels:

- The approach direction of the majority of grains was compatible with the flow direction of the interstellar helium gas as measured with Ulysses (Witte, 2004; Witte et al., 2004) during all three time intervals.
- The dust flux varied by a factor of about two during the three intervals, the lowest flux being measured in the period 1999 to 2000, while the highest flux occurred in 2005/2006 (Krüger et al., 2007).
- A subset of the grains detected in 2005 shows a clear shift in the detected impact direction away from the ecliptic plane towards southern ecliptic latitudes.

Our preliminary analysis indicates that this shift is about 30° away from the ecliptic plane towards southern ecliptic latitudes (Krüger et al., 2007). The reason for this shift remains

mysterious. Whether it is connected to a secondary stream of interstellar neutral atoms shifted from the main neutral gas flow (Collier et al., 2004; Wurz et al., 2004; Nakagawa et al., 2006) is presently unclear. Given, however, that the neutral gas stream is shifted along the ecliptic plane while the shift in the dust flow is offset from the ecliptic, a connection between both phenomena seems unlikely.

Even though Ulysses' position in the heliosphere and the dust detection conditions were very similar during all three time intervals considered in Figure 9, the configurations of the solar wind driven interplanetary magnetic field (IMF), which strongly affects the dynamics of the smallest grains, were completely different. We have to consider that the interstellar grains need approximately twenty years to travel from the heliospheric boundary to the inner solar system where they are detected by Ulysses. Thus, the effect of the IMF on the grain dynamics is the accumulated effect caused by the interaction with the IMF over several years: In the earlier time intervals (1993/1994 and 1999/2000) the grains had a recent dynamic history dominated by solar minimum conditions (Landgraf, 2000), while the grains detected during the third interval (2005/2006) had a recent history dominated by the much more disturbed solar maximum conditions of the IMF. During the solar maximum conditions the overall magnetic dipole field changed polarity. Morfill and Grün (1979) predicted that due to this effect in a 22-year cycle, small interstellar grains experience either focussing or defocusing conditions. During these times they are systematically deflected by the solar wind magnetic field either towards or away from the solar magnetic equator plane (close to the ecliptic plane). This latter configuration likely has a strong influence on the dust dynamics and the total interstellar flux in the inner heliosphere but it has not been modelled in detail. An explanation of the grain interaction with the IMF at the recent solar maximum conditions is still pending.

Detailed modelling of the dynamics of the electrically charged dust grains in the heliosphere can give us information about the local interstellar environment of the solar system where the particles originate from. The models developed by Landgraf et al. (2003) fit the observed flux variation by assuming a constant dust concentration in the local interstellar environment of our solar system. It implies that the local interstellar dust phase must be homogeneously distributed over length scales of 50 AU, which is the distance travelled by the Sun during the measurement period of Ulysses from 1992 to 2002. This conclusion is supported by the more recent Ulysses data until the end of 2004 (Krüger et al., 2006a). Our latest Ulysses dust data of 2005/2006, on the other hand, put a question mark onto this conclusion because if the observed shift in impact direction turns out to be intrinsic, it would imply that this homogeneity breaks down on larger length scales.

5.2 Interplanetary dust

Figure 10 shows the data (AR3 to AR6) from launch in 1990 until the end of the Ulysses mission in 2007 and compares them with two meteoroid environment models by Divine (1993) and Staubach et al. (1997). For most of the mission time, excluding the ecliptic plane crossings in 1995, 2001 and 2007 the Divine model predicts impacts from a very

broad range of directions, with spin angles from 45° to 300°. The impactors belong mostly to the so-called "halo" population which was introduced in the model to explain the Pioneer data (Divine, 1993). The Ulysses directionality of the impacts had not been available at the time of construction of the model, and they are not well fit by the "halo" population. In contrast, the Staubach et al. (1997) model was fit to 5 years of Ulysses data from the craft's first orbit about the Sun, taking the crucial directional information into account. It is in better agreement with the data and has been confirmed by Ulysses' second and third orbits. It places most of the impacts into the spin angle range from 30° to 120°. These are due to interstellar dust flowing through the solar system (Grün et al., 1994).

One more observation from these plots is that both the Divine and Staubach models predict higher flux during the ecliptic plane crossings than the data permit. The time dependence of the interstellar dust flux was asserted after the meteoroid models under review had been constructed (Landgraf, 2000). However, the disagreement at the ecliptic plane crossings was not anticipated, since almost all data incorporated in the models were taken from the ecliptic plane. Possible explanations of the discrepancy are the roughness of model fits as well as different representations of the data taken for model adjustments and displayed in Figure 10. While Figure 10 selects all impacts above a fixed threshold of charge released, the models were fitted using more uncertain inferred mass thresholds. The inference of mass is based on speed determination that is uncertain by a factor of 2.

5.3 β-meteoroids

When Ulysses was in the inner solar system in 1995 and in 2001, maxima were evident in the impact rate of the smallest particles (AR1; Papers V and IX). A similar maximum in the inner solar system occurred again in 2007 (Fig. 7; top panel). Although in all three cases the maximum was reached during a short period around ecliptic plane crossing, many particles were also detected at high ecliptic latitudes. These grains are attributed to a population of submicron-sized interplanetary particles whose dynamics is dominated by solar radiation pressure. They move on escape trajectories from the solar system (β-meteoroids, Baguhl et al., 1995b; Hamilton et al., 1996). β-meteoroids were identified with Ulysses over the Sun's poles in 1994/95 (Wehry and Mann, 1999) and 2000/01 (Wehry et al., 2004). Due to the detection geometry, however, they were undetectable outside these periods, explaining the lower impact rates in AR1. β-meteoroids were detectable again from mid-2006 until early-2008 (Wehry et al., 2004). In independent potential detection of β-meteoroids was recently reported from the plasma wave instrument on board the STEREO spacecraft (Meyer-Vernet et al., 2009).

Wehry and Mann (1999) and Wehry et al. (2004) identified a significant asymmetry in the flux of these particles between the northern and the southern hemisphere from the first two heliocentric orbits of Ulysses, the reason of which is presently unknown. A comprehensive analysis of these three data sets will be the subject of a future investigation and may reveal whether the asymmetry is connected with the solar cycle variation of the interplanetary magnetic field.

6 Conclusions

In this paper, the eleventh and final in a series of Ulysses and Galileo dust data papers, we present data from the Ulysses dust instrument for the period January 2005 to November 2007. In this time interval, starting from a heliocentric distance of 5.3 AU close to aphelion, the spacecraft approached the Sun, flew over the Sun's south pole, crossed the ecliptic plane at 1.4 AU heliocentric distance and reached a northern ecliptic latitude of 60°.

A total number of 609 dust impacts were recorded during this period. Together with 6110 impacts recorded in interplanetary space and near Jupiter between Ulysses' launch in October 1990 and December 2004 (Grün et al., 1995a; Krüger et al., 1999b, 2001b, 2006a), the complete dust data set measured during the entire Ulysses mission consists of 6719 impacts. Given its temporal coverage and Ulysses' unique orbital orientation, the Ulysses dust data set will be a treasure for decades to come.

The total recorded dust impact rate dropped from an initial value of 0.7 impacts per day in 2005 when Ulysses was at low ecliptic latitudes to a value of 0.3 impacts at higher latitudes. Most of these particles were of interstellar origin, in particular at higher ecliptic latitudes, a minor fraction being interplanetary particles. A maximum of 1.5 per day was measured in 2007 in the inner solar system; here the majority of the grains were of interplanetary origin.

The measurements from the entire Ulysses mission since launch in 1990 are in disagreement with the interplanetary dust flux model by Divine (1993). Instead, they are well matched by the model of Staubach et al. (1997) which was originally developed with a shorter data set from the first Ulysses orbit and with the dust measurements from Galileo's interplanetary cruise.

Noise tests performed regularly during the three years period revealed no degradation in the noise sensitivity of the dust instrument, and the nominal instrument operational configuration remained unchanged during the entire period. In particular, no change in the channeltron high voltage setting was required.

With Ulysses we had the unprecedented opportunity to measure dust in interplanetary space for approximately 17 years. In particular, due to the unique orientation of Ulysses' orbital plane approximately perpendicular to the flow direction of the interstellar dust through the solar system and the spacecraft's 6-year revolution period about the Sun, we obtained dust measurements from three traverses of the same spatial region at southern ecliptic latitudes. These passes were separated by six years in time and were obtained at different phases of the solar cycle. Variations in the interstellar dust flux by a factor of three are evident during the entire mission. Flux variations until 2002 have been explained by the interaction of the dust grains with the time-varying interplanetary magnetic field, while detailed modelling of the later data is still pending. The data obtained in 2005/2006 reveal an approximately 30° shift in the approach direction of the grains away from the approach direction of the interstellar helium gas. The reason for this shift remains mysterious and will be the subject of a future investigation.

Even though this is the final paper in our serious of Ulysses dust data papers published

during the last 15 years, the evaluation of this unique data set is continuing. A list of specific open questions raised in this and earlier data papers includes:

- *β-meteoroids:* The detailed evaluation of the measurements from Ulysses' third solar orbit is still pending. Open questions include the measured north-south asymmetry in the measured flux and the heliocentric distance range where these grains are generated. More measurements from other spacecraft (e.g. STEREO) would be advantageous to answer these questions.

- *Comparison with Pioneer 10 and 11 measurements:* The flux of particles with $m \geq 10^{-9}$ g as measured with Ulysses is about a factor of five lower than expected from the Pioneer 10/11 measurements. Potential reasons for this discrepancy are errors on the mass calibrations of the Ulysses and/or Pioneer detectors in this mass range, many of the Pioneer detections may not be due to actual meteoroid impacts, or the dust grains by Pioneer belong to a population of dust which could not or only partially be detected with Ulysses (Krüger et al., 1999b). Measurements with New Horizons in the outer solar system may shed new light onto this question.

- *Interstellar dust:* Earlier comprehensive investigations of the interstellar impactors were mostly performed in the late 1990s and relied upon the significantly smaller data set available at the time. In the meantime, until the end of the Ulysses mission, the interstellar dust data set has grown by at least a factor of two so that a complete re-analysis of the entire data set is worthwhile and can give new insights into, e.g., the grain dynamics inside the heliosphere and into the conditions in the local interstellar environment where these grains originate from. In particular, the reason for the observed 30° shift remains an open question.

- *Interplanetary dust:* The interplanetary dust model by Divine (1993) was developed before the Ulysses data became available and the model by Staubach et al. (1997) used only data from within the ecliptic plane and from a fraction of Ulysses' first heliocentric orbit. A new model is presently being developed by Dikarev et al. (2005) which will incorporate infrared observations of the zodiacal cloud by the COBE DIRBE instrument, in-situ flux measurements by the dust detectors on board Galileo and Ulysses, and the crater size distributions on lunar rock samples retrieved by the Apollo missions.

Acknowledgements. We dedicate this work to the memory of Dietmar Linkert who passed away in spring 2009. He was Principal Engineer for space instruments at MPI für Kernphysik including the dust instruments flown on the HEOS-2, Helios, Galileo, Ulysses and Cassini missions. His friends and colleagues around the world appreciated his experience and sought his professional advice. We thank the Ulysses project at ESA and NASA/JPL for effective and successful mission operations. This work has been supported by the Deutsches Zentrum für Luft- und Raumfahrt e.V. (DLR) under grants 50 0N 9107 and 50 QJ 9503. Support by Max-Planck-Institut für Kernphysik and Max-Planck-Institut für Sonnensystemforschung is also gratefully acknowledged.

References

Altobelli, N., Kempf, S., Krüger, H., Landgraf, M., Srama, R., and Grün, E.: 2005a, *In-Situ Monitoring of Interstellar Dust in the Inner Solar System*, in *AIP Conf. Proc. 761: The Spectral Energy Distributions of Gas-Rich Galaxies: Confronting Models with Data*, pp 149–152

Altobelli, N., Kempf, S., Krüger, H., Landgraf, M., Roy, M., and Grün, E.: 2005b, *Interstellar dust flux measurements by the Galileo dust instrument between Venus and Mars orbit*, *Journal of Geophysical Research* **110**, 7102–7115

Altobelli, N., Kempf, S., Landgraf, M., Srama, R., Dikarev, V., Krüger, H., Moragas-Klostermeyer, G., and Grün, E.: 2003, *Cassini between Venus and Earth: Detection of Interstellar Dust*, *Journal of Geophysical Research* **108**, A10, 7–1

Altobelli, N., Moissl, R., Krüger, H., Landgraf, M., and Grün, E.: 2004, *Influence of wall impacts on the Ulysses dust detector in modelling the interstellar dust flux*, *Planetary and Space Science* **52**, 1287–1295

Baggaley, W. J. and Neslušan, L.: 2002, *A model of the heliocentric orbits of a stream of Earth-impacting interstellar meteoroids*, *Astronomy and Astrophysics* **382**, 1118–1124

Baguhl, M., Grün, E., Hamilton, D. P., Linkert, G., Riemann, R., and Staubach, P.: 1995a, *The flux of interstellar dust observed by Ulysses and Galileo*, *Space Science Reviews* **72**, 471–476

Baguhl, M., Hamilton, D. P., Grün, E., Dermott, S. F., Fechtig, H., Hanner, M. S., Kissel, J., Lindblad, B. A., Linkert, D., Linkert, G., Mann, I., McDonnell, J. A. M., Morfill, G. E., Polanskey, C., Riemann, R., Schwehm, G. H., Staubach, P., and Zook, H. A.: 1995b, *Dust measurements at high ecliptic latitudes*, *Science* **268**, 1016–1020

Balogh, A., Marsden, R., and Smith, E. e.: 2001, *The heliosphere near solar minimum: The Ulysses Perspective*, Springer Praxis, Springer, Berlin, Heidelberg, New York

Collier, M. R., Moore, T. E., Simpson, D., Roberts, A., Szabo, A., Fuselier, S., Wurz, P., Lee, M. A., and Tsurutani, B. T.: 2004, *An unexplained* $10-40^{\circ}$ *shift in the location of some diverse neutral atom data at 1 AU*, *Advances in Space Research* **34**, 166–171

Czechowski, A. and Mann, I.: 2003a, *Local interstellar cloud grains outside the heliopause*, *Astronomy and Astrophysics* **410**, 165–173

Czechowski, A. and Mann, I.: 2003b, *Penetration of Interstellar Grains into the Heliosphere*, *Journal of Geophysical Research* **108**, A10, 8038, 10.1029/2003JA009917

Dikarev, V., Landgraf, M., Grün, E., Baggaley, W., and Galligan, D.: 2001, *Interplanetary Dust Model:From Micron sized Dust to Meteors*, *Proceedings of the Meteroids 2001 Conference* pp 609–615

651 Dikarev, V., Jehn, R., and Grün, E.: 2002, *Towards a new model of the interplanetary*
652 *metereoroid environment*, *Advances in Space Research* **29(8)**, 1171–1175

653 Dikarev, V., Grün, E., Baggaley, J., Galligan, D., Landgraf, M., and Jehn, R.: 2005, *The*
654 *new ESA meteoroid model*, *Advances in Space Research* **35**, 1282–1289

655 Divine, N.: 1993, *Five populations of interplanetary meteoroids*, *Journal of Geophysical*
656 *Research* **98**, 17029–17048

657 Flandes, A. and Krüger, H.: 2007, *Solar wind modulation of Jupiter dust stream detection*,
658 in H. Krüger and A. L. Graps (ed.), *Dust in planetary systems*, pp 87–90, ESA SP-643

659 Flandes, A., Krüger, H., Hamilton, D. P., and Valdés-Galicia, J. F.: 2009, *Magnetic field*
660 *modulated dust streams from Jupiter in interplanetary space*, *Icarus*, in preparation

661 Frisch, P. C., Dorschner, J., Geiß, J., Greenberg, J. M., Grün, E., Landgraf, M., Hoppe,
662 P., Jones, A. P., Krätschmer, W., Linde, T. J., Morfill, G. E., Reach, W. T., Slavin,
663 J., Svestka, J., Witt, A., and Zank, G. P.: 1999, *Dust in the Local Interstellar Wind*,
664 *Astrophysical Journal* **525**, 492–516

665 Frisch, P. C. and Slavin, J. D.: 2003, *The Chemical Composition and Gas-to-Dust Mass*
666 *Ratio of Nearby Interstellar Matter*, *Astrophysical Journal* **594**, 844–858

667 Graps, A. L., Grün, E., Svedhem, H., Krüger, H., Horányi, M., Heck, A., and Lammers,
668 S.: 2000, *Io as a source of the Jovian dust streams*, *Nature* **405**, 48–50

669 Grün, E., Fechtig, H., Hanner, M. S., Kissel, J., Lindblad, B. A., Linkert, D., Maas, D.,
670 Morfill, G. E., and Zook, H. A.: 1992a, *The Galileo dust detector*, *Space Science*
671 *Reviews* **60**, 317–340

672 Grün, E., Fechtig, H., Kissel, J., Linkert, D., Maas, D., McDonnell, J. A. M., Morfill, G. E.,
673 Schwehm, G. H., Zook, H. A., and Giese, R. H.: 1992b, *The Ulysses dust experiment*,
674 *Astronomy and Astrophysics, Supplement* **92**, 411–423

675 Grün, E., Zook, H. A., Baguhl, M., Balogh, A., Bame, S. J., Fechtig, H., Forsyth, R.,
676 Hanner, M. S., Horányi, M., Kissel, J., Lindblad, B. A., Linkert, D., Linkert, G., Mann,
677 I., McDonnell, J. A. M., Morfill, G. E., Phillips, J. L., Polanskey, C., Schwehm, G. H.,
678 Siddique, N., Staubach, P., Svestka, J., and Taylor, A.: 1993, *Discovery of Jovian dust*
679 *streams and interstellar grains by the Ulysses spacecraft*, *Nature* **362**, 428–430

680 Grün, E., Gustafson, B. E., Mann, I., Baguhl, M., Morfill, G. E., Staubach, P., Taylor, A.,
681 and Zook, H. A.: 1994, *Interstellar dust in the heliosphere*, *Astronomy and Astrophysics*
682 **286**, 915–924

683 Grün, E., Baguhl, M., Divine, N., Fechtig, H., Hamilton, D. P., Hanner, M. S., Kissel,
684 J., Lindblad, B. A., Linkert, D., Linkert, G., Mann, I., McDonnell, J. A. M., Morfill,
685 G. E., Polanskey, C., Riemann, R., Schwehm, G. H., Siddique, N., Staubach, P., and

686 Zook, H. A.: 1995a, *Two years of Ulysses dust data*, *Planetary and Space Science* **43**,
687 971–999, Paper III

688 Grün, E., Baguhl, M., Divine, N., Fechtig, H., Hamilton, D. P., Hanner, M. S., Kissel,
689 J., Lindblad, B. A., Linkert, D., Linkert, G., Mann, I., McDonnell, J. A. M., Morfill,
690 G. E., Polanskey, C., Riemann, R., Schwehm, G. H., Siddique, N., Staubach, P., and
691 Zook, H. A.: 1995b, *Three years of Galileo dust data*, *Planetary and Space Science* **43**,
692 953–969, Paper II

693 Grün, E., Baguhl, M., Hamilton, D. P., Kissel, J., Linkert, D., Linkert, G., and Riemann,
694 R.: 1995c, *Reduction of Galileo and Ulysses dust data*, *Planetary and Space Science*
695 **43**, 941–951, Paper I

696 Grün, E., Staubach, P., Baguhl, M., Hamilton, D. P., Zook, H. A., Dermott, S. F., Gustafson,
697 B. A., Fechtig, H., Kissel, J., Linkert, D., Linkert, G., Srama, R., Hanner, M. S.,
698 Polanskey, C., Horányi, M., Lindblad, B. A., Mann, I., McDonnell, J. A. M., Mor-
699 fill, G. E., and Schwehm, G. H.: 1997, *South-North and Radial Traverses through the*
700 *Interplanetary Dust Cloud*, *Icarus* **129**, 270–288

701 Grün, E., Krüger, H., Graps, A., Hamilton, D. P., Heck, A., Linkert, G., Zook, H., Dermott,
702 S. F., Fechtig, H., Gustafson, B., Hanner, M., Horányi, M., Kissel, J., Lindblad, B.,
703 Linkert, G., Mann, I., McDonnell, J. A. M., Morfill, G. E., Polanskey, C., Schwehm,
704 G. H., and Srama, R.: 1998, *Galileo observes electromagnetically coupled dust in the*
705 *Jovian magnetosphere*, *Journal of Geophysical Research* **103**, 20011–20022

706 Grün, E. and Landgraf, M.: 2000, *Collisional consequences of big interstellar grains*,
707 *Journal of Geophysical Research* **105 no A5**, 10,291–10,298

708 Grün, E., Krüger, H., and Landgraf, M.: 2001, *Cosmic Dust*, in A. Balogh, R. Marsden,
709 and E. Smith (eds.), *The heliosphere at solar minimum: The Ulysses perspective*, pp
710 373–404, Springer Praxis

711 Hamilton, D. P. and Burns, J. A.: 1993, *Ejection of dust from Jupiter's gossamer ring*,
712 *Nature* **364**, 695–699

713 Hamilton, D. P., Grün, E., and Baguhl, M.: 1996, *Electromagnetic escape of dust from the*
714 *solar system*, in B. A. S. Gustafson and M. S. Hanner (eds.), *Physics, Chemistry and*
715 *Dynamics of Interplanetary Dust, ASP Conference Series*, Vol. 104, pp 31–34

716 Horányi, M., Morfill, G. E., and Grün, E.: 1993, *Mechanism for the acceleration and*
717 *ejection of dust grains from Jupiter's magnetosphere*, *Nature* **363**, 144–146

718 Horányi, M., Grün, E., and Heck, A.: 1997, *Modeling the Galileo dust measurements at*
719 *Jupiter*, *Geophysical Research Letters* **24**, 2175–2178

720 Jones, G. H. and Balogh, A.: 2003, *A survey of strong interplanetary field enhacements at*
721 *Ulysses*, *Icarus* **166**, 297–310

Kempf, S., Srama, R., Altobelli, N., Auer, S., Tschernjawski, V., Bradley, J., Burton, M. E., Helfert, S., Johnson, T. V., Krüger, H., Moragas-Klostermeyer, G., and Grün, E.: 2004, *Cassini between Earth and asteroid belt: first in-situ charge measurements of interplanetary grains*, *Icarus* **171**, 317–335

Krüger, H., Grün, E., Hamilton, D. P., Baguhl, M., Dermott, S. F., Fechtig, H., Gustafson, B. A., Hanner, M. S., Horányi, M., Kissel, J., Lindblad, B. A., Linkert, D., Linkert, G., Mann, I., McDonnell, J. A. M., Morfill, G. E., Polanskey, C., Riemann, R., Schwehm, G. H., Srama, R., and Zook, H. A.: 1999a, *Three years of Galileo dust data: II. 1993 to 1995*, *Planetary and Space Science* **47**, 85–106, Paper IV

Krüger, H., Grün, E., Landgraf, M., Baguhl, M., Dermott, S. F., Fechtig, H., Gustafson, B. A., Hamilton, D. P., Hanner, M. S., Horányi, M., Kissel, J., Lindblad, B., Linkert, D., Linkert, G., Mann, I., McDonnell, J. A. M., Morfill, G. E., Polanskey, C., Schwehm, G. H., Srama, R., and Zook, H. A.: 1999b, *Three years of Ulysses dust data: 1993 to 1995*, *Planetary and Space Science* **47**, 363–383, Paper V

Krüger, H., Grün, E., Graps, A. L., Bindschadler, D. L., Dermott, S. F., Fechtig, H., Gustafson, B. A., Hamilton, D. P., Hanner, M. S., Horányi, M., Kissel, J., Lindblad, B., Linkert, D., Linkert, G., Mann, I., McDonnell, J. A. M., Morfill, G. E., Polanskey, C., Schwehm, G. H., Srama, R., and Zook, H. A.: 2001a, *One year of Galileo dust data from the jovian system: 1996*, *Planetary and Space Science* **49**, 1285–1301, Paper VI

Krüger, H., Grün, E., Landgraf, M., Dermott, S. F., Fechtig, H., Gustafson, B. A., Hamilton, D. P., Hanner, M. S., Horányi, M., Kissel, J., Lindblad, B., Linkert, D., Linkert, G., Mann, I., McDonnell, J. A. M., Morfill, G. E., Polanskey, C., Schwehm, G. H., Srama, R., and Zook, H. A.: 2001b, *Four years of Ulysses dust data: 1996 to 1999*, *Planetary and Space Science* **49**, 1303–1324, Paper VII

Krüger, H., Forsyth, R. J., Graps, A. L., and Grün, E.: 2005a, *Electromagnetically Interacting Dust Streams During Ulysses' Second Jupiter Encounter*, in Boufendi, L., Mikikian, M. and Shukla, P. K., AIP conference proceedings (ed.), *New Vistas in Dusty Plasmas*, pp 157–160

Krüger, H., Grün, E., Linkert, D., Linkert, G., and Moissl, R.: 2005b, *Galileo long-term dust monitoring in the jovian magnetosphere*, *Planetary and Space Science* **53**, 1109–1120

Krüger, H., Altobelli, N., Anweiler, B., Dermott, S. F., Dikarev, V., Graps, A. L., Grün, E., Gustafson, B. A., Hamilton, D. P., Hanner, M. S., Horányi, M., Kissel, J., Landgraf, M., Lindblad, B., Linkert, D., Linkert, G., Mann, I., McDonnell, J. A. M., Morfill, G. E., Polanskey, C., Schwehm, G. H., Srama, R., and Zook, H. A.: 2006a, *Five years of Ulysses dust data: 2000 to 2004*, *Planetary and Space Science* **54**, 932–956, Paper IX

Krüger, H., Bindschadler, D., Dermott, S. F., Graps, A. L., Grün, E., Gustafson, B. A., Hamilton, D. P., Hanner, M. S., Horányi, M., Kissel, J., Lindblad, B., Linkert, D.,

760 Linkert, G., Mann, I., McDonnell, J. A. M., Moissl, R., Morfill, G. E., Polanskey, C.,
761 Schwehm, G. H., Srama, R., and Zook, H. A.: 2006b, *Galileo dust data from the jovian*
762 *system: 1997 to 1999*, *Planetary and Space Science* **54**, 879–910, Paper VIII

763 Krüger, H., Graps, A. L., Hamilton, D. P., Flandes, A., Forsyth, R. J., Horányi, M., and
764 Grün, E.: 2006c, *Ulysses jovian latitude scan of high-velocity dust streams originating*
765 *from the jovian system*, *Planetary and Space Science* **54**, 919–931

766 Krüger, H., Landgraf, M., Altobelli, N., and Grün, E.: 2007, *Interstellar dust in the solar*
767 *system*, *Space Science Reviews* **130**, 401–408

768 Krüger, H. and Grün, E.: 2009, *Interstellar Dust Inside and Outside the Heliosphere*, in
769 Linsky, J. and Izmodenov, V. and Möbius, E. (ed.), *From the outer heliosphere to the*
770 *local bubble*, Springer Heidelberg

771 Krüger, H., Bindschadler, D., Dermott, S. F., Graps, A. L., Grün, E., Gustafson, B. A.,
772 Hamilton, D. P., Hanner, M. S., Horányi, M., Kissel, J., Linkert, D., Linkert, G., Mann,
773 I., McDonnell, J. A. M., Moissl, R., Morfill, G. E., Polanskey, C., Roy, M., Schwehm,
774 G. H., and Srama, R.: 2010, *Galileo dust data from the jovian system: 2000 to 2003*,
775 *Planetary and Space Science*, Paper X, submitted

776 Landgraf, M.: 1998, *Modellierung der Dynamik und Interpretation der In-situ-Messung in-*
777 *terstellaren Staubs in der lokalen Umgebung des Sonnensystems*, *Ph.D. thesis*, Ruprecht-
778 Karls-Universität Heidelberg

779 Landgraf, M., Augustsson, K., Grün, E., and Gustafson, B. A. S.: 1999, *Deflection of the*
780 *local interstellar dust flow by solar radiation pressure*, *Science* **286**, 2,319–2,322

781 Landgraf, M.: 2000, *Modelling the Motion and Distribution of Interstellar Dust inside the*
782 *Heliosphere*, *Journal of Geophysical Research* **105, no. A5**, 10,303–10316

783 Landgraf, M., Baggeley, W. J., Grün, E., Krüger, H., and Linkert, G.: 2000, *Aspects*
784 *of the Mass Distribution of Interstellar Dust Grains in the Solar System from in situ*
785 *Measurements*, *Journal of Geophysical Research* **105, no. A5**, 10,343–10352

786 Landgraf, M., Krüger, H., Altobelli, N., and Grün, E.: 2003, *Penetration of the Heliosphere*
787 *by the interstellar dust stream during solar maximum*, *Journal of Geophysical Research*
788 **108**, 5–1

789 Mann, I., Grün, E., and Wilck, M.: 1996, *The Contribution of Asteroid Dust to the Inter-*
790 *planetary Dust Cloud: The Impact of ULYSSES Results on the Understanding of Dust*
791 *Production in the Asteroid Belt and of the Formation of the IRAS Dust Bands*, *Icarus*
792 **120**, 399–407

793 Mann, I. and Kimura, H.: 2000, *Interstellar dust properties dervied from mass density,*
794 *mass distribution, and flux rates in the heliosphere*, *Journal of Geophysical Research*
795 **105 No. A5**, 10,317–10,328

Mann, I., Kimura, H., Biesecker, D. A., Tsurutani, B. T., Grün, E., McKibben, R. B., Liou, J.-C., MacQueen, R. M., Mukai, T., Guhathakurta, M., and Lamy, P.: 2004, *Dust Near The Sun*, *Space Science Reviews* **110**, 269–305

Mann, I. and Czechowski, A.: 2005, *Dust Destruction and Ion Formation in the Inner Solar System*, *Astrophysical Journal, Letters* **621**, L73–L76

Meyer-Vernet, N., Maksimovic, M., Czechowski, A., Mann, I., Zouganelis, I., Goetz, K., Kaiser, M. L., St. Cyr, O. C., Bougeret, J.-L., and Bale, S. D.: 2009, *Dust Detection by the Wave Instrument on STEREO: Nanoparticles Picked up by the Solar Wind?*, *Solar Physics* **256**, 463–474

Morfill, G. E. and Grün, E.: 1979, *The motion of charged dust particles in interplanetary space II -Interstellar grains* , *Planetary and Space Science* **27**, 1283–1292

Nakagawa, H., Bzowski, M., Yamazaki, A., Fukunishi, H., Watanabe, S., Takahashi, Y., and Taguchi, M.: 2006, *Secondary population of interstellar neutrals seems deflected to the side*, in *36th COSPAR Scientific Assembly*, Vol. 36 of *COSPAR, Plenary Meeting*, p 1170

Staubach, P., Grün, E., and Jehn, R.: 1997, *The meteoroid environment near earth*, *Advances in Space Research* **19**, 301–308

Stone, R. G., Bougeret, J. L., Caldwell, J., Canu, P., de Conchy, Y., Cornilleau-Wehrlin, N., Desch, M. D., Fainberg, J., Goetz, K., Goldstein, M. L., Harvey, C. C., Hoang, S., Howard, R., Kaiser, M. L., Kellogg, P., Klein, B., Knoll, R., Lecacheux, A., Langyel-Frey, D., MacDowall, R. J., Manning, R., Meetre, C. A., Meyer, A., Monge, N., Monson, S., Nicol, G., Reiner, M. J., Steinbert, J. L., Torres, E., de Villedary, C., Wouters, F., and Zarka, P.: 1992, *The unified radio and plasma wave investigation*, *Astronomy and Astrophysics, Supplement* **92**, 291–316

Svestka, J., Auer, S., Baguhl, M., and Grün, E.: 1996, *Measurements of dust electric charges by the Ulysses and Galileo dust detectors*, in B. A. Gustafson and M. S. Hanner (eds.), *Physics, Chemistry and Dynamics of Interplanetary Dust, ASP Conference Series*, Vol. 104, pp 481–484

Taylor, A. D., Baggeley, W. J., and Steel, D. I.: 1996, *Discovery of interstellar dust entering the Earth's atmosphere*, *Nature* **380**, 323–325

Wehry, A. and Mann, I.: 1999, *Identification of β-meteoroids from measurements of the dust detector onboard the Ulysses spacecraft*, *Astronomy and Astrophysics* **341**, 296–303

Wehry, A., Krüger, H., and Grün, E.: 2004, *Analysis of Ulysses data: Radiation pressure effects on dust particles*, *Astronomy and Astrophysics* **419**, 1169–1174

Wenzel, K., Marsden, R., Page, D., and Smith, E.: 1992, *The Ulysses mission*, *Astronomy and Astrophysics, Supplement* **92**, 207–219

Willis, M. J., Burchell, M., Ahrens, T. J., Krüger, H., and Grün, E.: 2005, *Decreased values of cosmic dust number density estimates in the solar system*, *Icarus* **176**, 440–452

Witte, M., Banaszkiewicz, H., and Rosenbauer, H.: 1996, *Recent results on the parameters of interstellar helium from the Ulysses/GAS experiment*, *Space Science Reviews* **78, no. 1/2**, 289–296

Witte, M.: 2004, *Kinetic parameters of interstellar neutral helium. Review of results obtained during one solar cycle with the Ulysses/GAS-instrument*, *Astronomy and Astrophysics* **426**, 835–844

Witte, M., Banaszkiewicz, M., Rosenbauer, H., and McMullin, D.: 2004, *Kinetic parameters of interstellar neutral helium: updated results from the Ulysses/GAS instrument*, *Advances in Space Research* **34**, 61–65

Wurz, P., Collier, M. R., Moore, T. E., Simpson, D., Fuselier, S., and Lennartson, W.: 2004, *Possible Origin of the Secondary Stream of Neutral Fluxes at 1 AU*, in V. Florinski, N. V. Pogorelov, and G. P. Zank (eds.), *Physics of the Outer Heliosphere*, Vol. 719 of *American Institute of Physics Conference Series*, pp 195–200

Zook, H. A., Grün, E., Baguhl, M., Hamilton, D. P., Linkert, G., Linkert, D., Liou, J.-C., Forsyth, R., and Phillips, J. L.: 1996, *Solar wind magnetic field bending of Jovian dust trajectories*, *Science* **274**, 1501–1503

Table 1: Summary of Ulysses data papers, significant mission events and dust detector switch-off times. Jupiter distance $R_J = 71492\,km$.

Time Interval	Significant Mission Events	Dust Detector off	Paper Number
1990 – 1992	Ulysses launch (6 Oct 1990), Jupiter flyby (8 Feb 1992, distance 6.3 R_J)	Before 27 Oct 1990, 14 Jun 1991 - 18 Jun 1991	III (Grün et al., 1995a)
1993 – 1995	Maximum southern latitude $-79°$ (3 Oct 1994), Perihelion (12 Mar 1995), Maximum northern latitude 79° (19 Aug 1995)	8 Aug 1993 - 11 Aug 1993, 27 Nov 1993 - 28 Nov 1993, 10 Oct 1994 - 11 Oct 1994, 10 Dec 1995	V (Krüger et al., 1999b)
1996 – 1999	Aphelion (20 Apr 1998),	17 Aug 1996 - 18 Aug 1996, 1 Apr 1997 - 2 Apr 1997, 15 Feb 1999 - 16 Feb 1999	VII (Krüger et al., 2001b)
2000 – 2004	Maximum southern latitude $-80°$ (27 Nov 2000), Perihelion (23 May 2001), Maximum northern latitude 80° (13 Oct 2001), Jupiter flyby (4 Feb 2004, distance 0.8 AU), Aphelion (30 Jun 2004)	26 Mar 2002 - 8 Apr 2002, 1 Dec 2002 - 3 Jun 2003, 28 Jun 2003 - 22 Aug 2003, 30 Nov 2003 - 2 Dec 2003	IX (Krüger et al., 2006a)
2005 – 2007	Maximum southern latitude $-80°$ (7 Feb 2007), Perihelion (18 Aug 2007)	28 Sep 2006 - 9 Mar 2007, 2 Apr 2007 - 30 Apr 2007, After 30 Nov 2007	XI (this paper)

Table 2: Ulysses mission and dust detector (GRU) configuration, tests and other events. Only selected events are given before 2005. See Section 2 for details.

Yr-day	Date	Time	Event
90-279	06.10.90		Ulysses launch
03-154	03.06.03	03:38	GRU 0.8 W heater on
04-182	30.06.04		Ulysses aphelion passage (5.4 AU)
04-337	02.12.04	11:00	GRU nominal configuration: HV=4, EVD=C,I, SSEN=0001
05-006	06.01.05	07:00	GRU noise test
05-034	03.02.05	04:20	GRU noise test
05-063	04.03.05	03:00	GRU noise test
05-090	31.03.05	01:00	GRU noise test
05-120	30.04.05	00:00	GRU noise test
05-146	26.05.05	04:00	GRU noise test
05-174	23.06.05	20:00	GRU noise test
05-201	20.07.05	17:27	GRU noise test
05-229	17.08.05	11:49	GRU noise test
05-259	16.09.05	19:00	GRU noise test
05-285	12.10.05	09:00	GRU noise test
05-314	10.11.05	13:14	GRU noise test
05-342	08.12.05	11:00	GRU noise test
06-005	05.01.06	08:30	GRU noise test
06-033	02.02.06	09:16	GRU noise test
06-061	02.03.06	04:00	GRU noise test
06-089	30.03.06	02:00	GRU noise test
06-118	28.04.06	00:30	GRU noise test
06-148	28.05.06	06:28	GRU noise test
06-173	22.06.06	07:33	GRU noise test
06-202	21.07.06	19:00	GRU noise test
06-232	20.08.06	17:00	GRU noise test
06-256	13.09.06	20:11	GRU noise test
06-271	28.09.06	16:28	GRU off (both heaters off)
07-038	07.02.07		Ulysses maximum south solar latitude (-79.7°)
07-067	08.03.07	18:08	GRU 0.8 W heater on
07-067	08.03.07	18:28	GRU 0.4 W heater on
07-068	09.03.07	16:44	GRU 0.8 W heater off
07-068	09.03.07	17:31	GRU on
07-069	10.03.07	07:54	GRU nominal configuration
07-079	20.03.07	08:40	GRU noise test
07-092	02.04.07	18:11	GRU off (both heaters off)
07-120	30.04.07	01:23	GRU 0.8 W heater on
07-120	30.04.07	01:33	GRU 0.4 W heater on
07-120	30.04.07	21:37	GRU 0.8 W heater off
07-120	30.04.07	21:38	GRU on
07-121	01.05.07	04:07	GRU nominal configuration
07-130	10.05.07	20:00	GRU noise test
07-158	07.06.07	01:00	GRU noise test
07-187	06.07.07	16:15	GRU noise test
07-214	02.08.07	01:53	GRU noise test
07-231	18.08.07		Ulysses perihelion passage (1.39 AU)
07-232	19.08.07		Ulysses ecliptic plane crossing
07-242	30.08.07	00:17	GRU noise test
07-270	27.09.07	17:00	GRU noise test
07-298	25.10.07	13:00	GRU noise test
07-326	22.11.07	15:00	GRU noise test
07-334	30.11.07	16:20	GRU off (both heaters off)
08-014	14.01.08		Ulysses maximum north solar latitude (79.8°)
09-181	30.06.09		Ulysses end of mission

Abbreviations used: HV: channeltron high voltage step; EVD: event definition, ion- (I), channeltron- (C), or electron-channel (E); SSEN: detection thresholds, ICP, CCP, ECP and PCP. Times when no data could be collected with the dust instrument: 28 September 2006 to 9 March 2007, 2 April to 30 April 2007 and after 30 November 2007.

Table 3. Overview of dust impacts detected with the Ulysses dust detector between 1 January 2005 and 30 November 2007 as derived from the accumulators†. Switch-on of the instrument is indicated by horizontal lines. The heliocentric distance R, the lengths of the time interval Δt (days) from the previous table entry, and the corresponding numbers of impacts are given for the 24 accumulators. The accumulators are arranged with increasing signal amplitude ranges (AR), with four event classes for each amplitude range (CLN = 0,1,2,3); e.g. AC31 means counter for AR = 1 and CLN = 3. The Δt in the first line (05-006) is the time interval counted from the last entry in Table 2 in Paper IX. The totals of counted impacts†, of impacts with complete data, and of all events (noise plus impact events) for the entire period are given as well.

Date	Time	R [AU]	Δt [d]	AC 01†	AC 11†	AC 21	AC 31	AC 02†	AC 12	AC 22	AC 32	AC 03	AC 13	AC 23	AC 33	AC 04	AC 14	AC 24	AC 34	AC 05	AC 15	AC 25	AC 35	AC 06	AC 16	AC 26	AC 36
05-006	11:45	5.300	7.561	-	-	-	-	-	-	-	1	-	-	-	-	-	-	-	1	*	-	-	-	*	-	-	-
05-039	23:36	5.258	33.49	-	1	11	2	-	-	5	2	-	-	-	-	-	-	-	-	*	-	-	-	*	-	-	-
05-061	19:36	5.227	21.83	-	3	8	3	-	-	-	2	-	-	-	1	-	-	1	-	*	-	-	-	*	-	-	-
05-089	09:46	5.184	27.59	-	1	11	3	-	1	5	2	-	-	-	1	-	-	-	-	*	-	-	-	*	-	-	-
05-104	17:01	5.158	15.30	-	-	4	2	-	-	3	-	-	-	-	-	-	-	-	1	*	-	-	-	*	-	-	-
05-140	22:27	5.089	36.22	-	5	6	1	-	-	5	2	-	-	-	-	-	-	-	1	*	-	-	-	*	-	-	-
05-177	01:56	5.013	36.14	-	5	4	2	-	-	9	9	-	-	-	-	-	-	-	-	*	-	-	-	*	-	-	-
05-204	13:40	4.949	27.48	-	2	5	1	-	-	2	2	-	-	-	3	-	-	-	-	*	-	-	-	*	-	-	-
05-227	18:13	4.891	23.18	-	4	5	2	-	-	3	7	-	-	1	6	-	-	-	-	*	-	-	-	*	-	-	-
05-250	17:23	4.831	22.96	-	1	6	-	-	1	1	7	-	-	-	2	-	-	-	1	*	-	-	-	*	-	-	-
05-284	14:06	4.734	33.86	-	2	3	-	-	-	2	4	-	-	1	7	-	-	-	-	*	-	-	-	*	-	-	-
05-310	21:37	4.654	26.31	-	1	3	-	-	-	5	5	-	-	-	3	-	-	-	-	*	-	-	-	*	-	-	-
05-337	10:38	4.568	26.54	-	3	-	-	-	-	2	2	-	-	-	1	-	-	-	1	*	-	-	-	*	-	-	-
05-364	06:07	4.475	26.81	-	1	-	-	-	-	1	1	-	-	-	1	-	-	-	-	*	-	-	-	*	-	-	-
06-028	18:17	4.368	29.50	-	2	2	1	-	1	3	4	-	-	-	1	-	-	-	-	*	-	-	-	*	-	-	-
06-052	22:35	4.274	24.17	-	2	3	-	-	-	2	4	-	-	-	2	-	-	-	-	*	-	-	-	*	-	-	-
06-078	05:59	4.172	25.30	-	2	2	-	-	-	1	-	-	-	-	3	-	-	-	-	*	-	-	-	*	-	-	-
06-100	06:53	4.078	22.03	-	-	1	-	-	-	3	1	-	-	1	1	-	-	-	-	*	-	-	-	*	-	-	-
06-132	07:12	3.935	32.01	-	-	2	-	-	-	2	1	-	-	-	5	-	-	-	-	*	-	-	-	*	-	-	-
06-165	22:45	3.776	33.64	-	1	2	1	-	-	1	2	-	-	-	2	-	-	-	1	*	-	-	-	*	-	-	-
06-192	21:07	3.642	26.93	-	-	1	-	-	-	1	1	-	-	-	1	-	-	-	-	*	-	-	-	*	-	-	-
06-217	08:19	3.514	24.46	-	1	1	-	-	-	-	1	-	-	-	1	-	-	-	1	*	-	-	-	*	-	-	-
06-238	08:40	3.400	21.01	-	-	2	-	-	-	-	1	-	-	-	1	-	-	-	-	*	-	-	-	*	-	-	-
06-271	16:30	3.211	33.32	-	-	1	-	-	-	1	2	-	-	-	1	-	-	-	1	*	-	-	-	*	-	-	-
07-069	07:54	2.163	162.6																								
07-092	18:15	2.004	23.43	-	1	-	-	-	1	2	2	-	-	1	1	-	-	-	-	*	-	-	1	*	-	-	-
07-121	04:07	1.818	28.41																								
07-152	04:50	1.634	31.02	-	1	6	-	-	1	-	1	-	-	1	-	-	-	-	-	*	-	-	-	*	-	-	-
07-182	21:34	1.489	30.69	-	13	10	4	-	-	-	1	-	-	-	2	-	-	1	-	*	-	-	-	*	-	-	-
07-200	08:56	1.433	17.47	2	12	6	1	-	-	8	5	-	-	-	1	-	-	-	1	*	-	-	-	*	-	-	-
07-222	17:12	1.396	22.34	2	25	17	3	-	1	3	2	-	-	3	-	-	-	1	3	*	-	-	-	*	-	-	-
07-243	23:21	1.402	21.25	3	25	8	1	-	3	9	2	-	-	3	5	-	-	1	2	*	-	2	1	*	-	1	-
07-266	13:56	1.452	22.60	-	5	13	4	-	2	6	-	-	-	4	5	-	-	-	2	*	-	-	-	*	-	-	-
07-288	22:33	1.538	22.35	-	8	9	-	-	1	1	-	-	-	1	2	-	-	-	1	*	-	-	-	*	-	-	-
07-309	22:37	1.644	21.00	-	1	5	-	-	-	2	-	-	-	-	2	-	-	-	2	*	-	-	-	*	-	-	-

Table 3 continued.

Date	Time	R [AU]	Δt [d]	AC 01†	AC 11†	AC 21	AC 31	AC 02†	AC 12	AC 22	AC 32	AC 03	AC 13	AC 23	AC 33	AC 04	AC 14	AC 24	AC 34	AC 05	AC 15	AC 25	AC 35	AC 06	AC 16	AC 26	AC 36
07-334	16:30	1.790	24.74	-	3	2	-	-	-	-	-	-	-	1	-	-	-	-	-	*	-	-	-	*	-	-	-
Impacts (counted)				7†	131†	159	31	0†	12	88	76	0	0	17	61	0	0	4	19	*	0	2	2	*	0	1	0
Impacts (complete data)				7	131	158	31	0	12	88	76	0	0	17	61	0	0	4	19	*	0	2	2	*	0	1	0
All events(complete data)				6243	132	159	31	120	12	88	76	2	0	17	61	1	0	4	19	*	0	2	2	*	0	1	0

†: Entries for AC01, AC11 and AC02 are the number of impacts with complete data. Due to the noise contamination of these three categories the number of impacts cannot be determined from the accumulators. The method to separate dust impacts from noise events in these three categories has been given by Baguhl et al. (1993).
∗: No entries are given for AC05 and AC06 because they count the overflows of accumulators AC21 and AC31 since the reprogramming in December 2004 (Paper IX).

Table 4. Raw data: No., impact time, CLN, AR, SEC, IA, EA, CA, IT, ET, EIT, EIC, ICC, PA, PET, EVD, ICP, ECP, CCP, PCP, HV and evaluated data: R, LON, LAT, D_{Jup}, rotation angle (ROT), instr. pointing (S_{LON}, S_{LAT}), impact speed (v, in km s^{-1}), speed error factor (VEF), mass (m, in grams) and mass error factor (MEF).

No.	IMP. DATE	CLN	AR	SEC	IA	EA	CA	IT	ET	EIT	EIC	ICC	PA	PET	EVD	ICP	ECP	CCP	PCP	HV	R	LON	LAT	D_{Jup}	ROT	S_{LON}	S_{LAT}	V	VEF	M	MEF
6111	05-006 03:30	3	4	17	29	49	13	9	5	7	0	1	46	0	1	0	0	0	1	4	5.29763	159.2	-8.8	2.70789	280	76	11	7.8	1.9	$5.4 \cdot 10^{-10}$	10.5
6112	05-006 11:45	3	2	156	10	20	9	9	7	9	0	1	36	0	1	0	0	0	1	4	5.29735	159.2	-8.8	2.70959	116	269	-23	14.1	1.9	$8.9 \cdot 10^{-13}$	10.5
6113	05-010 12:16	3	2	166	10	20	1	8	6	7	0	1	37	0	1	0	0	0	1	4	5.29256	159.2	-9.0	2.73766	132	274	-39	21.4	1.9	$1.9 \cdot 10^{-13}$	10.5
6114	05-010 15:01	2	1	87	2	6	0	9	10	11	0	0	0	0	1	0	0	0	1	4	5.29242	159.2	-9.0	2.73851	21	245	69	26.5	2.0	$3.3 \cdot 10^{-15}$	12.5
6115	05-011 21:22	2	1	105	5	9	0	8	8	7	0	0	0	0	1	0	0	0	1	4	5.29094	159.2	-9.1	2.74700	46	255	44	28.0	1.6	$7.4 \cdot 10^{-15}$	6.0
6116	05-014 23:24	2	1	193	6	10	0	7	8	8	0	0	0	0	1	0	0	0	1	4	5.28737	159.3	-9.2	2.76737	169	311	-70	35.4	1.6	$4.8 \cdot 10^{-15}$	6.0
6117	05-017 00:12	2	1	102	5	10	0	8	8	8	0	0	0	0	1	0	0	0	1	4	5.28481	159.3	-9.4	2.78178	43	254	47	28.0	1.6	$8.8 \cdot 10^{-15}$	6.0
6118	05-018 08:39	2	1	51	3	7	0	9	9	9	0	0	0	0	1	0	0	0	1	4	5.28329	159.3	-9.4	2.79025	331	87	61	21.0	1.6	$1.1 \cdot 10^{-14}$	6.0
6119	05-019 14:03	3	1	87	2	6	10	15	8	10	0	1	0	0	1	0	0	0	1	4	5.28176	159.3	-9.5	2.79871	21	244	68	36.7	2.0	$1.1 \cdot 10^{-15}$	12.5
6120	05-021 13:52	1	1	98	5	2	0	8	15	0	1	0	0	0	1	0	0	0	1	4	5.27929	159.3	-9.6	2.81224	40	251	50	21.4	1.9	$6.4 \cdot 10^{-15}$	10.5
6121	05-022 22:45	2	1	204	7	12	0	7	7	6	0	0	34	0	1	0	0	0	1	4	5.27758	159.4	-9.7	2.82153	189	15	-71	43.7	1.6	$3.3 \cdot 10^{-15}$	6.0
6122	05-023 08:32	2	2	186	8	13	0	7	8	6	0	0	34	0	1	0	0	0	1	4	5.27711	159.4	-9.7	2.82406	163	300	-66	35.4	1.6	$1.1 \cdot 10^{-14}$	6.0
6123	05-023 10:04	2	2	248	13	12	1	6	15	0	1	1	27	31	1	0	0	0	1	4	5.27695	159.4	-9.7	2.82491	250	68	-17	43.5	1.9	$8.9 \cdot 10^{-15}$	10.5
6124	05-024 05:20	2	1	241	6	11	0	8	8	7	0	0	0	0	1	0	0	0	1	4	5.27601	159.4	-9.7	2.82997	240	65	-27	28.0	1.6	$1.2 \cdot 10^{-14}$	6.0
6125	05-025 11:04	2	1	217	5	10	0	9	8	7	0	0	0	0	1	0	0	0	1	4	5.27444	159.4	-9.8	2.83841	210	49	-55	22.7	1.6	$1.8 \cdot 10^{-14}$	6.0
6126	05-030 11:00	3	2	179	12	21	2	8	5	6	0	1	39	0	1	0	0	0	1	4	5.26804	159.4	-10.0	2.87210	158	293	-62	21.4	1.9	$3.1 \cdot 10^{-13}$	10.5
6127	05-032 05:43	2	2	157	9	19	0	8	5	8	0	0	37	0	1	0	0	0	1	4	5.26592	159.4	-10.1	2.88303	127	270	-33	21.4	1.9	$1.2 \cdot 10^{-13}$	10.5
6128	05-032 19:14	2	1	187	3	8	0	9	8	12	0	0	0	0	1	0	0	0	1	4	5.26494	159.5	-10.2	2.88807	174	326	-71	22.7	1.6	$9.4 \cdot 10^{-15}$	6.0
6129	05-034 00:12	2	2	76	8	13	0	7	8	6	0	0	35	0	1	0	0	0	1	4	5.26330	159.5	-10.2	2.89647	18	234	71	35.4	1.6	$1.1 \cdot 10^{-14}$	6.0
6130	05-034 23:18	2	1	21	5	10	0	8	8	7	0	0	0	0	1	0	0	0	1	4	5.26214	159.5	-10.3	2.90234	300	76	30	28.0	1.6	$8.8 \cdot 10^{-15}$	6.0
6131	05-035 00:03	2	1	115	7	12	0	8	8	6	0	0	0	0	1	0	0	0	1	4	5.26198	159.5	-10.3	2.90318	72	256	19	28.0	1.6	$1.7 \cdot 10^{-14}$	6.0
6132	05-037 05:39	3	1	161	4	8	13	8	9	7	0	1	0	0	1	0	0	0	1	4	5.25915	159.5	-10.4	2.91743	141	277	-47	25.9	1.6	$6.9 \cdot 10^{-15}$	6.0
6133	05-039 23:36	2	2	92	12	21	0	7	4	6	0	0	42	0	1	0	0	0	1	4	5.25545	159.5	-10.5	2.93585	43	248	47	34.1	1.9	$6.0 \cdot 10^{-14}$	10.5
6134	05-041 16:13	2	1	125	2	6	0	9	10	10	0	0	6	21	1	0	0	0	1	4	5.25307	159.6	-10.6	2.94755	98	260	-6	26.5	2.0	$3.3 \cdot 10^{-15}$	12.5
6135	05-041 18:10	1	1	209	4	3	0	9	15	0	1	0	0	0	1	0	0	0	1	4	5.25290	159.6	-10.6	2.94839	216	49	-49	14.1	1.9	$2.8 \cdot 10^{-14}$	10.5
6136	05-041 21:24	3	1	91	2	6	3	9	9	9	0	1	0	0	1	0	0	0	1	4	5.25273	159.6	-10.6	2.94922	50	249	40	31.3	2.0	$1.9 \cdot 10^{-15}$	12.5
6137	05-042 12:20	2	1	111	6	10	0	8	8	6	0	0	0	0	1	0	0	0	1	4	5.25187	159.6	-10.7	2.95340	78	256	13	28.0	1.6	$1.0 \cdot 10^{-14}$	6.0
6138	05-042 22:42	1	1	185	4	1	0	11	12	0	1	0	37	31	1	0	0	0	1	4	5.25136	159.6	-10.7	2.95591	182	349	-71	7.8	1.9	$9.3 \cdot 10^{-14}$	10.5
6139	05-043 00:56	2	1	237	3	7	0	9	8	9	0	0	0	0	1	0	0	0	1	4	5.25119	159.6	-10.7	2.95674	255	65	-13	22.7	1.6	$7.8 \cdot 10^{-15}$	6.0
6140	05-043 12:24	2	1	96	3	8	0	9	8	9	0	0	0	0	1	0	0	0	1	4	5.25050	159.6	-10.7	2.96008	56	251	34	22.7	1.6	$9.4 \cdot 10^{-15}$	6.0
6141	05-044 19:41	3	1	196	4	9	5	8	8	7	0	1	0	0	1	0	0	0	1	4	5.24878	159.6	-10.8	2.96842	196	26	-65	28.0	1.6	$6.2 \cdot 10^{-15}$	6.0
6142	05-045 06:28	2	1	155	3	9	0	8	7	9	0	0	0	0	1	0	0	0	1	4	5.24808	159.6	-10.8	2.97176	149	282	-53	34.6	1.6	$2.7 \cdot 10^{-15}$	6.0
6143	05-045 10:34	3	1	139	7	11	1	7	7	8	0	1	0	0	1	0	0	0	1	4	5.24791	159.6	-10.8	2.97259	127	268	-33	43.7	1.6	$2.9 \cdot 10^{-15}$	6.0
6144	05-046 17:38	2	1	68	7	12	0	7	8	7	0	0	34	0	1	0	0	0	1	4	5.24617	159.6	-10.9	2.98092	26	237	63	35.4	1.6	$8.1 \cdot 10^{-15}$	6.0
6145	05-047 12:38	2	4	166	27	30	8	6	5	4	1	1	1	0	1	0	0	0	1	4	5.24494	159.6	-10.9	2.98676	164	300	-64	34.6	1.6	$2.1 \cdot 10^{-12}$	6.0
6146	05-047 23:00	2	1	137	4	9	0	8	8	8	0	0	0	0	1	0	0	0	1	4	5.24442	159.6	-11.0	2.98925	123	267	-29	28.0	1.6	$6.2 \cdot 10^{-15}$	6.0
6147	05-049 02:18	3	3	151	21	26	6	5	6	6	0	1	45	0	1	0	0	0	1	4	5.24283	159.6	-11.0	2.99674	142	276	-47	35.4	1.6	$3.9 \cdot 10^{-13}$	6.0
6148	05-053 15:58	3	2	150	12	20	4	7	5	6	0	1	38	0	1	0	0	0	1	4	5.23624	159.7	-11.3	3.02747	169	310	-67	34.1	1.9	$5.2 \cdot 10^{-14}$	10.5
6149	05-055 18:09	1	1	192	2	1	0	15	15	0	1	0	0	0	1	0	0	0	1	4	5.23317	159.7	-11.4	3.04156	227	52	-38	11.8	11.8	$2.4 \cdot 10^{-14}$	5858.3
6150	05-056 13:51	3	2	133	14	22	10	8	7	5	0	1	40	0	1	0	0	0	1	4	5.23208	159.7	-11.4	3.04653	144	276	-49	21.4	1.9	$5.0 \cdot 10^{-13}$	10.5
6151	05-061 19:36	2	1	229	7	12	0	8	8	7	0	0	34	0	1	0	0	0	1	4	5.22434	159.8	-11.7	3.08123	318	78	48	28.0	1.6	$1.7 \cdot 10^{-14}$	6.0
6152	05-062 07:18	2	1	35	1	6	0	15	9	13	0	0	9	21	1	0	0	0	1	4	5.22359	159.8	-11.7	3.08453	45	242	44	31.3	2.0	$1.5 \cdot 10^{-15}$	12.5
6153	05-065 13:55	2	2	152	12	20	0	8	5	6	0	0	40	0	1	0	0	0	1	4	5.21870	159.8	-11.9	3.10594	226	48	-39	21.4	1.9	$2.6 \cdot 10^{-13}$	10.5
6154	05-066 11:46	2	1	73	6	11	0	8	8	7	0	0	0	0	1	0	0	0	1	4	5.21737	159.8	-11.9	3.11170	116	260	-22	28.0	1.6	$1.2 \cdot 10^{-14}$	6.0
6155	05-069 03:40	2	1	95	1	6	0	15	9	13	0	0	0	0	1	0	0	0	1	4	5.21317	159.9	-12.1	3.12977	148	278	-52	31.3	2.0	$1.5 \cdot 10^{-15}$	12.5
6156	05-069 05:19	2	2	13	8	9	5	12	15	0	1	1	23	31	1	0	0	0	1	4	5.21317	159.9	-12.1	3.12977	33	235	56	5.0	1.9	$2.9 \cdot 10^{-12}$	10.5
6157	05-069 19:19	2	1	5	4	9	0	8	8	8	0	0	0	0	1	0	0	0	1	4	5.21221	159.9	-12.1	3.13387	30	232	59	28.0	1.6	$6.2 \cdot 10^{-15}$	6.0
6158	05-070 00:31	3	1	29	3	7	8	8	9	9	0	1	5	22	1	0	0	0	1	4	5.21183	159.9	-12.1	3.13551	64	245	26	25.9	1.6	$4.9 \cdot 10^{-15}$	6.0
6159	05-070 00:37	2	1	1	6	10	0	8	8	8	0	0	0	0	1	0	0	0	1	4	5.21183	159.9	-12.1	3.13551	25	227	64	28.0	1.6	$1.0 \cdot 10^{-14}$	6.0
6160	05-070 20:02	2	1	252	3	8	0	9	9	9	0	0	0	0	1	0	0	0	1	4	5.21067	159.9	-12.2	3.14043	18	220	70	21.0	1.6	$1.3 \cdot 10^{-14}$	6.0

No.	IMP. DATE	CLN	AR	SEC	IA	EA	CA	IT	ET	EIT	EIC	IIC	PA	PET	EVD	ICP	ECP	CCP	PCP	HV	R	LON	LAT	D_{Jup}	ROT	S_{LON}	S_{LAT}	V	VEF	M	MEF
6161	05-073 02:49	3	1	187	7	12	1	7	7	6	0	1	4	21	1	0	0	0	1	4	5.20717	159.9	-12.3	3.15517	288	67	19	43.7	1.6	$3.3 \cdot 10^{-15}$	6.0
6162	05-074 22:31	2	1	71	5	5	1	10	15	0	1	1	0	0	1	0	0	0	1	4	5.20423	159.9	-12.4	3.16744	133	266	-38	10.4	1.9	$9.3 \cdot 10^{-14}$	10.5
6163	05-076 13:07	3	2	52	8	12	10	7	8	6	0	1	0	0	1	0	0	0	1	4	5.20167	159.9	-12.5	3.17805	107	256	-14	35.4	1.6	$9.7 \cdot 10^{-15}$	6.0
6164	05-078 06:56	3	3	92	19	22	7	6	5	6	0	1	41	0	1	0	0	0	1	4	5.19889	160.0	-12.6	3.18947	169	307	-66	34.6	1.6	$1.4 \cdot 10^{-13}$	6.0
6165	05-078 08:08	2	2	91	8	13	0	8	8	6	0	0	34	0	1	0	0	0	1	4	5.19889	160.0	-12.6	3.18947	168	304	-65	28.0	1.6	$2.4 \cdot 10^{-14}$	6.0
6166	05-078 18:10	2	1	101	2	6	0	10	9	10	0	0	0	0	1	0	0	0	1	4	5.19809	160.0	-12.6	3.19273	182	342	-69	31.3	2.0	$1.9 \cdot 10^{-15}$	12.5
6167	05-081 13:15	2	2	114	13	21	0	8	6	6	0	0	39	0	1	0	0	0	1	4	5.19367	160.0	-12.7	3.21063	202	24	-59	21.4	1.9	$3.6 \cdot 10^{-13}$	10.5
6168	05-081 13:19	3	2	101	12	20	8	7	5	6	0	1	38	0	1	0	0	0	1	4	5.19367	160.0	-12.7	3.21063	184	346	-68	34.1	1.9	$5.2 \cdot 10^{-14}$	10.5
6169	05-082 00:30	2	1	122	5	4	1	9	15	0	1	1	0	0	1	0	0	0	1	4	5.19286	160.0	-12.8	3.21389	214	36	-50	14.1	1.9	$3.8 \cdot 10^{-14}$	10.5
6170	05-082 16:49	1	1	168	3	1	0	9	15	0	1	0	2	21	1	0	0	0	1	4	5.19185	160.0	-12.8	3.21795	279	63	10	14.1	1.9	$1.8 \cdot 10^{-14}$	10.5
6171	05-082 17:46	1	2	41	10	1	0	6	15	0	1	0	7	31	1	0	0	0	1	4	5.19185	160.0	-12.8	3.21795	100	253	-7	43.5	1.9	$9.0 \cdot 10^{-16}$	10.5
6172	05-083 08:36	2	1	113	4	9	0	8	7	8	0	0	3	21	1	0	0	0	1	4	5.19084	160.0	-12.8	3.22201	205	27	-56	34.6	1.6	$3.2 \cdot 10^{-15}$	6.0
6173	05-086 08:55	3	1	127	6	11	3	8	8	6	0	1	0	0	1	0	0	0	1	4	5.18593	160.0	-13.0	3.24147	227	44	-39	28.0	1.6	$1.2 \cdot 10^{-14}$	6.0
6174	05-086 13:47	2	1	90	3	8	0	8	8	8	0	0	0	0	1	0	0	0	1	4	5.18552	160.0	-13.0	3.24309	175	319	-68	28.0	1.6	$4.5 \cdot 10^{-15}$	6.0
6175	05-089 09:46	2	2	72	8	12	0	9	10	9	0	0	0	0	1	0	0	0	1	4	5.18076	160.1	-13.1	3.26170	153	278	-55	19.3	1.6	$8.8 \cdot 10^{-14}$	6.0
6176	05-091 14:38	2	2	253	11	19	0	8	5	7	0	0	37	0	1	0	0	0	1	4	5.17721	160.1	-13.3	3.27543	48	235	41	21.4	1.9	$1.7 \cdot 10^{-13}$	10.5
6177	05-093 22:13	3	1	96	6	11	1	8	8	8	0	1	0	0	1	0	0	0	1	4	5.17321	160.1	-13.4	3.29074	188	355	-67	28.0	1.6	$1.2 \cdot 10^{-14}$	6.0
6178	05-094 00:05	2	1	160	4	8	0	8	8	8	0	0	0	0	1	0	0	0	1	4	5.17299	160.1	-13.4	3.29154	278	60	10	28.0	1.6	$5.2 \cdot 10^{-15}$	6.0
6179	05-094 20:54	2	1	185	5	10	0	7	7	7	0	0	0	0	1	0	0	0	1	4	5.17172	160.1	-13.4	3.29637	314	71	44	43.7	1.6	$1.7 \cdot 10^{-15}$	6.0
6180	05-096 05:25	2	1	201	1	5	0	15	9	10	0	0	8	22	1	0	0	0	1	4	5.16938	160.2	-13.5	3.30522	337	86	65	31.3	2.0	$1.3 \cdot 10^{-15}$	12.5
6181	05-097 04:05	2	2	7	9	4	9	9	13	0	1	1	11	21	1	0	0	0	1	4	5.16767	160.2	-13.6	3.31164	66	240	25	14.1	1.9	$7.5 \cdot 10^{-14}$	10.5
6182	05-097 14:47	3	1	150	7	12	8	7	7	6	0	1	3	21	1	0	0	0	1	4	5.16703	160.2	-13.6	3.31405	267	56	0	43.7	1.6	$3.3 \cdot 10^{-15}$	6.0
6183	05-100 15:28	2	1	24	2	7	0	15	8	10	0	0	0	0	1	0	0	0	1	4	5.16163	160.2	-13.8	3.33409	91	247	0	36.7	2.0	$1.3 \cdot 10^{-15}$	12.5
6184	05-100 20:16	2	2	234	10	9	6	8	8	0	1	1	0	0	1	0	0	0	1	4	5.16142	160.2	-13.8	3.33489	26	222	62	21.4	1.9	$4.7 \cdot 10^{-14}$	10.5
6185	05-104 17:01	3	4	40	30	49	14	7	5	5	0	1	46	0	1	0	0	0	1	4	5.15464	160.3	-14.0	3.35967	115	254	-21	14.1	1.9	$1.4 \cdot 10^{-10}$	10.5
6186	05-105 05:18	2	1	231	6	11	0	9	8	8	0	0	0	0	1	0	0	0	1	4	5.15376	160.3	-14.0	3.36286	25	218	63	22.7	1.6	$2.5 \cdot 10^{-14}$	6.0
6187	05-114 14:37	1	1	50	1	5	0	15	15	0	1	0	11	31	1	0	0	0	1	4	5.13694	160.4	-14.5	3.42242	133	261	-38	2.3	2.0	$6.1 \cdot 10^{-12}$	12.5
6188	05-116 12:48	3	2	96	12	21	1	8	6	6	0	1	39	0	1	0	0	0	1	4	5.13328	160.4	-14.6	3.43506	199	13	-61	21.4	1.9	$3.1 \cdot 10^{-13}$	10.5
6189	05-118 08:10	2	2	84	13	9	3	9	15	0	1	1	42	31	1	0	0	0	1	4	5.13005	160.4	-14.7	3.44611	183	337	-68	14.1	1.9	$3.5 \cdot 10^{-13}$	10.5
6190	05-119 14:49	1	1	161	5	3	0	8	15	0	1	0	0	0	1	0	0	0	1	4	5.12774	160.4	-14.8	3.45399	291	60	22	21.4	1.9	$7.3 \cdot 10^{-15}$	10.5
6191	05-122 09:46	2	1	185	4	9	0	8	8	8	0	0	0	0	1	0	0	0	1	4	5.12237	160.5	-14.9	3.47206	326	74	55	28.0	1.6	$6.2 \cdot 10^{-15}$	6.0
6192	05-123 05:19	3	4	7	30	49	17	8	5	5	0	1	46	0	1	0	0	0	1	4	5.12097	160.5	-15.0	3.47677	76	240	15	10.4	1.9	$3.0 \cdot 10^{-10}$	10.5
6193	05-123 07:10	2	1	50	5	4	2	9	15	0	1	1	0	0	1	0	0	0	1	4	5.12073	160.5	-15.0	3.47755	136	262	-41	14.1	1.9	$3.8 \cdot 10^{-14}$	10.5
6194	05-123 14:27	2	1	29	7	12	0	8	8	7	0	0	35	0	1	0	0	0	1	4	5.12026	160.5	-15.0	3.47912	107	249	-14	28.0	1.6	$1.7 \cdot 10^{-14}$	6.0
6195	05-123 18:00	3	1	245	7	12	11	7	8	6	0	1	0	0	1	0	0	0	1	4	5.11979	160.5	-15.0	3.48069	51	232	39	35.4	1.6	$8.1 \cdot 10^{-15}$	6.0
6196	05-123 20:44	1	1	85	3	2	0	9	15	0	1	0	0	0	1	0	0	0	1	4	5.11979	160.5	-15.0	3.48069	186	345	-67	14.1	1.9	$2.1 \cdot 10^{-14}$	10.5
6197	05-124 06:04	2	2	105	9	20	0	8	6	7	0	0	37	0	1	0	0	0	1	4	5.11885	160.5	-15.0	3.48383	214	30	-49	21.4	1.9	$1.6 \cdot 10^{-13}$	10.5
6198	05-124 20:40	3	2	26	14	21	19	8	7	6	0	1	40	0	1	0	0	0	1	4	5.11791	160.5	-15.1	3.48696	103	248	-10	21.4	1.9	$4.2 \cdot 10^{-13}$	10.5
6199	05-127 19:53	1	1	106	4	3	0	9	15	0	1	0	0	0	1	0	0	0	1	4	5.11221	160.5	-15.2	3.50574	217	32	-47	14.1	1.9	$2.8 \cdot 10^{-14}$	10.5
6200	05-128 02:41	1	1	67	2	2	0	9	15	0	1	0	0	0	1	0	0	0	1	4	5.11173	160.5	-15.2	3.50730	162	287	-61	11.8	11.8	$2.8 \cdot 10^{-14}$	5858.3
6201	05-128 14:07	2	1	72	5	3	4	9	15	0	1	1	0	0	1	0	0	0	1	4	5.11077	160.5	-15.3	3.51042	169	301	-65	14.1	1.9	$3.3 \cdot 10^{-14}$	10.5
6202	05-129 22:22	2	2	64	12	5	4	9	15	0	1	1	36	31	1	0	0	0	1	4	5.10814	160.5	-15.3	3.51900	158	282	-59	14.1	1.9	$1.4 \cdot 10^{-13}$	10.5
6203	05-130 07:30	2	2	6	9	13	0	8	8	6	0	0	34	0	1	0	0	0	1	4	5.10741	160.6	-15.4	3.52134	77	240	14	28.0	1.6	$2.8 \cdot 10^{-14}$	6.0
6204	05-137 21:14	2	2	83	10	19	0	7	7	7	0	0	37	0	1	0	0	0	1	4	5.09255	160.6	-15.8	3.56870	187	348	-67	34.1	1.9	$2.9 \cdot 10^{-14}$	10.5
6205	05-140 22:27	2	1	73	4	8	0	8	8	8	0	0	0	0	1	0	0	0	1	4	5.08660	160.7	-16.0	3.58724	174	313	-67	28.0	1.6	$5.2 \cdot 10^{-15}$	6.0
6206	05-141 01:29	3	2	66	11	20	1	7	5	7	0	1	37	0	1	0	0	0	1	4	5.08635	160.7	-16.0	3.58801	164	292	-63	34.1	1.9	$4.4 \cdot 10^{-14}$	10.5
6207	05-141 21:34	1	1	92	3	2	0	10	15	0	1	0	0	0	1	0	0	0	1	4	5.08460	160.7	-16.0	3.59341	201	15	-59	10.4	1.9	$4.4 \cdot 10^{-14}$	10.5
6208	05-144 12:30	2	2	64	8	12	0	7	8	8	0	0	0	0	1	0	0	0	1	4	5.07933	160.7	-16.2	3.60956	162	288	-62	35.4	1.6	$9.7 \cdot 10^{-15}$	6.0
6209	05-146 03:05	1	1	21	2	1	0	11	15	0	1	0	36	31	1	0	0	0	1	4	5.07604	160.7	-16.2	3.61954	102	248	-9	11.8	11.8	$2.4 \cdot 10^{-14}$	5858.3
6210	05-146 13:17	1	1	25	5	2	0	9	15	0	1	0	12	31	1	0	0	0	1	4	5.07528	160.7	-16.3	3.62184	108	249	-15	14.1	1.9	$2.9 \cdot 10^{-14}$	10.5
6211	05-146 14:21	2	2	34	10	14	0	7	8	7	0	0	35	0	1	0	0	0	1	4	5.07528	160.7	-16.3	3.62184	121	254	-27	35.4	1.6	$1.8 \cdot 10^{-14}$	6.0
6212	05-151 03:57	3	2	37	13	22	1	8	6	6	0	1	40	0	1	0	0	0	1	4	5.06582	160.8	-16.5	3.65014	126	256	-32	21.4	1.9	$4.2 \cdot 10^{-13}$	10.5
6213	05-151 08:00	2	1	53	2	7	0	15	8	11	0	0	8	21	1	0	0	0	1	4	5.06556	160.8	-16.5	3.65091	149	271	-52	36.7	2.0	$1.3 \cdot 10^{-15}$	12.5
6214	05-151 17:04	1	1	21	3	3	0	9	15	0	1	0	0	0	1	0	0	0	1	4	5.06479	160.8	-16.6	3.65319	104	248	-11	14.1	1.9	$2.4 \cdot 10^{-14}$	10.5
6215	05-151 21:37	1	1	7	1	1	0	15	15	0	1	0	0	0	1	0	0	0	1	4	5.06427	160.8	-16.6	3.65472	84	242	7	11.8	11.8	$1.9 \cdot 10^{-14}$	5858.3

No.	IMP. DATE	CLN	AR	SEC	IA	EA	CA	IT	ET	EIT	EIC	IIC	PA	PET	EVD	ICP	ECP	CCP	PCP	HV	R	LON	LAT	D_{Jup}	ROT	S_{LON}	S_{LAT}	V	VEF	M	MEF
6216	05-152 08:34	2	2	97	9	19	0	8	6	7	0	0	37	0	1	0	0	0	1	4	5.06350	160.8	-16.6	3.65701	211	27	-52	21.4	1.9	$1.2 \cdot 10^{-13}$	10.5
6217	05-152 19:34	3	2	52	12	20	2	8	5	6	0	1	38	0	1	0	0	0	1	4	5.06247	160.8	-16.6	3.66006	148	270	-51	21.4	1.9	$2.6 \cdot 10^{-13}$	10.5
6218	05-152 23:51	3	2	50	12	20	3	9	7	6	0	1	38	0	1	0	0	0	1	4	5.06221	160.8	-16.6	3.66082	145	268	-49	14.1	1.9	$1.2 \cdot 10^{-12}$	10.5
6219	05-157 23:57	3	1	66	5	9	13	7	8	7	0	1	0	0	1	0	0	0	1	4	5.05177	160.9	-16.9	3.69120	169	301	-65	35.4	1.6	$3.5 \cdot 10^{-15}$	6.0
6220	05-160 17:43	2	2	93	10	19	0	8	6	7	0	0	36	0	1	0	0	0	1	4	5.04596	160.9	-17.1	3.70785	208	24	-54	21.4	1.9	$1.5 \cdot 10^{-13}$	10.5
6221	05-164 23:25	2	2	68	14	21	0	8	5	6	0	0	40	0	1	0	0	0	1	4	5.03688	161.0	-17.3	3.73346	174	313	-67	21.4	1.9	$4.2 \cdot 10^{-13}$	10.5
6222	05-164 23:43	2	1	21	6	11	0	9	9	8	0	0	0	0	1	0	0	0	1	4	5.03688	161.0	-17.3	3.73346	108	249	-15	21.0	1.6	$3.6 \cdot 10^{-14}$	6.0
6223	05-169 11:56	3	2	52	10	14	1	9	10	8	0	1	0	0	1	0	0	0	1	4	5.02714	161.0	-17.6	3.76046	152	276	-54	19.3	1.6	$1.7 \cdot 10^{-13}$	6.0
6224	05-173 14:39	2	1	38	1	1	0	15	1	11	0	0	5	24	1	0	0	0	1	4	5.01809	161.1	-17.8	3.78508	134	261	-39	11.8	11.8	$1.9 \cdot 10^{-14}$	5858.3
6225	05-173 19:34	3	2	59	8	12	10	7	8	7	0	1	0	0	1	0	0	0	1	4	5.01754	161.1	-17.8	3.78657	163	291	-62	35.4	1.6	$9.7 \cdot 10^{-15}$	6.0
6226	05-173 23:29	2	2	19	8	12	0	7	8	7	0	0	34	0	1	0	0	0	1	4	5.01727	161.1	-17.8	3.78731	107	250	-14	35.4	1.6	$9.7 \cdot 10^{-15}$	6.0
6227	05-174 12:06	2	2	59	8	13	0	8	8	6	0	0	34	0	1	0	0	0	1	4	5.01588	161.1	-17.8	3.79103	163	292	-62	28.0	1.6	$2.4 \cdot 10^{-14}$	6.0
6228	05-175 11:05	3	2	48	13	21	1	8	6	6	0	1	39	0	1	0	0	0	1	4	5.01395	161.1	-17.9	3.79623	148	273	-51	21.4	1.9	$3.6 \cdot 10^{-13}$	10.5
6229	05-175 17:44	3	1	112	6	10	3	7	8	6	0	1	0	0	1	0	0	0	1	4	5.01339	161.1	-17.9	3.79772	238	46	-28	35.4	1.6	$4.8 \cdot 10^{-15}$	6.0
6230	05-175 22:10	2	2	72	12	20	0	7	5	6	0	0	38	0	1	0	0	0	1	4	5.01284	161.1	-17.9	3.79920	182	337	-67	34.1	1.9	$5.2 \cdot 10^{-14}$	10.5
6231	05-176 16:57	3	2	44	10	20	12	7	5	6	0	1	36	0	1	0	0	0	1	4	5.01117	161.1	-18.0	3.80365	143	268	-47	34.1	1.9	$3.8 \cdot 10^{-14}$	10.5
6232	05-176 17:16	2	1	54	3	8	0	9	8	10	0	0	0	21	1	0	0	0	1	4	5.01117	161.1	-18.0	3.80365	157	283	-58	22.7	1.6	$9.4 \cdot 10^{-15}$	6.0
6233	05-176 18:49	2	2	56	13	8	9	10	11	0	1	1	35	9	1	0	0	0	1	4	5.01089	161.1	-18.0	3.80440	160	287	-60	10.4	1.9	$6.0 \cdot 10^{-13}$	10.5
6234	05-177 01:56	3	2	4	13	21	21	8	7	6	0	1	39	0	1	0	0	0	1	4	5.01033	161.1	-18.0	3.80588	87	245	4	21.4	1.9	$3.6 \cdot 10^{-13}$	10.5
6235	05-177 06:08	3	1	63	5	9	4	7	8	8	0	1	0	0	1	0	0	0	1	4	5.00977	161.1	-18.0	3.80736	170	305	-65	35.4	1.6	$3.5 \cdot 10^{-15}$	6.0
6236	05-178 21:22	3	2	39	9	13	4	9	9	7	0	1	0	0	1	0	0	0	1	4	5.00614	161.2	-18.1	3.81699	137	264	-41	21.0	1.6	$8.3 \cdot 10^{-14}$	6.0
6237	05-184 03:54	2	1	238	3	9	0	9	8	9	0	0	0	0	1	0	0	0	1	4	4.99428	161.2	-18.4	3.84796	59	238	31	22.7	1.6	$1.1 \cdot 10^{-14}$	6.0
6238	05-186 01:59	1	1	65	7	4	0	11	15	0	1	0	40	31	1	0	0	0	1	4	4.99000	161.2	-18.5	3.85897	176	321	-67	7.8	1.9	$2.4 \cdot 10^{-13}$	10.5
6239	05-186 17:18	2	1	250	5	3	8	9	15	0	1	1	0	0	1	0	0	0	1	4	4.98857	161.3	-18.5	3.86264	76	243	14	14.1	1.9	$3.3 \cdot 10^{-14}$	10.5
6240	05-189 06:06	2	1	167	7	14	0	7	7	7	0	0	36	0	1	0	0	0	1	4	4.98253	161.3	-18.7	3.87800	321	75	50	34.1	1.9	$1.3 \cdot 10^{-14}$	10.5
6241	05-189 17:19	2	1	40	5	8	3	11	15	0	1	1	1	31	1	0	0	0	1	4	4.98166	161.3	-18.7	3.88019	143	270	-46	4.2	1.6	$2.4 \cdot 10^{-12}$	6.0
6242	05-190 20:37	3	2	29	11	20	1	8	5	6	0	1	37	0	1	0	0	0	1	4	4.97905	161.3	-18.8	3.88676	128	261	-33	21.4	1.9	$2.2 \cdot 10^{-13}$	10.5
6243	05-192 03:33	3	3	63	19	24	1	6	6	6	0	1	43	0	1	0	0	0	1	4	4.97586	161.3	-18.9	3.89477	176	322	-67	28.0	1.6	$3.8 \cdot 10^{-13}$	6.0
6244	05-197 12:28	3	3	40	23	28	8	6	5	5	0	1	46	0	1	0	0	0	1	4	4.96324	161.4	-19.2	3.92597	146	274	-49	34.6	1.6	$8.3 \cdot 10^{-13}$	6.0
6245	05-197 19:36	2	1	62	5	4	2	9	15	0	1	1	0	0	1	0	0	0	1	4	4.96265	161.4	-19.2	3.92742	177	326	-67	14.1	1.9	$3.8 \cdot 10^{-14}$	10.5
6246	05-199 20:21	2	2	73	8	20	0	9	4	9	0	0	39	0	1	0	0	0	1	4	4.95790	161.4	-19.3	3.93897	193	6	-63	14.1	1.9	$6.5 \cdot 10^{-13}$	10.5
6247	05-201 14:07	3	3	234	19	23	3	6	6	6	0	1	42	0	1	0	0	0	1	4	4.95373	161.4	-19.4	3.94905	61	241	29	28.0	1.6	$3.3 \cdot 10^{-13}$	6.0
6248	05-201 18:03	2	2	84	11	20	0	7	5	6	0	0	37	0	0	0	0	0	1	4	4.95313	161.4	-19.4	3.95048	211	31	-52	34.1	1.9	$4.4 \cdot 10^{-14}$	10.5
6249	05-204 13:40	1	1	36	3	1	0	9	15	0	1	0	0	0	1	0	0	0	1	4	4.94652	161.5	-19.6	3.96628	144	273	-47	14.1	1.9	$1.8 \cdot 10^{-14}$	10.5
6250	05-206 08:15	3	2	15	8	13	20	7	8	6	0	1	0	0	1	0	0	0	1	4	4.94229	161.5	-19.7	3.97630	117	259	-23	35.4	1.6	$1.1 \cdot 10^{-14}$	6.0
6251	05-208 10:23	2	2	27	9	13	0	8	8	8	0	0	35	0	1	0	0	0	1	4	4.93712	161.5	-19.8	3.98843	134	267	-39	28.0	1.6	$2.8 \cdot 10^{-14}$	6.0
6252	05-208 20:15	2	1	37	7	12	0	7	8	7	0	0	0	0	1	0	0	0	1	4	4.93621	161.5	-19.8	3.99057	149	278	-51	35.4	1.6	$8.1 \cdot 10^{-15}$	6.0
6253	05-209 02:16	3	2	4	10	20	12	8	6	6	0	1	36	0	1	0	0	0	1	4	4.93560	161.5	-19.8	3.99199	102	254	-9	21.4	1.9	$1.9 \cdot 10^{-13}$	10.5
6254	05-209 08:06	1	1	124	3	3	0	9	15	0	1	0	35	31	1	0	0	0	1	4	4.93499	161.5	-19.9	3.99342	271	61	3	14.1	1.9	$2.4 \cdot 10^{-14}$	10.5
6255	05-209 15:45	2	1	31	7	3	2	8	15	0	1	1	0	0	1	0	0	0	1	4	4.93407	161.6	-19.9	3.99555	141	271	-44	21.4	1.9	$1.0 \cdot 10^{-14}$	10.5
6256	05-209 22:02	2	2	224	8	5	7	10	13	0	1	1	10	18	1	0	0	0	1	4	4.93346	161.6	-19.9	3.99698	52	238	38	10.4	1.9	$1.6 \cdot 10^{-13}$	10.5
6257	05-210 08:54	3	2	23	11	20	11	8	6	6	0	1	37	0	1	0	0	0	1	4	4.93254	161.6	-19.9	3.99911	130	264	-35	21.4	1.9	$2.2 \cdot 10^{-13}$	10.5
6258	05-210 11:08	3	2	34	14	22	9	7	5	6	0	1	40	0	1	0	0	0	1	4	4.93224	161.6	-19.9	3.99982	145	275	-48	34.1	1.9	$9.7 \cdot 10^{-14}$	10.5
6259	05-211 09:50	3	3	21	21	25	18	7	8	6	0	1	43	0	1	0	0	0	1	4	4.92978	161.6	-20.0	4.00551	129	265	-34	19.3	1.6	$3.0 \cdot 10^{-12}$	6.0
6260	05-211 17:32	2	1	26	7	5	10	9	13	0	1	1	0	0	1	0	0	0	1	4	4.92917	161.6	-20.0	4.00693	136	269	-40	14.1	1.9	$6.4 \cdot 10^{-14}$	10.5
6261	05-211 22:26	2	1	186	6	11	0	8	8	7	0	0	0	0	1	0	0	0	1	4	4.92855	161.6	-20.0	4.00835	1	162	78	28.0	1.6	$1.2 \cdot 10^{-14}$	6.0
6262	05-212 16:59	3	1	119	7	11	3	7	8	6	0	1	0	0	1	0	0	0	1	4	4.92670	161.6	-20.1	4.01260	267	60	0	35.4	1.6	$6.9 \cdot 10^{-15}$	6.0
6263	05-215 13:25	1	1	190	6	6	0	9	15	0	1	0	0	0	1	0	0	0	1	4	4.91958	161.6	-20.2	4.02887	11	198	74	14.1	1.9	$6.3 \cdot 10^{-14}$	10.5
6264	05-215 13:30	2	3	70	21	21	22	12	9	0	1	1	23	14	1	0	0	0	1	4	4.91958	161.6	-20.2	4.02887	202	23	-58	2.0	1.9	$2.3 \cdot 10^{-09}$	10.5
6265	05-216 05:04	3	3	75	19	23	1	6	6	6	0	1	41	0	1	0	0	0	1	4	4.91803	161.6	-20.3	4.03240	209	32	-53	28.0	1.6	$3.3 \cdot 10^{-13}$	6.0
6266	05-216 23:05	3	1	23	7	12	2	9	10	9	0	1	3	21	1	0	0	0	1	4	4.91616	161.7	-20.3	4.03663	136	270	-41	19.3	1.6	$7.3 \cdot 10^{-14}$	6.0
6267	05-217 08:18	3	2	7	11	19	1	7	5	6	0	1	37	0	1	0	0	0	1	4	4.91522	161.7	-20.3	4.03874	114	259	-20	34.1	1.9	$3.3 \cdot 10^{-14}$	10.5
6268	05-219 23:17	3	3	34	20	24	6	5	5	6	0	1	43	0	1	0	0	0	1	4	4.90864	161.7	-20.5	4.05351	156	289	-57	43.7	1.6	$9.8 \cdot 10^{-14}$	6.0
6269	05-220 18:31	3	2	48	12	20	21	7	5	6	0	1	38	0	1	0	0	0	1	4	4.90644	161.7	-20.5	4.05842	176	328	-66	34.1	1.9	$5.2 \cdot 10^{-14}$	10.5
6270	05-223 21:13	3	2	18	11	20	13	7	5	6	0	1	38	0	1	0	0	0	1	4	4.89853	161.7	-20.7	4.07591	139	274	-43	34.1	1.9	$4.4 \cdot 10^{-14}$	10.5

No.	IMP. DATE	CLN	AR	SEC	IA	EA	CA	IT	ET	EIT	EIC	IIC	PA	PET	EVD	ICP	ECP	CCP	PCP	HV	R	LON	LAT	D_{Jup}	ROT	S_{LON}	S_{LAT}	V	VEF	M	MEF
6271	05-224 03:53	1	1	76	2	4	0	11	15	0	1	0	8	31	1	0	0	0	1	4	4.89789	161.8	-20.7	4.07730	221	43	-43	11.8	11.8	$3.6 \cdot 10^{-14}$	5858.3
6272	05-225 20:41	3	3	27	20	24	1	5	5	6	0	1	44	0	1	0	0	0	1	4	4.89375	161.8	-20.8	4.08636	153	285	-54	43.7	1.6	$9.8 \cdot 10^{-14}$	6.0
6273	05-226 03:58	3	3	25	19	23	5	6	7	6	0	1	41	0	1	0	0	0	1	4	4.89279	161.8	-20.9	4.08845	150	283	-52	25.9	1.6	$4.3 \cdot 10^{-13}$	6.0
6274	05-226 13:00	3	3	230	22	29	11	6	3	5	0	1	46	0	1	0	0	0	1	4	4.89183	161.8	-20.9	4.09054	78	249	12	21.4	1.9	$4.4 \cdot 10^{-12}$	10.5
6275	05-226 18:20	1	1	206	5	5	0	10	15	0	1	0	13	31	1	0	0	0	1	4	4.89119	161.8	-20.9	4.09193	45	238	44	10.4	1.9	$9.3 \cdot 10^{-14}$	10.5
6276	05-226 19:20	2	2	3	9	3	5	9	15	0	1	1	0	0	1	0	0	0	1	4	4.89119	161.8	-20.9	4.09193	119	263	-25	14.1	1.9	$6.6 \cdot 10^{-14}$	10.5
6277	05-227 18:13	2	1	52	5	1	6	9	13	0	1	1	0	0	1	0	0	0	1	4	4.88863	161.8	-21.0	4.09748	189	360	-65	14.1	1.9	$2.5 \cdot 10^{-14}$	10.5
6278	05-228 19:33	2	1	246	4	1	3	9	15	15	0	1	0	0	1	0	0	0	1	4	4.88606	161.8	-21.0	4.10303	107	259	-13	14.1	1.9	$2.1 \cdot 10^{-14}$	10.5
6279	05-228 22:34	2	1	53	2	5	0	15	9	10	0	0	0	0	1	0	0	0	1	4	4.88573	161.8	-21.0	4.10372	195	14	-62	31.3	2.0	$1.6 \cdot 10^{-15}$	12.5
6280	05-229 08:28	1	2	239	13	14	0	12	15	0	1	0	24	31	1	0	0	0	1	4	4.88477	161.8	-21.1	4.10580	97	256	-4	5.0	1.9	$1.4 \cdot 10^{-11}$	10.5
6281	05-229 15:08	3	2	247	14	21	14	9	9	7	0	1	39	0	1	0	0	0	1	4	4.88380	161.8	-21.1	4.10788	108	259	-15	14.1	1.9	$1.9 \cdot 10^{-12}$	10.5
6282	05-229 15:23	3	2	245	10	20	1	7	6	6	0	1	36	0	1	0	0	0	1	4	4.88380	161.8	-21.1	4.10788	106	258	-12	34.1	1.9	$3.8 \cdot 10^{-14}$	10.5
6283	05-231 03:05	3	2	251	9	14	4	8	8	6	0	1	36	0	1	0	0	0	1	4	4.87992	161.8	-21.2	4.11618	115	262	-21	28.0	1.6	$3.3 \cdot 10^{-14}$	6.0
6284	05-232 23:06	3	2	249	14	22	4	7	6	6	0	1	41	0	1	0	0	0	1	4	4.87537	161.9	-21.3	4.12584	119	264	-25	34.1	1.9	$9.7 \cdot 10^{-14}$	10.5
6285	05-233 17:50	3	2	43	9	13	2	9	9	8	0	1	0	0	1	0	0	0	1	4	4.87342	161.9	-21.3	4.12997	190	3	-64	21.0	1.6	$8.3 \cdot 10^{-14}$	6.0
6286	05-235 04:56	2	1	5	7	11	0	8	8	7	0	0	0	0	1	0	0	0	1	4	4.86950	161.9	-21.4	4.13822	137	274	-41	28.0	1.6	$1.5 \cdot 10^{-14}$	6.0
6287	05-235 20:36	1	1	58	4	1	0	10	15	0	1	0	0	0	1	0	0	0	1	4	4.86786	161.9	-21.4	4.14165	211	36	-51	10.4	1.9	$4.3 \cdot 10^{-14}$	10.5
6288	05-238 01:14	3	2	253	11	20	1	8	5	7	0	1	37	0	1	0	0	0	1	4	4.86194	161.9	-21.6	4.15398	133	272	-38	21.4	1.9	$2.2 \cdot 10^{-13}$	10.5
6289	05-240 14:27	3	3	28	19	23	1	6	5	6	0	1	41	0	1	0	0	0	1	4	4.85533	162.0	-21.7	4.16763	177	334	-66	34.6	1.6	$1.7 \cdot 10^{-13}$	6.0
6290	05-243 09:49	2	1	233	6	11	0	7	7	8	0	0	0	0	1	0	0	0	1	4	4.84766	162.0	-21.9	4.18327	116	265	-22	43.7	1.6	$2.3 \cdot 10^{-15}$	6.0
6291	05-244 00:30	2	1	157	4	8	0	8	8	8	0	0	0	0	1	0	0	0	1	4	4.84599	162.0	-21.9	4.18666	9	196	74	28.0	1.6	$5.2 \cdot 10^{-15}$	6.0
6292	05-244 07:08	3	4	25	27	49	28	8	8	5	0	1	46	0	1	0	0	0	1	4	4.84532	162.0	-22.0	4.18801	183	349	-66	10.4	1.9	$1.9 \cdot 10^{-10}$	10.5
6293	05-246 17:55	3	3	24	19	25	1	6	5	6	0	1	44	0	1	0	0	0	1	4	4.83893	162.1	-22.1	4.20086	191	8	-63	34.6	1.6	$2.3 \cdot 10^{-13}$	6.0
6294	05-246 20:27	2	1	191	2	6	0	9	7	10	0	0	3	21	1	0	0	0	1	4	4.83860	162.1	-22.1	4.20153	66	249	24	56.0	2.0	$1.8 \cdot 10^{-16}$	12.5
6295	05-249 07:11	3	2	137	9	14	1	8	8	6	0	1	36	0	1	0	0	0	1	4	4.83183	162.1	-22.3	4.21500	1	165	76	28.0	1.6	$3.3 \cdot 10^{-14}$	6.0
6296	05-250 17:23	2	2	0	8	6	5	8	15	0	1	1	0	0	1	0	0	0	1	4	4.82809	162.1	-22.3	4.22239	167	314	-62	21.4	1.9	$2.0 \cdot 10^{-14}$	10.5
6297	05-253 04:35	2	2	252	11	20	0	7	5	7	0	0	38	0	1	0	0	0	1	4	4.82126	162.2	-22.5	4.23578	171	323	-64	34.1	1.9	$4.4 \cdot 10^{-14}$	10.5
6298	05-253 12:40	3	2	240	14	21	7	8	6	6	0	1	39	0	1	0	0	0	1	4	4.82023	162.2	-22.5	4.23778	154	294	-54	21.4	1.9	$4.2 \cdot 10^{-13}$	10.5
6299	05-254 21:23	3	3	194	19	22	7	7	6	6	0	1	41	0	1	0	0	0	1	4	4.81645	162.2	-22.6	4.24512	89	258	2	22.7	1.6	$5.8 \cdot 10^{-13}$	6.0
6300	05-255 14:08	3	2	5	14	22	22	7	5	6	0	1	40	0	1	0	0	0	1	4	4.81472	162.2	-22.7	4.24845	183	351	-65	34.1	1.9	$9.7 \cdot 10^{-14}$	10.5
6301	05-255 19:29	3	2	209	14	21	2	7	5	6	0	1	39	0	1	0	0	0	1	4	4.81403	162.2	-22.7	4.24978	110	265	-16	34.1	1.9	$8.3 \cdot 10^{-14}$	10.5
6302	05-255 21:02	1	1	163	4	2	0	9	15	0	1	0	2	21	1	0	0	0	1	4	4.81369	162.2	-22.7	4.25045	45	242	44	14.1	1.9	$2.5 \cdot 10^{-14}$	10.5
6303	05-255 22:30	1	1	245	3	10	0	14	15	0	1	0	58	31	1	0	0	0	1	4	4.81369	162.2	-22.7	4.25045	160	302	-58	2.0	1.9	$3.9 \cdot 10^{-11}$	10.5
6304	05-256 11:26	3	3	227	19	23	23	7	6	6	0	1	41	0	1	0	0	0	1	4	4.81231	162.2	-22.7	4.25311	135	277	-39	22.7	1.6	$6.8 \cdot 10^{-13}$	6.0
6305	05-256 23:37	3	3	218	19	25	8	7	7	6	0	1	43	0	1	0	0	0	1	4	4.81093	162.2	-22.7	4.25576	130	275	-34	21.0	1.6	$1.3 \cdot 10^{-12}$	6.0
6306	05-260 20:31	3	3	208	20	26	13	5	6	5	0	1	44	0	1	0	0	0	1	4	4.80015	162.3	-23.0	4.27629	122	271	-27	35.4	1.6	$3.3 \cdot 10^{-13}$	6.0
6307	05-267 02:36	2	3	230	21	26	12	5	5	5	0	1	44	0	1	0	0	0	1	4	4.78255	162.4	-23.4	4.30913	164	311	-60	43.7	1.6	$1.6 \cdot 10^{-13}$	6.0
6308	05-270 06:15	2	1	161	6	11	0	8	8	7	0	0	0	0	1	0	0	0	1	4	4.77329	162.4	-23.6	4.32607	72	255	19	28.0	1.6	$1.2 \cdot 10^{-14}$	6.0
6309	05-272 18:16	3	3	199	19	23	3	5	6	6	0	1	42	0	1	0	0	0	1	4	4.76611	162.5	-23.7	4.33904	124	275	-29	35.4	1.6	$1.5 \cdot 10^{-13}$	6.0
6310	05-274 00:02	2	1	162	3	7	1	13	15	0	1	1	42	31	1	0	0	0	1	4	4.76251	162.5	-23.8	4.34551	77	257	14	2.4	1.6	$1.1 \cdot 10^{-11}$	6.0
6311	05-276 19:00	3	3	185	20	25	13	7	8	6	0	1	43	0	1	0	0	0	1	4	4.75454	162.5	-24.0	4.35968	113	271	-18	19.3	1.6	$2.5 \cdot 10^{-12}$	6.0
6312	05-276 23:19	3	2	220	15	23	7	8	7	6	0	1	41	0	1	0	0	0	1	4	4.75418	162.5	-24.0	4.36032	162	311	-58	21.4	1.9	$6.4 \cdot 10^{-13}$	10.5
6313	05-282 13:17	3	3	132	21	29	2	7	3	6	0	1	46	0	1	0	0	0	1	4	4.73772	162.6	-24.3	4.38910	40	242	48	14.1	1.9	$1.7 \cdot 10^{-11}$	10.5
6314	05-283 22:28	2	1	164	4	1	8	10	15	15	0	1	4	21	1	0	0	0	1	4	4.73366	162.6	-24.4	4.39609	89	263	2	10.4	1.9	$4.3 \cdot 10^{-14}$	10.5
6315	05-284 14:06	2	2	172	12	21	0	8	5	6	0	0	44	0	1	0	0	0	1	4	4.73181	162.6	-24.5	4.39926	100	267	-7	21.4	1.9	$3.1 \cdot 10^{-13}$	10.5
6316	05-289 00:07	3	3	212	19	23	10	7	6	6	0	1	41	0	1	0	0	0	1	4	4.71842	162.7	-24.8	4.42200	160	312	-56	22.7	1.6	$6.8 \cdot 10^{-13}$	6.0
6317	05-289 00:41	2	2	126	9	5	11	9	15	0	1	1	0	0	1	0	0	0	1	4	4.71842	162.7	-24.8	4.42200	40	243	48	14.1	1.9	$8.9 \cdot 10^{-14}$	10.5
6318	05-289 23:58	2	2	209	13	21	0	8	6	6	0	0	39	0	1	0	0	0	1	4	4.71580	162.7	-24.8	4.42639	156	305	-54	21.4	1.9	$3.6 \cdot 10^{-13}$	10.5
6319	05-290 02:27	2	1	199	7	7	9	10	15	0	1	1	0	0	1	0	0	0	1	4	4.71542	162.7	-24.8	4.42702	142	291	-43	10.4	1.9	$1.9 \cdot 10^{-13}$	10.5
6320	05-290 14:30	3	3	227	19	22	2	8	6	6	0	1	42	0	1	0	0	0	1	4	4.71392	162.7	-24.9	4.42953	181	352	-63	19.5	1.6	$1.1 \cdot 10^{-12}$	6.0
6321	05-291 19:17	2	2	225	10	6	2	9	15	0	1	1	0	0	1	0	0	0	1	4	4.71016	162.7	-24.9	4.43580	182	355	-62	14.1	1.9	$1.3 \cdot 10^{-13}$	10.5
6322	05-293 12:50	2	2	249	14	22	0	8	5	6	0	0	42	0	1	0	0	0	1	4	4.70488	162.8	-25.1	4.44455	215	47	-46	21.4	1.9	$5.0 \cdot 10^{-13}$	10.5
6323	05-295 05:39	3	2	203	14	21	8	9	9	6	0	1	40	0	1	0	0	0	1	4	4.69996	162.8	-25.2	4.45264	149	299	-49	14.1	1.9	$1.9 \cdot 10^{-12}$	10.5
6324	05-295 09:41	1	1	170	7	1	0	7	15	0	1	0	42	31	1	0	0	0	1	4	4.69920	162.8	-25.2	4.45389	103	270	-9	34.1	1.9	$1.5 \cdot 10^{-15}$	10.5
6325	05-300 12:04	3	2	183	12	20	6	8	6	6	0	1	37	0	1	0	0	0	1	4	4.68354	162.9	-25.5	4.47926	126	283	-30	21.4	1.9	$2.6 \cdot 10^{-13}$	10.5

No.	IMP. DATE	CLN	AR	SEC	IA	EA	CA	IT	ET	EIT	EIC	IIC	PA	PET	EVD	ICP	ECP	CCP	PCP	HV	R	LON	LAT	D_{Jup}	ROT	S_{LON}	S_{LAT}	V	VEF	M	MEF
6326	05-301 06:10	3	3	187	21	25	8	5	5	6	0	1	44	0	1	0	0	0	1	4	4.68123	162.9	-25.6	4.48295	132	286	-34	43.7	1.6	$1.4 \cdot 10^{-13}$	6.0
6327	05-301 14:22	2	1	7	3	8	0	9	8	9	0	0	0	0	1	0	0	0	1	4	4.68046	162.9	-25.6	4.48418	238	64	-26	22.7	1.6	$9.4 \cdot 10^{-15}$	6.0
6328	05-307 08:03	2	1	155	3	7	0	9	8	9	0	0	0	0	1	0	0	0	1	4	4.66263	163.0	-26.0	4.51229	84	264	7	22.7	1.6	$7.8 \cdot 10^{-15}$	6.0
6329	05-308 03:39	3	2	210	13	21	20	7	5	6	0	1	39	0	1	0	0	0	1	4	4.65990	163.0	-26.0	4.51655	168	330	-58	34.1	1.9	$7.1 \cdot 10^{-14}$	10.5
6330	05-308 14:42	3	2	218	12	21	1	8	7	6	0	1	38	0	1	0	0	0	1	4	4.65872	163.0	-26.0	4.51837	179	352	-61	21.4	1.9	$3.1 \cdot 10^{-13}$	10.5
6331	05-310 21:22	3	2	191	13	21	10	9	9	6	0	1	38	0	1	0	0	0	1	4	4.65127	163.1	-26.2	4.52986	140	295	-41	14.1	1.9	$1.7 \cdot 10^{-12}$	10.5
6332	05-310 21:37	2	2	94	9	14	0	8	8	6	0	0	36	0	1	0	0	0	1	4	4.65127	163.1	-26.2	4.52986	4	186	71	28.0	1.6	$3.3 \cdot 10^{-14}$	6.0
6333	05-312 05:11	2	2	216	10	8	9	9	15	0	1	1	0	0	1	0	0	0	1	4	4.64733	163.1	-26.3	4.53589	179	352	-60	14.1	1.9	$1.8 \cdot 10^{-13}$	10.5
6334	05-314 15:17	3	2	156	13	22	5	8	6	7	0	1	40	0	1	0	0	0	0	5	4.63941	163.1	-26.4	4.54790	94	270	0	21.4	1.9	$4.2 \cdot 10^{-13}$	10.5
6335	05-318 21:22	3	3	150	19	23	12	7	9	6	0	1	41	0	1	0	0	0	1	4	4.62586	163.2	-26.7	4.56819	88	269	4	16.9	1.6	$2.3 \cdot 10^{-12}$	6.0
6336	05-323 02:13	1	1	206	3	4	0	11	15	0	1	0	18	30	1	0	0	0	1	4	4.61257	163.3	-27.0	4.58770	169	335	-57	7.8	1.9	$1.2 \cdot 10^{-13}$	10.5
6337	05-323 08:49	1	1	104	1	2	0	15	15	0	1	0	0	0	1	0	0	0	1	4	4.61176	163.3	-27.0	4.58888	26	230	58	11.8	11.8	$2.3 \cdot 10^{-14}$	5858.3
6338	05-330 12:19	1	1	215	6	3	0	9	15	0	1	0	0	0	1	0	0	0	1	4	4.58811	163.4	-27.5	4.62277	183	2	-58	14.1	1.9	$3.9 \cdot 10^{-14}$	10.5
6339	05-332 22:39	2	2	128	11	9	7	6	15	0	1	1	39	31	1	0	0	0	1	4	4.58027	163.4	-27.7	4.63376	60	257	29	43.5	1.9	$3.9 \cdot 10^{-15}$	10.5
6340	05-336 10:51	3	4	161	24	31	12	8	6	5	0	1	46	0	1	0	0	0	1	4	4.56865	163.5	-27.9	4.64985	109	280	-14	10.4	1.9	$7.5 \cdot 10^{-11}$	10.5
6341	05-337 10:38	3	2	168	11	20	9	9	8	7	0	1	36	0	1	0	0	0	1	4	4.56532	163.5	-28.0	4.65443	119	286	-22	14.1	1.9	$1.0 \cdot 10^{-12}$	10.5
6342	05-337 21:40	3	2	154	14	20	14	9	11	7	0	1	38	0	1	0	0	0	1	4	4.56365	163.5	-28.0	4.65671	99	275	-5	10.4	1.6	$3.4 \cdot 10^{-12}$	6.0
6343	05-352 18:12	1	1	189	1	1	0	15	15	0	1	0	4	21	1	0	0	0	1	4	4.51310	163.8	-29.0	4.72350	154	317	-47	11.8	11.8	$1.9 \cdot 10^{-14}$	5858.3
6344	05-354 00:23	3	3	156	19	23	8	6	6	6	0	1	42	0	1	0	0	0	1	4	4.50878	163.8	-29.1	4.72901	107	281	-11	28.0	1.6	$3.3 \cdot 10^{-13}$	6.0
6345	05-364 06:07	2	2	200	9	6	2	9	15	0	1	1	0	0	1	0	0	0	1	4	4.47290	164.0	-29.9	4.77357	178	355	-52	14.1	1.9	$1.1 \cdot 10^{-13}$	10.5
6346	06-001 17:36	3	2	152	13	20	14	9	8	6	0	1	37	0	1	0	0	0	1	4	4.46448	164.1	-30.0	4.78374	110	283	-13	14.1	1.9	$1.4 \cdot 10^{-12}$	10.5
6347	06-002 08:42	2	1	118	1	6	0	15	9	11	0	0	0	0	1	0	0	0	1	4	4.46225	164.1	-30.1	4.78641	62	257	27	31.3	2.0	$1.5 \cdot 10^{-15}$	12.5
6348	06-005 07:11	3	3	136	19	23	6	6	6	6	0	1	41	0	1	0	0	0	1	4	4.45154	164.1	-30.3	4.79915	91	273	2	28.0	1.6	$3.3 \cdot 10^{-13}$	6.0
6349	06-005 08:33	2	1	156	4	6	4	11	15	0	1	1	38	31	0	0	0	0	1	4	4.45154	164.1	-30.3	4.79915	119	290	-20	4.2	1.6	$1.4 \cdot 10^{-12}$	6.0
6350	06-007 05:26	2	2	123	10	14	9	10	15	0	1	1	46	31	1	0	0	0	1	4	4.44480	164.2	-30.4	4.80707	72	263	18	4.9	1.7	$9.6 \cdot 10^{-12}$	7.7
6351	06-009 06:00	3	2	181	13	20	9	8	6	6	0	1	39	0	1	0	0	0	1	4	4.43714	164.2	-30.6	4.81599	153	320	-43	21.4	1.9	$3.1 \cdot 10^{-13}$	10.5
6352	06-013 19:03	3	2	164	13	19	10	9	9	8	0	1	36	0	1	0	0	0	1	4	4.42080	164.3	-30.9	4.83473	134	301	-31	16.9	1.6	$6.1 \cdot 10^{-13}$	6.0
6353	06-016 15:04	1	2	160	8	5	0	8	15	0	1	0	0	0	1	0	0	0	1	4	4.41029	164.4	-31.1	4.84658	134	301	-30	21.4	1.9	$1.7 \cdot 10^{-14}$	10.5
6354	06-017 06:04	3	1	254	3	8	13	8	8	9	0	1	0	0	1	0	0	0	1	4	4.40799	164.4	-31.2	4.84915	266	81	0	28.0	1.6	$4.5 \cdot 10^{-15}$	6.0
6355	06-018 04:42	2	2	182	8	8	4	8	15	0	1	1	4	21	1	0	0	0	1	4	4.40477	164.4	-31.2	4.85273	165	335	-46	21.4	1.9	$2.9 \cdot 10^{-14}$	10.5
6356	06-019 07:32	3	2	118	13	20	11	7	6	6	0	1	39	0	1	0	0	0	1	4	4.40063	164.4	-31.3	4.85733	74	262	16	34.1	1.9	$6.1 \cdot 10^{-14}$	10.5
6357	06-020 03:05	1	1	206	5	2	0	10	15	0	1	0	34	31	1	0	0	0	1	4	4.39740	164.4	-31.4	4.86090	198	24	-45	10.4	1.9	$6.1 \cdot 10^{-14}$	10.5
6358	06-026 14:41	1	1	114	3	11	0	13	15	0	1	0	45	31	1	0	0	0	1	4	4.37368	164.6	-31.8	4.88662	80	264	11	2.5	1.9	$1.8 \cdot 10^{-11}$	10.5
6359	06-028 18:17	2	2	120	8	3	6	10	15	0	1	1	35	31	1	0	0	0	1	4	4.36524	164.6	-32.0	4.89559	88	269	5	10.4	1.9	$1.2 \cdot 10^{-13}$	10.5
6360	06-030 01:25	3	3	147	23	30	26	8	5	5	0	1	46	0	1	0	0	0	1	4	4.36053	164.6	-32.1	4.90055	126	294	-23	10.4	1.9	$5.8 \cdot 10^{-11}$	10.5
6361	06-030 23:04	1	1	98	6	9	0	11	15	0	1	0	14	31	1	0	0	0	1	4	4.35723	164.6	-32.2	4.90402	57	248	29	4.2	1.6	$3.3 \cdot 10^{-12}$	6.0
6362	06-032 08:21	3	2	136	13	21	1	8	6	6	0	1	39	0	1	0	0	0	1	4	4.35202	164.7	-32.3	4.90944	110	282	-11	21.4	1.9	$3.6 \cdot 10^{-13}$	10.5
6363	06-033 13:06	2	2	114	9	14	0	8	8	7	0	0	36	0	1	0	0	0	1	4	4.34728	164.7	-32.4	4.91435	87	267	5	28.0	1.6	$3.3 \cdot 10^{-14}$	6.0
6364	06-033 15:24	2	1	176	3	8	0	8	8	9	0	0	0	0	1	0	0	0	1	4	4.34681	164.7	-32.4	4.91484	175	347	-45	28.0	1.6	$4.5 \cdot 10^{-15}$	6.0
6365	06-034 15:58	3	2	138	15	22	1	8	6	6	0	1	41	0	1	0	0	0	1	4	4.34301	164.7	-32.5	4.91875	121	289	-19	21.4	1.9	$5.4 \cdot 10^{-13}$	10.5
6366	06-035 15:36	2	2	120	10	14	8	8	8	6	0	1	34	0	1	0	0	0	1	4	4.33920	164.7	-32.5	4.92266	95	272	0	28.0	1.6	$3.9 \cdot 10^{-14}$	6.0
6367	06-041 14:21	3	2	135	13	21	11	7	6	6	0	1	40	0	1	0	0	0	1	4	4.31665	164.9	-33.0	4.94537	122	290	-20	34.1	1.9	$7.1 \cdot 10^{-14}$	10.5
6368	06-043 03:59	1	1	186	1	1	0	15	15	0	1	0	0	0	1	0	0	0	1	4	4.31037	164.9	-33.1	4.95158	203	23	-38	11.8	11.8	$1.9 \cdot 10^{-14}$	5858.3
6369	06-043 19:53	3	3	143	21	25	26	5	5	5	0	1	44	0	1	0	0	0	1	4	4.30795	164.9	-33.2	4.95396	142	306	-32	43.7	1.6	$1.4 \cdot 10^{-13}$	6.0
6370	06-048 15:51	3	2	151	14	22	25	7	5	6	0	1	41	0	1	0	0	0	1	4	4.28895	165.0	-33.5	4.97238	162	327	-39	34.1	1.9	$9.7 \cdot 10^{-14}$	10.5
6371	06-049 00:07	2	1	44	4	8	0	8	9	8	0	0	0	0	1	0	0	0	1	4	4.28749	165.0	-33.6	4.97378	11	189	52	25.9	1.6	$6.9 \cdot 10^{-15}$	6.0
6372	06-052 22:35	2	1	55	5	9	0	7	8	8	0	0	0	0	1	0	0	0	1	4	4.27224	165.1	-33.9	4.98821	35	219	41	35.4	1.6	$3.5 \cdot 10^{-15}$	6.0
6373	06-053 16:07	3	3	123	19	23	14	6	8	6	0	1	41	0	1	0	0	0	1	4	4.26928	165.2	-33.9	4.99099	130	293	-24	23.8	1.6	$5.8 \cdot 10^{-13}$	6.0
6374	06-055 20:22	1	1	185	2	2	0	15	15	0	1	0	7	20	1	0	0	0	1	4	4.26086	165.2	-34.1	4.99881	218	35	-30	11.8	11.8	$2.8 \cdot 10^{-14}$	5858.3
6375	06-056 08:25	2	1	117	3	8	0	8	7	9	0	0	0	0	1	0	0	0	1	4	4.25887	165.2	-34.1	5.00064	130	292	-23	34.6	1.6	$2.3 \cdot 10^{-15}$	6.0
6376	06-063 10:15	2	2	140	14	10	12	10	15	0	1	1	39	31	1	0	0	0	1	4	4.23035	165.4	-34.7	5.02643	170	334	-39	10.4	1.9	$10.0 \cdot 10^{-13}$	10.5
6377	06-064 09:03	3	3	73	23	30	9	6	4	5	0	1	46	0	1	0	0	0	1	4	4.22632	165.4	-34.8	5.03001	76	251	14	21.4	1.9	$6.1 \cdot 10^{-12}$	10.5
6378	06-070 00:28	1	1	183	4	2	0	12	15	0	1	0	11	31	1	0	0	0	1	4	4.20348	165.5	-35.2	5.04988	242	51	-15	5.0	1.9	$4.6 \cdot 10^{-13}$	10.5
6379	06-077 16:49	2	1	72	5	9	0	8	8	7	0	0	0	0	1	0	0	0	1	4	4.17211	165.7	-35.8	5.07622	104	265	-5	28.0	1.6	$7.4 \cdot 10^{-15}$	6.0
6380	06-078 05:59	3	3	77	20	26	6	5	6	6	0	1	45	0	1	0	0	0	1	4	4.17004	165.7	-35.9	5.07792	111	270	-10	35.4	1.6	$3.3 \cdot 10^{-13}$	6.0

No.	IMP. DATE	CLN	AR	SEC	IA	EA	CA	IT	ET	EIT	EIC	IIC	PA	PET	EVD	ICP	ECP	CCP	PCP	HV	R	LON	LAT	D_{Jup}	ROT	S_{LON}	S_{LAT}	V	VEF	M	MEF
6381	06-085 16:50	3	3	97	19	23	18	6	6	5	0	1	42	0	1	0	0	0	1	4	4.13870	165.9	-36.5	5.10310	156	308	-34	28.0	1.6	$3.3 \cdot 10^{-13}$	6.0
6382	06-090 17:18	2	3	96	22	28	29	5	5	5	0	1	46	0	1	0	0	0	1	4	4.11756	166.1	-36.9	5.11949	157	308	-34	43.7	1.6	$2.7 \cdot 10^{-13}$	6.0
6383	06-091 02:03	2	2	71	14	12	6	9	15	0	1	1	36	31	1	0	0	0	1	4	4.11597	166.1	-36.9	5.12071	122	274	-17	14.1	1.9	$6.7 \cdot 10^{-13}$	10.5
6384	06-092 10:11	2	2	58	9	10	7	9	9	0	1	1	0	0	1	0	0	0	1	4	4.11012	166.1	-37.1	5.12516	112	264	-10	14.1	1.9	$2.2 \cdot 10^{-13}$	10.5
6385	06-094 02:05	2	1	45	5	10	0	8	8	7	0	0	0	0	1	0	0	0	1	4	4.10318	166.2	-37.2	5.13039	94	251	1	28.0	1.6	$8.8 \cdot 10^{-15}$	6.0
6386	06-099 10:30	3	2	60	12	20	5	8	6	8	0	1	36	0	1	0	0	0	1	4	4.08008	166.3	-37.7	5.14745	123	271	-17	21.4	1.9	$2.6 \cdot 10^{-13}$	10.5
6387	06-100 06:53	2	2	64	9	14	0	8	8	7	0	0	36	0	1	0	0	0	1	4	4.07630	166.3	-37.7	5.15019	129	276	-21	28.0	1.6	$3.3 \cdot 10^{-14}$	6.0
6388	06-100 11:10	2	2	43	14	5	12	9	15	0	1	1	37	31	1	0	0	0	1	4	4.07576	166.3	-37.7	5.15058	99	253	-2	14.1	1.9	$2.0 \cdot 10^{-13}$	10.5
6389	06-102 07:49	3	3	107	20	25	6	6	6	6	0	1	44	0	1	0	0	0	1	4	4.06763	166.4	-37.9	5.15642	190	345	-38	28.0	1.6	$5.9 \cdot 10^{-13}$	6.0
6390	06-104 23:53	2	1	239	5	10	0	7	7	8	0	0	0	0	1	0	0	0	1	4	4.05621	166.5	-38.1	5.16453	17	177	47	43.7	1.6	$1.7 \cdot 10^{-15}$	6.0
6391	06-109 23:14	2	2	111	10	4	4	9	15	0	1	1	34	31	1	0	0	0	1	4	4.03428	166.6	-38.6	5.17972	204	1	-34	14.1	1.9	$8.9 \cdot 10^{-14}$	10.5
6392	06-112 08:49	2	1	111	2	7	0	15	8	11	0	0	0	0	1	0	0	0	1	4	4.02380	166.7	-38.8	5.18683	205	2	-34	36.7	2.0	$1.3 \cdot 10^{-15}$	12.5
6393	06-116 21:11	3	3	39	19	23	3	6	5	6	0	1	42	0	1	0	0	0	1	4	4.00325	166.8	-39.2	5.20046	112	258	-11	34.6	1.6	$1.7 \cdot 10^{-13}$	6.0
6394	06-118 16:34	3	3	42	19	24	10	7	6	6	0	1	42	0	1	0	0	0	1	4	3.99543	166.9	-39.3	5.20555	116	261	-14	22.7	1.6	$7.9 \cdot 10^{-13}$	6.0
6395	06-118 19:52	3	3	51	21	27	6	5	5	6	0	1	46	0	1	0	0	0	1	4	3.99487	166.9	-39.3	5.20591	129	272	-22	43.7	1.6	$1.9 \cdot 10^{-13}$	6.0
6396	06-120 07:42	3	3	39	19	24	5	6	5	6	0	1	44	0	1	0	0	0	1	4	3.98814	166.9	-39.5	5.21023	113	259	-12	34.6	1.6	$1.9 \cdot 10^{-13}$	6.0
6397	06-132 07:12	3	2	79	12	20	7	9	6	7	0	1	37	0	1	0	0	0	1	4	3.93366	167.3	-40.6	5.24378	179	326	-41	14.1	1.9	$1.2 \cdot 10^{-12}$	10.5
6398	06-137 10:15	2	1	206	5	9	0	8	8	7	0	0	0	0	1	0	0	0	1	4	3.91002	167.5	-41.0	5.25753	359	146	52	28.0	1.6	$7.4 \cdot 10^{-15}$	6.0
6399	06-137 19:25	3	2	58	14	21	8	8	6	6	0	1	39	0	1	0	0	0	1	4	3.90828	167.5	-41.1	5.25852	151	292	-34	21.4	1.9	$4.2 \cdot 10^{-13}$	10.5
6400	06-139 02:15	3	3	35	19	22	5	7	9	6	0	1	39	0	1	0	0	0	1	4	3.90248	167.5	-41.2	5.26182	120	262	-16	16.9	1.6	$2.0 \cdot 10^{-12}$	6.0
6401	06-141 00:15	2	2	15	12	6	3	8	15	0	1	1	39	31	1	0	0	0	1	4	3.89317	167.6	-41.4	5.26704	92	242	2	21.4	1.9	$3.7 \cdot 10^{-14}$	10.5
6402	06-141 17:10	3	1	108	7	10	1	8	8	6	0	1	0	0	1	0	0	0	1	4	3.89025	167.6	-41.4	5.26866	223	18	-27	28.0	1.6	$1.2 \cdot 10^{-14}$	6.0
6403	06-141 20:06	3	2	129	9	13	1	7	8	6	0	1	0	0	1	0	0	0	1	4	3.88967	167.6	-41.4	5.26899	253	42	-8	35.4	1.6	$1.3 \cdot 10^{-14}$	6.0
6404	06-157 01:25	1	1	79	2	2	0	11	15	0	1	0	39	31	1	0	0	0	1	4	3.81747	168.1	-42.9	5.30691	194	347	-41	11.8	11.8	$2.8 \cdot 10^{-14}$	5858.3
6405	06-158 11:56	3	3	53	21	27	12	5	5	5	0	1	46	0	1	0	0	0	1	4	3.81086	168.2	-43.0	5.31017	158	299	-39	43.7	1.6	$1.9 \cdot 10^{-13}$	6.0
6406	06-165 22:45	3	4	32	27	49	25	6	4	5	0	1	46	0	1	0	0	0	1	4	3.77454	168.5	-43.8	5.32751	134	276	-27	21.4	1.9	$2.0 \cdot 10^{-11}$	10.5
6407	06-172 18:16	3	3	35	23	29	8	5	4	5	0	1	46	0	1	0	0	0	1	4	3.74082	168.8	-44.4	5.34272	141	282	-31	48.9	1.6	$2.3 \cdot 10^{-13}$	6.0
6408	06-176 21:48	2	1	12	5	9	0	8	8	7	0	0	4	22	1	0	0	0	1	4	3.72039	168.9	-44.9	5.35153	110	257	-11	28.0	1.6	$7.4 \cdot 10^{-15}$	6.0
6409	06-184 16:06	2	2	239	9	9	4	10	15	0	1	1	38	31	1	0	0	0	1	4	3.68162	169.3	-45.7	5.36741	75	236	14	10.4	1.9	$3.8 \cdot 10^{-13}$	10.5
6410	06-192 21:07	3	2	32	13	21	3	8	6	6	0	1	40	0	1	0	0	0	1	4	3.63976	169.6	-46.5	5.38339	149	294	-36	21.4	1.9	$3.6 \cdot 10^{-13}$	10.5
6411	06-206 22:08	3	3	14	22	27	23	5	5	5	0	1	46	0	1	0	0	0	1	4	3.56738	170.3	-48.0	5.40823	134	283	-28	43.7	1.6	$2.2 \cdot 10^{-13}$	6.0
6412	06-210 16:33	3	4	1	25	49	12	9	5	5	0	1	46	0	1	0	0	0	1	4	3.54769	170.5	-48.5	5.41439	117	269	-16	7.8	1.9	$2.9 \cdot 10^{-10}$	10.5
6413	06-211 06:40	1	1	182	3	2	0	9	15	0	1	0	41	31	1	0	0	0	1	4	3.54440	170.5	-48.5	5.41540	12	177	53	14.1	1.9	$2.1 \cdot 10^{-14}$	10.5
6414	06-215 23:39	3	2	56	10	19	2	7	7	7	0	1	36	0	1	0	0	0	1	4	3.51993	170.8	-49.0	5.42267	199	5	-40	34.1	1.9	$2.9 \cdot 10^{-14}$	10.5
6415	06-217 08:19	2	1	2	7	11	0	8	8	6	0	0	0	0	1	0	0	0	1	4	3.51262	170.8	-49.2	5.42477	124	276	-21	28.0	1.6	$1.5 \cdot 10^{-14}$	6.0
6416	06-223 21:49	2	1	208	6	5	6	10	15	0	1	1	43	31	1	0	0	0	1	4	3.47715	171.2	-50.0	5.43450	59	233	26	10.4	1.9	$1.1 \cdot 10^{-13}$	10.5
6417	06-228 19:44	3	3	205	19	24	11	10	9	6	0	1	42	0	1	0	0	0	1	4	3.45081	171.5	-50.5	5.44123	60	235	26	10.0	1.6	$1.1 \cdot 10^{-11}$	6.1
6418	06-228 22:13	2	1	4	5	9	0	8	8	7	0	0	0	0	1	0	0	0	1	4	3.45013	171.5	-50.5	5.44140	137	291	-29	28.0	1.6	$7.4 \cdot 10^{-15}$	6.0
6419	06-238 08:40	3	2	254	13	21	1	8	5	6	0	1	39	0	1	0	0	0	1	4	3.39886	172.1	-51.7	5.45331	139	296	-30	21.4	1.9	$3.6 \cdot 10^{-13}$	10.5
6420	06-254 09:14	3	2	217	12	19	1	8	6	7	0	1	37	0	1	0	0	0	1	4	3.30884	173.2	-53.6	5.47063	100	272	-3	21.4	1.9	$2.0 \cdot 10^{-13}$	10.5
6421	06-263 18:27	3	3	199	20	24	11	5	6	6	0	1	43	0	1	0	0	0	1	4	3.25543	174.0	-54.8	5.47883	83	263	9	35.4	1.6	$2.4 \cdot 10^{-13}$	6.0
6422	06-266 05:23	2	1	4	2	6	1	12	15	0	1	1	2	31	1	0	0	0	1	4	3.24178	174.2	-55.2	5.48069	173	348	-40	2.3	2.0	$8.9 \cdot 10^{-12}$	12.5
6423	06-266 06:35	3	4	230	29	49	10	11	9	6	0	1	31	0	1	0	0	0	1	4	3.24106	174.2	-55.2	5.48079	131	301	-24	2.5	1.9	$2.3 \cdot 10^{-08}$	10.5
6424	06-267 08:17	2	2	165	11	10	8	10	15	0	1	1	39	31	1	0	0	0	1	4	3.23529	174.3	-55.3	5.48154	39	230	38	10.4	1.9	$6.1 \cdot 10^{-13}$	10.5
6425	06-268 21:29	3	2	222	15	23	9	9	7	6	0	1	41	0	1	0	0	0	1	4	3.22591	174.4	-55.5	5.48273	119	291	-16	14.1	1.9	$2.9 \cdot 10^{-12}$	10.5
6426	07-069 15:55	2	2	207	9	10	1	7	15	0	1	1	46	31	1	0	0	0	1	4	2.16070	256.1	-78.5	5.38376	119	82	-7	34.1	1.9	$9.3 \cdot 10^{-15}$	10.5
6427	07-071 07:26	1	2	165	8	10	0	8	15	0	1	0	38	31	1	0	0	0	1	4	2.14962	258.6	-78.4	5.38082	59	31	18	7.0	2.9	$1.2 \cdot 10^{-12}$	46.7
6428	07-073 02:06	3	2	106	14	22	9	7	6	6	0	1	40	0	1	0	0	0	1	4	2.13769	261.3	-78.3	5.37762	337	301	30	34.1	1.9	$9.7 \cdot 10^{-14}$	10.5
6429	07-080 13:31	2	3	91	20	23	10	6	7	3	1	1	42	0	1	0	0	0	1	4	2.08669	272.4	-77.5	5.36357	316	286	25	25.9	1.6	$5.8 \cdot 10^{-13}$	6.0
6430	07-084 02:27	3	2	116	15	23	8	8	8	6	0	1	41	0	1	0	0	0	1	4	2.06297	277.2	-77.0	5.35684	352	328	34	21.4	1.9	$6.4 \cdot 10^{-13}$	10.5
6431	07-084 21:11	1	1	163	5	5	0	8	15	15	1	0	38	31	1	0	0	0	1	4	2.05704	278.4	-76.8	5.35514	58	43	20	21.4	1.9	$9.8 \cdot 10^{-15}$	10.5
6432	07-089 22:03	3	3	84	21	27	7	6	6	5	0	1	46	0	1	0	0	0	1	4	2.02329	284.6	-75.8	5.34531	308	285	23	28.0	1.6	$9.8 \cdot 10^{-13}$	6.0
6433	07-091 07:11	3	5	100	53	53	30	9	6	5	0	1	46	0	1	0	0	0	1	4	2.01403	286.2	-75.5	5.34258	331	310	31	7.8	1.9	$3.7 \cdot 10^{-09}$	10.5
6434	07-091 08:53	2	2	122	14	11	1	7	15	15	1	1	47	31	1	0	0	0	1	4	2.01403	286.2	-75.5	5.34258	2	347	36	34.1	1.9	$2.4 \cdot 10^{-14}$	10.5
6435	07-123 21:05	2	1	139	3	18	3	6	15	15	0	1	36	22	1	0	0	0	1	4	1.80059	311.6	-65.2	5.27535	40	54	32	43.5	1.9	$2.6 \cdot 10^{-15}$	10.5

No.	IMP. DATE	CLN	AR	SEC	IA	EA	CA	IT	ET	EIT	EIC	IIC	PA	PET	EVD	ICP	ECP	CCP	PCP	HV	R	LON	LAT	D_{Jup}	ROT	S_{LON}	S_{LAT}	V	VEF	M	MEF
6436	07-130 08:34	3	2	137	11	19	1	7	5	7	0	1	37	0	1	0	0	0	1	4	1.76099	314.6	-62.5	5.26218	41	59	32	34.1	1.9	$3.3 \cdot 10^{-14}$	10.5
6437	07-132 00:14	2	1	123	4	2	0	7	15	12	0	0	2	31	1	0	0	0	1	4	1.75028	315.4	-61.8	5.25860	23	39	40	34.1	1.9	$1.1 \cdot 10^{-15}$	10.5
6438	07-132 11:44	2	1	162	4	8	0	8	8	8	0	0	2	24	1	0	0	0	1	4	1.74800	315.6	-61.6	5.25784	78	92	12	28.0	1.6	$5.2 \cdot 10^{-15}$	6.0
6439	07-136 03:34	2	1	154	5	8	0	8	8	7	0	0	2	25	1	0	0	0	1	4	1.72537	317.1	-59.9	5.25023	69	87	17	28.0	1.6	$6.2 \cdot 10^{-15}$	6.0
6440	07-146 04:00	2	1	165	6	1	0	0	15	12	0	0	2	25	1	0	0	0	1	4	1.66706	320.6	-55.2	5.23056	91	108	3	11.8	11.8	$4.4 \cdot 10^{-14}$	5858.3
6441	07-147 06:12	2	1	141	5	9	0	8	8	7	0	0	3	25	1	0	0	0	1	4	1.66071	320.9	-54.6	5.22842	58	83	25	28.0	1.6	$7.4 \cdot 10^{-15}$	6.0
6442	07-149 00:16	1	2	106	10	7	0	9	15	0	1	0	46	31	1	0	0	0	1	4	1.65091	321.5	-53.8	5.22511	9	29	46	14.1	1.9	$1.5 \cdot 10^{-13}$	10.5
6443	07-149 22:51	2	3	100	20	7	2	10	15	0	1	1	47	29	1	0	0	0	1	4	1.64606	321.7	-53.3	5.22348	2	18	47	5.0	1.9	$1.1 \cdot 10^{-11}$	10.5
6444	07-152 04:50	1	1	79	2	3	0	15	2	0	1	0	46	13	1	0	0	0	1	4	1.63439	322.4	-52.2	5.21955	333	339	42	11.8	11.8	$3.2 \cdot 10^{-14}$	5858.3
6445	07-154 06:49	1	1	62	5	1	0	7	15	0	1	0	3	31	1	0	0	0	1	4	1.62218	323.0	-51.0	5.21545	311	316	31	34.1	1.9	$1.1 \cdot 10^{-15}$	10.5
6446	07-157 06:41	1	1	173	2	4	0	15	15	0	1	0	38	30	1	0	0	0	1	4	1.60630	323.8	-49.4	5.21014	109	125	-8	11.8	11.8	$3.6 \cdot 10^{-14}$	5858.3
6447	07-157 13:06	3	1	88	6	10	12	7	7	6	0	1	3	25	1	0	0	0	1	4	1.60499	323.9	-49.3	5.20970	350	2	48	43.7	1.6	$2.0 \cdot 10^{-15}$	6.0
6448	07-157 20:10	2	1	141	2	6	0	15	8	10	0	0	3	31	1	0	0	0	1	4	1.60369	323.9	-49.2	5.20927	64	92	21	36.7	2.0	$1.1 \cdot 10^{-15}$	12.5
6449	07-157 21:26	2	1	52	1	1	0	15	15	11	0	0	3	31	1	0	0	0	1	4	1.60304	324.0	-49.1	5.20905	299	307	24	11.8	11.8	$1.9 \cdot 10^{-14}$	5858.3
6450	07-158 03:43	2	1	11	5	9	0	8	7	7	0	0	34	0	1	0	0	0	0	5	1.60174	324.0	-49.0	5.20862	242	264	-14	34.6	1.6	$3.8 \cdot 10^{-15}$	6.0
6451	07-158 09:31	1	1	115	2	1	0	9	15	0	1	0	3	31	1	0	0	0	1	4	1.60044	324.1	-48.8	5.20819	28	58	42	11.8	11.8	$2.4 \cdot 10^{-14}$	5858.3
6452	07-159 01:50	2	1	134	5	10	0	7	7	8	0	0	3	31	1	0	0	0	1	4	1.59721	324.3	-48.5	5.20712	55	85	27	43.7	1.6	$1.7 \cdot 10^{-15}$	6.0
6453	07-159 17:01	1	1	147	6	2	0	7	15	15	1	0	35	31	1	0	0	0	1	4	1.59400	324.4	-48.1	5.20605	74	100	15	34.1	1.9	$1.5 \cdot 10^{-15}$	10.5
6454	07-161 05:17	2	1	110	7	7	1	8	15	0	1	1	37	31	1	0	0	0	1	4	1.58636	324.8	-47.3	5.20353	23	52	45	21.4	1.9	$2.0 \cdot 10^{-14}$	10.5
6455	07-162 17:23	2	4	165	26	22	3	8	12	0	1	1	63	29	1	0	0	0	1	4	1.57883	325.2	-46.5	5.20105	101	121	-3	10.4	1.9	$2.5 \cdot 10^{-11}$	10.5
6456	07-164 19:50	1	1	177	2	15	0	9	0	0	1	0	47	31	1	0	0	0	1	4	1.56834	325.7	-45.3	5.19762	119	135	-16	11.8	11.8	$2.2 \cdot 10^{-13}$	5858.3
6457	07-165 00:47	3	1	247	7	12	5	7	7	6	0	1	3	31	1	0	0	0	1	4	1.56712	325.8	-45.1	5.19723	218	245	-29	43.7	1.6	$3.3 \cdot 10^{-15}$	6.0
6458	07-165 12:02	3	3	11	19	24	14	6	7	6	0	1	43	0	1	0	0	0	1	4	1.56469	325.9	-44.8	5.19644	246	269	-12	25.9	1.6	$5.0 \cdot 10^{-13}$	6.0
6459	07-165 14:29	3	1	8	5	9	1	7	7	7	0	1	2	31	1	0	0	0	1	4	1.56469	325.9	-44.8	5.19644	242	266	-15	43.7	1.6	$1.4 \cdot 10^{-15}$	6.0
6460	07-165 18:37	2	1	224	1	6	0	15	9	12	0	0	3	31	1	0	0	0	1	4	1.56348	325.9	-44.7	5.19605	186	208	-39	31.3	2.0	$1.5 \cdot 10^{-15}$	12.5
6461	07-165 19:56	1	1	133	5	13	0	9	15	15	1	0	58	28	1	0	0	0	1	4	1.56348	325.9	-44.7	5.19605	58	90	26	14.1	1.9	$1.8 \cdot 10^{-13}$	10.5
6462	07-165 22:29	2	1	169	5	1	0	6	2	12	0	0	3	31	1	0	0	0	1	4	1.56288	326.0	-44.6	5.19585	109	127	-9	43.5	1.9	$3.9 \cdot 10^{-16}$	10.5
6463	07-169 23:20	1	1	81	3	10	0	7	15	0	1	0	46	31	1	0	0	0	1	4	1.54399	326.9	-42.3	5.18979	348	2	50	34.1	1.9	$3.4 \cdot 10^{-15}$	10.5
6464	07-170 07:57	1	1	196	3	9	0	9	15	15	1	0	19	31	1	0	0	0	1	4	1.54226	326.9	-42.0	5.18925	150	163	-33	5.7	2.1	$8.2 \cdot 10^{-13}$	15.7
6465	07-171 00:28	3	2	134	10	19	8	7	5	6	0	1	3	31	1	0	0	0	1	4	1.53883	327.1	-41.6	5.18816	63	95	23	34.1	1.9	$2.9 \cdot 10^{-14}$	10.5
6466	07-173 19:19	2	1	206	3	8	0	8	8	8	0	0	2	31	1	0	0	0	1	4	1.52651	327.7	-39.9	5.18432	166	183	-40	28.0	1.6	$4.5 \cdot 10^{-15}$	6.0
6467	07-175 13:26	3	1	249	5	10	3	7	7	6	0	1	2	25	1	0	0	0	1	4	1.51890	328.1	-38.9	5.18198	227	257	-25	43.7	1.6	$1.7 \cdot 10^{-15}$	6.0
6468	07-176 23:13	1	1	176	2	2	0	9	15	0	1	0	3	31	1	0	0	0	1	4	1.51304	328.3	-38.0	5.18021	126	141	-21	11.8	11.8	$2.8 \cdot 10^{-14}$	5858.3
6469	07-177 09:20	2	1	102	5	14	0	15	12	12	0	0	15	1	1	0	0	0	1	4	1.51094	328.5	-37.7	5.17958	22	56	48	2.0	1.9	$1.0 \cdot 10^{-10}$	10.5
6470	07-177 16:13	1	1	179	4	8	0	5	7	0	1	0	45	31	1	0	0	0	1	4	1.50989	328.5	-37.5	5.17926	130	145	-24	62.6	1.6	$2.3 \cdot 10^{-16}$	6.0
6471	07-177 19:34	3	3	49	19	24	4	5	5	5	0	1	43	0	1	0	0	0	1	4	1.50937	328.5	-37.5	5.17911	308	316	31	43.7	1.6	$7.3 \cdot 10^{-14}$	6.0
6472	07-179 07:57	2	1	9	6	11	0	7	7	6	0	0	2	31	1	0	0	0	1	4	1.50319	328.8	-36.5	5.17728	252	277	-9	43.7	1.6	$2.3 \cdot 10^{-15}$	6.0
6473	07-181 16:16	1	1	48	2	7	0	9	15	15	1	0	46	30	1	0	0	0	1	4	1.49370	329.3	-35.0	5.17453	309	316	32	2.3	2.0	$1.1 \cdot 10^{-11}$	12.5
6474	07-182 14:46	1	1	47	3	1	0	7	0	0	1	0	46	7	1	0	0	0	1	4	1.49031	329.5	-34.5	5.17358	308	316	31	34.1	1.9	$7.7 \cdot 10^{-16}$	10.5
6475	07-182 21:34	1	1	195	4	11	0	5	15	0	1	0	47	31	1	0	0	0	1	4	1.48886	329.5	-34.2	5.17317	156	171	-38	70.0	1.9	$2.5 \cdot 10^{-16}$	10.5
6476	07-183 14:00	3	4	67	24	30	17	8	6	5	0	1	47	0	1	0	0	0	1	4	1.48647	329.6	-33.8	5.17251	337	346	49	19.5	1.6	$1.1 \cdot 10^{-11}$	6.0
6477	07-184 04:39	1	1	118	3	10	0	9	15	15	1	0	19	31	1	0	0	0	1	4	1.48411	329.8	-33.4	5.17185	49	87	34	14.1	1.9	$8.0 \cdot 10^{-14}$	10.5
6478	07-184 13:14	1	1	120	3	8	0	9	15	0	1	0	4	31	1	0	0	0	1	4	1.48270	329.8	-33.2	5.17147	52	90	32	5.7	2.1	$6.9 \cdot 10^{-13}$	15.7
6479	07-184 13:46	3	2	75	8	12	5	7	7	6	0	1	3	31	1	0	0	0	1	4	1.48270	329.8	-33.2	5.17147	348	4	53	43.7	1.6	$4.0 \cdot 10^{-15}$	6.0
6480	07-185 02:29	2	1	126	6	5	1	7	15	15	1	1	3	31	1	0	0	0	1	4	1.48085	329.9	-32.9	5.17096	61	97	26	34.1	1.9	$2.3 \cdot 10^{-15}$	10.5
6481	07-185 03:01	2	1	110	4	15	0	7	0	8	0	0	3	31	1	0	0	0	1	4	1.48038	330.0	-32.8	5.17084	38	78	41	34.1	1.9	$8.4 \cdot 10^{-15}$	10.5
6482	07-185 03:19	1	1	111	5	1	0	11	15	0	1	0	41	28	1	0	0	0	1	4	1.48038	330.0	-32.8	5.17084	40	79	40	7.8	1.9	$1.1 \cdot 10^{-13}$	10.5
6483	07-185 05:28	3	1	153	1	5	1	15	7	11	0	1	3	31	1	0	0	0	1	4	1.48038	330.0	-32.8	5.17084	99	122	-2	56.0	2.0	$1.3 \cdot 10^{-16}$	12.5
6484	07-185 08:52	2	2	28	9	13	0	7	7	6	0	0	36	0	1	0	0	0	1	4	1.47992	330.0	-32.7	5.17071	283	298	13	43.7	1.6	$5.4 \cdot 10^{-15}$	6.0
6485	07-185 11:05	3	2	133	10	19	1	7	6	6	0	1	37	0	1	0	0	0	1	4	1.47946	330.0	-32.6	5.17059	71	104	18	34.1	1.9	$2.9 \cdot 10^{-14}$	10.5
6486	07-185 13:45	3	2	113	11	19	1	7	5	6	0	1	38	0	1	0	0	0	1	4	1.47900	330.0	-32.5	5.17047	43	82	38	34.1	1.9	$3.3 \cdot 10^{-14}$	10.5
6487	07-185 14:19	2	1	126	5	9	0	8	8	8	0	0	3	31	1	0	0	0	1	4	1.47900	330.0	-32.5	5.17047	61	97	25	28.0	1.6	$7.4 \cdot 10^{-15}$	6.0
6488	07-186 01:23	1	1	35	4	2	0	8	15	0	1	0	36	31	1	0	0	0	1	4	1.47718	330.1	-32.2	5.16998	293	304	21	21.4	1.9	$5.4 \cdot 10^{-15}$	10.5
6489	07-187 03:18	1	1	82	2	9	0	8	15	0	1	0	47	31	1	0	0	0	1	4	1.47313	330.3	-31.5	5.16891	360	23	56	11.8	11.8	$8.8 \cdot 10^{-14}$	5858.3
6490	07-187 14:58	1	1	143	5	8	0	7	13	0	1	0	46	31	1	0	0	0	1	4	1.47180	330.4	-31.2	5.16857	86	114	6	16.2	1.7	$5.1 \cdot 10^{-14}$	7.4

No.	IMP. DATE	CLN	AR	SEC	IA	EA	CA	IT	ET	EIT	EIC	IIC	PA	PET	EVD	ICP	ECP	CCP	PCP	HV	R	LON	LAT	D_{Jup}	ROT	S_{LON}	S_{LAT}	V	VEF	M	MEF
6491	07-187 16:13	2	2	221	8	13	0	7	7	6	0	0	35	0	1	0	0	0	1	4	1.47136	330.4	-31.1	5.16845	196	225	-43	43.7	1.6	$4.7 \cdot 10^{-15}$	6.0
6492	07-189 03:45	3	3	115	20	26	3	7	6	6	0	1	45	0	1	0	0	0	1	4	1.46615	330.7	-30.1	5.16713	48	88	35	22.7	1.6	$1.5 \cdot 10^{-12}$	6.0
6493	07-189 16:45	1	1	181	2	7	0	15	13	15	1	0	14	31	1	0	0	0	1	4	1.46445	330.8	-29.8	5.16671	141	154	-32	7.7	2.0	$1.9 \cdot 10^{-13}$	12.5
6494	07-190 00:00	1	1	154	1	1	0	15	14	15	1	0	3	31	1	0	0	0	1	4	1.46319	330.8	-29.6	5.16640	103	125	-6	11.8	11.8	$1.9 \cdot 10^{-14}$	5858.3
6495	07-190 04:34	2	1	66	6	9	1	8	15	0	1	1	44	30	1	0	0	0	1	4	1.46277	330.9	-29.5	5.16630	339	349	52	7.0	2.9	$6.8 \cdot 10^{-13}$	46.7
6496	07-191 01:13	2	2	46	14	21	0	7	7	7	0	0	41	0	1	0	0	0	1	4	1.45987	331.0	-28.9	5.16560	312	318	35	34.1	1.9	$8.3 \cdot 10^{-14}$	10.5
6497	07-191 15:49	1	1	156	1	1	0	15	14	15	1	0	4	31	1	0	0	0	1	4	1.45783	331.1	-28.5	5.16512	107	128	-9	11.8	11.8	$1.9 \cdot 10^{-14}$	5858.3
6498	07-191 20:50	2	2	159	8	13	0	7	7	6	0	0	36	0	1	0	0	0	1	4	1.45742	331.2	-28.4	5.16502	111	130	-12	43.7	1.6	$4.7 \cdot 10^{-15}$	6.0
6499	07-193 08:01	2	2	183	8	15	9	7	0	6	0	1	3	31	1	0	0	0	1	4	1.45266	331.4	-27.4	5.16394	146	159	-36	34.1	1.9	$1.7 \cdot 10^{-14}$	10.5
6500	07-195 12:39	1	1	235	1	12	0	15	15	15	1	0	45	30	1	0	0	0	1	4	1.44582	331.8	-25.8	5.16249	220	254	-33	11.8	11.8	$1.2 \cdot 10^{-13}$	5858.3
6501	07-195 16:32	2	1	27	7	12	0	7	7	7	0	0	2	31	1	0	0	0	1	4	1.44545	331.8	-25.8	5.16242	288	300	17	43.7	1.6	$3.3 \cdot 10^{-15}$	6.0
6502	07-196 10:09	2	2	96	12	20	0	7	6	6	0	0	38	0	1	0	0	0	1	4	1.44326	332.0	-25.2	5.16198	25	66	51	34.1	1.9	$5.2 \cdot 10^{-14}$	10.5
6503	07-196 22:21	2	2	50	11	7	12	9	15	0	1	1	2	26	1	0	0	0	1	4	1.44183	332.0	-24.9	5.16171	321	325	43	14.1	1.9	$1.7 \cdot 10^{-13}$	10.5
6504	07-197 03:32	1	1	166	1	11	0	15	10	15	1	0	13	31	1	0	0	0	1	4	1.44112	332.1	-24.7	5.16157	124	139	-23	11.8	11.8	$1.0 \cdot 10^{-13}$	5858.3
6505	07-197 12:26	0	1	29	3	7	0	10	6	10	1	0	18	21	1	0	0	0	1	4	1.44006	332.1	-24.5	5.16138	292	302	20	27.0	2.3	$4.3 \cdot 10^{-15}$	19.8
6506	07-197 14:55	2	1	255	7	12	0	7	7	6	0	0	3	26	1	0	0	0	1	4	1.44006	332.1	-24.5	5.16138	250	277	-12	43.7	1.6	$3.3 \cdot 10^{-15}$	6.0
6507	07-197 17:23	3	2	40	9	14	1	7	7	6	0	1	36	0	1	0	0	0	1	4	1.43971	332.2	-24.4	5.16131	307	313	33	43.7	1.6	$6.4 \cdot 10^{-15}$	6.0
6508	07-198 11:59	1	1	183	3	9	0	10	15	15	1	0	19	30	1	0	0	0	1	4	1.43764	332.3	-23.9	5.16094	149	161	-39	4.9	1.7	$1.3 \cdot 10^{-12}$	7.7
6509	07-199 14:15	3	2	40	8	13	6	7	7	7	0	1	35	0	1	0	0	0	1	4	1.43461	332.5	-23.1	5.16043	308	313	34	43.7	1.6	$4.7 \cdot 10^{-15}$	6.0
6510	07-199 22:18	0	1	61	2	1	0	15	0	1	1	0	21	2	1	0	0	0	1	4	1.43363	332.5	-22.8	5.16028	338	344	54	11.8	11.8	$2.4 \cdot 10^{-14}$	5858.3
6511	07-200 08:56	2	2	74	9	11	11	11	15	0	1	1	6	30	1	0	0	0	1	4	1.43265	332.6	-22.6	5.16012	357	16	60	4.2	1.6	$7.9 \cdot 10^{-12}$	6.0
6512	07-200 15:12	1	1	174	2	8	0	15	15	0	1	0	47	31	1	0	0	0	1	4	1.43169	332.7	-22.3	5.15998	137	149	-33	2.3	2.0	$1.3 \cdot 10^{-11}$	12.5
6513	07-200 16:33	2	3	37	20	15	5	7	0	6	0	1	27	1	1	0	0	0	1	4	1.43169	332.7	-22.3	5.15998	305	310	31	14.1	1.9	$2.1 \cdot 10^{-12}$	10.5
6514	07-201 23:34	2	2	65	10	9	5	9	15	0	1	1	39	30	1	0	0	0	1	4	1.42855	332.9	-21.4	5.15954	345	354	58	14.1	1.9	$2.2 \cdot 10^{-13}$	10.5
6515	07-203 22:58	1	1	41	5	3	0	8	15	0	1	0	36	30	1	0	0	0	1	4	1.42379	333.2	-20.0	5.15899	312	314	38	21.4	1.9	$7.3 \cdot 10^{-15}$	10.5
6516	07-205 08:36	2	1	117	5	10	0	8	7	7	0	0	3	31	1	0	0	0	1	4	1.42071	333.4	-19.0	5.15872	60	100	28	34.6	1.6	$4.5 \cdot 10^{-15}$	6.0
6517	07-205 19:39	1	1	127	1	1	0	15	0	0	1	0	3	31	1	0	0	0	1	4	1.41962	333.5	-18.7	5.15864	74	108	16	11.8	11.8	$1.9 \cdot 10^{-14}$	5858.3
6518	07-205 20:27	2	1	43	5	9	0	7	7	6	0	0	3	26	1	0	0	0	1	4	1.41962	333.5	-18.7	5.15864	316	316	41	43.7	1.6	$1.4 \cdot 10^{-15}$	6.0
6519	07-206 11:10	1	1	121	2	10	0	8	15	15	1	0	47	31	1	0	0	0	1	4	1.41830	333.6	-18.2	5.15856	66	103	23	11.8	11.8	$1.1 \cdot 10^{-13}$	5858.3
6520	07-206 23:24	1	1	198	4	13	0	6	14	0	1	0	47	31	1	0	0	0	1	4	1.41726	333.7	-17.9	5.15851	175	193	-53	43.5	1.9	$2.4 \cdot 10^{-15}$	10.5
6521	07-207 07:24	2	1	60	5	10	0	8	7	7	0	0	2	26	1	0	0	0	1	4	1.41650	333.7	-17.6	5.15848	341	343	59	34.6	1.6	$4.5 \cdot 10^{-15}$	6.0
6522	07-207 08:16	1	1	172	1	8	0	15	14	15	1	0	19	31	1	0	0	0	1	4	1.41650	333.7	-17.6	5.15848	138	146	-36	11.8	11.8	$6.1 \cdot 10^{-14}$	5858.3
6523	07-209 18:08	1	1	174	1	9	0	15	15	15	1	0	47	31	1	0	0	0	1	4	1.41171	334.1	-15.8	5.15846	143	148	-39	11.8	11.8	$7.3 \cdot 10^{-14}$	5858.3
6524	07-209 22:45	2	1	57	2	7	0	15	7	10	0	0	3	31	1	0	0	0	1	4	1.41148	334.1	-15.7	5.15846	338	336	58	56.0	2.0	$2.2 \cdot 10^{-16}$	12.5
6525	07-210 09:13	3	1	65	5	9	3	7	7	6	0	1	2	26	1	0	0	0	1	4	1.41059	334.2	-15.4	5.15850	350	356	64	43.7	1.6	$1.4 \cdot 10^{-15}$	6.0
6526	07-210 20:30	2	1	62	3	11	0	8	5	13	0	0	24	0	1	0	0	0	1	4	1.40994	334.3	-15.1	5.15853	346	348	63	21.4	1.9	$2.1 \cdot 10^{-14}$	10.5
6527	07-211 07:09	1	1	200	2	11	0	15	15	0	1	0	63	31	1	0	0	0	1	4	1.40909	334.4	-14.7	5.15859	180	200	-56	11.8	11.8	$1.2 \cdot 10^{-13}$	5858.3
6528	07-211 07:11	1	1	205	1	10	0	15	15	15	1	0	46	31	1	0	0	0	1	4	1.40909	334.4	-14.7	5.15859	187	213	-55	11.8	11.8	$8.6 \cdot 10^{-14}$	5858.3
6529	07-212 03:24	0	1	42	2	7	0	15	10	14	1	0	45	28	1	0	0	0	1	4	1.40765	334.5	-14.1	5.15872	318	312	44	26.5	2.0	$3.9 \cdot 10^{-15}$	12.5
6530	07-212 11:35	2	1	123	1	5	0	15	10	10	0	0	4	31	1	0	0	0	1	4	1.40725	334.5	-13.9	5.15876	72	106	18	26.5	2.0	$2.2 \cdot 10^{-15}$	12.5
6531	07-212 21:29	1	1	53	2	11	0	15	15	0	1	0	46	31	1	0	0	0	1	4	1.40646	334.6	-13.5	5.15886	334	326	57	11.8	11.8	$1.2 \cdot 10^{-13}$	5858.3
6532	07-213 15:25	1	1	249	1	11	0	15	15	0	1	0	46	31	1	0	0	0	1	4	1.40535	334.7	-13.0	5.15905	250	276	-15	11.8	11.8	$1.0 \cdot 10^{-13}$	5858.3
6533	07-213 19:17	2	1	23	6	11	0	7	7	7	0	0	3	26	1	0	0	0	1	4	1.40516	334.7	-12.9	5.15908	292	295	22	43.7	1.6	$2.3 \cdot 10^{-15}$	6.0
6534	07-213 19:30	1	1	25	2	7	0	15	13	15	1	0	45	31	1	0	0	0	1	4	1.40516	334.7	-12.9	5.15908	295	296	24	7.7	2.0	$1.9 \cdot 10^{-13}$	12.5
6535	07-213 22:26	2	3	146	22	1	17	9	15	15	0	1	47	0	1	0	0	0	1	4	1.40498	334.8	-12.8	5.15911	105	121	-10	7.8	1.9	$1.4 \cdot 10^{-12}$	10.5
6536	07-214 06:23	1	1	14	2	11	0	15	15	0	1	0	10	31	1	0	0	0	1	4	1.40444	334.8	-12.5	5.15921	280	289	11	11.8	11.8	$1.2 \cdot 10^{-13}$	5858.3
6537	07-214 09:44	3	4	85	27	49	18	6	5	5	0	1	47	0	1	0	0	0	1	4	1.40426	334.8	-12.5	5.15925	20	65	62	21.4	1.9	$2.0 \cdot 10^{-11}$	10.5
6538	07-214 11:07	2	1	123	6	11	0	10	3	14	0	0	56	7	1	0	0	0	1	4	1.40426	334.8	-12.5	5.15925	73	106	17	27.0	2.3	$1.4 \cdot 10^{-14}$	19.8
6539	07-214 15:43	2	2	115	9	19	0	7	6	7	0	0	35	31	1	0	0	0	1	4	1.40391	334.9	-12.3	5.15932	62	101	28	34.1	1.9	$2.4 \cdot 10^{-14}$	10.5
6540	07-215 01:58	2	4	61	25	26	9	8	10	5	0	1	47	0	1	0	0	0	1	4	1.40339	334.9	-12.0	5.15944	346	343	66	10.4	1.9	$4.0 \cdot 10^{-11}$	10.5
6541	07-215 02:29	0	1	84	3	11	0	8	10	14	1	0	19	29	1	0	0	0	1	4	1.40339	334.9	-12.0	5.15944	18	63	63	21.4	1.9	$2.1 \cdot 10^{-14}$	10.5
6542	07-215 03:03	3	1	50	7	11	1	7	7	6	0	1	3	31	1	0	0	0	1	4	1.40323	335.0	-11.9	5.15948	331	319	55	43.7	1.6	$2.9 \cdot 10^{-15}$	6.0
6543	07-215 03:15	1	1	78	1	1	0	15	15	0	1	0	3	31	1	0	0	0	1	4	1.40323	335.0	-11.9	5.15948	10	46	68	11.8	11.8	$1.9 \cdot 10^{-14}$	5858.3
6544	07-215 12:21	2	3	18	17	2	1	15	0	12	0	1	26	0	1	0	0	0	1	4	1.40273	335.0	-11.6	5.15960	286	291	16	2.0	1.9	$6.9 \cdot 10^{-11}$	10.5
6545	07-215 19:34	1	1	57	2	2	0	9	15	0	1	0	36	30	1	0	0	0	1	4	1.40240	335.1	-11.5	5.15969	341	331	63	11.8	11.8	$2.8 \cdot 10^{-14}$	5858.3

No.	IMP. DATE	CLN	AR	SEC	IA	EA	CA	IT	ET	EIT	EIC	IIC	PA	PET	EVD	ICP	ECP	CCP	PCP	HV	R	LON	LAT	D_{Jup}	ROT	S_{LON}	S_{LAT}	V	VEF	M	MEF
6546	07-216 01:58	1	1	123	2	2	0	15	15	15	1	0	3	31	1	0	0	0	1	4	1.40208	335.1	-11.3	5.15978	73	106	17	11.8	11.8	$2.8 \cdot 10^{-14}$	5858.3
6547	07-216 07:21	1	1	44	2	1	0	15	8	0	1	0	23	31	1	0	0	0	1	4	1.40176	335.1	-11.1	5.15987	322	310	49	11.8	11.8	$2.4 \cdot 10^{-14}$	5858.3
6548	07-216 08:51	2	1	161	1	5	0	15	7	11	0	0	3	31	1	0	0	0	1	4	1.40176	335.1	-11.1	5.15987	127	130	-30	56.0	2.0	$1.3 \cdot 10^{-16}$	12.5
6549	07-216 12:22	1	1	241	1	9	0	15	15	0	1	0	46	31	1	0	0	0	1	4	1.40145	335.2	-10.9	5.15997	240	270	-24	11.8	11.8	$7.3 \cdot 10^{-14}$	5858.3
6550	07-216 16:35	1	1	92	2	10	0	15	15	0	1	0	47	31	1	0	0	0	1	4	1.40130	335.2	-10.8	5.16002	30	80	56	11.8	11.8	$1.1 \cdot 10^{-13}$	5858.3
6551	07-216 16:59	3	4	43	28	49	26	8	6	5	0	1	47	0	1	0	0	0	1	4	1.40130	335.2	-10.8	5.16002	321	308	48	10.4	1.9	$2.2 \cdot 10^{-10}$	10.5
6552	07-216 22:10	3	4	83	27	49	10	6	5	5	0	1	47	0	1	0	0	0	1	4	1.40100	335.2	-10.6	5.16012	17	63	65	21.4	1.9	$2.0 \cdot 10^{-11}$	10.5
6553	07-216 23:15	2	1	117	5	9	0	7	7	8	0	0	4	31	1	0	0	0	1	4	1.40100	335.2	-10.6	5.16012	65	103	25	43.7	1.6	$1.4 \cdot 10^{-15}$	6.0
6554	07-217 01:22	2	1	19	6	12	0	7	7	7	0	0	34	0	1	0	0	0	1	4	1.40085	335.2	-10.5	5.16018	287	290	18	43.7	1.6	$2.7 \cdot 10^{-15}$	6.0
6555	07-217 03:29	1	1	173	2	9	0	9	15	0	1	0	47	31	1	0	0	0	1	4	1.40070	335.3	-10.4	5.16023	144	142	-44	11.8	11.8	$8.8 \cdot 10^{-14}$	5858.3
6556	07-217 09:12	2	1	148	2	7	0	15	8	10	0	0	4	31	1	0	0	0	1	4	1.40041	335.3	-10.3	5.16034	109	120	-14	36.7	2.0	$1.3 \cdot 10^{-15}$	12.5
6557	07-217 12:15	2	1	155	3	7	0	9	8	9	0	0	3	31	1	0	0	0	1	4	1.40026	335.3	-10.2	5.16039	119	124	-23	22.7	1.6	$7.8 \cdot 10^{-15}$	6.0
6558	07-218 06:46	2	1	47	4	10	0	8	7	8	0	0	2	26	1	0	0	0	1	4	1.39943	335.4	-9.6	5.16074	327	310	54	34.6	1.6	$3.8 \cdot 10^{-15}$	6.0
6559	07-218 12:54	3	2	96	12	20	1	7	7	6	0	1	39	0	1	0	0	0	1	4	1.39917	335.5	-9.4	5.16087	36	87	51	34.1	1.9	$5.2 \cdot 10^{-14}$	10.5
6560	07-218 21:05	1	1	104	2	15	0	9	0	0	1	0	47	31	1	0	0	0	1	4	1.39878	335.5	-9.2	5.16106	47	94	41	11.8	11.8	$2.2 \cdot 10^{-13}$	5858.3
6561	07-218 21:31	1	1	182	2	15	0	9	0	0	1	0	47	31	1	0	0	0	1	4	1.39878	335.5	-9.2	5.16106	157	153	-55	11.8	11.8	$2.2 \cdot 10^{-13}$	5858.3
6562	07-219 14:12	2	1	3	2	1	0	15	0	13	0	0	46	0	1	0	0	0	1	4	1.39816	335.6	-8.7	5.16140	266	280	-1	11.8	11.8	$2.4 \cdot 10^{-14}$	5858.3
6563	07-220 01:27	1	1	62	3	13	0	7	15	0	1	0	3	31	1	0	0	0	1	4	1.39768	335.7	-8.3	5.16168	348	337	72	34.1	1.9	$5.5 \cdot 10^{-15}$	10.5
6564	07-220 19:30	2	1	155	5	10	0	7	7	8	0	0	2	31	1	0	0	0	1	4	1.39702	335.8	-7.8	5.16213	119	121	-25	43.7	1.6	$1.7 \cdot 10^{-15}$	6.0
6565	07-221 07:13	2	1	109	4	9	0	7	7	7	0	0	3	31	1	0	0	0	1	4	1.39660	335.9	-7.4	5.16245	55	98	35	43.7	1.6	$1.2 \cdot 10^{-15}$	6.0
6566	07-221 14:32	1	2	11	11	3	0	12	7	15	1	0	57	30	1	0	0	0	1	4	1.39640	335.9	-7.2	5.16261	277	282	8	5.0	1.9	$1.7 \cdot 10^{-12}$	10.5
6567	07-221 16:36	3	1	143	3	7	1	7	7	8	0	1	2	31	1	0	0	0	1	4	1.39630	335.9	-7.1	5.16269	102	114	-9	43.7	1.6	$7.2 \cdot 10^{-16}$	6.0
6568	07-221 22:53	3	2	60	13	21	9	8	9	6	0	1	39	0	1	0	0	0	1	4	1.39611	336.0	-7.0	5.16286	346	324	71	21.4	1.9	$3.6 \cdot 10^{-13}$	10.5
6569	07-222 01:05	2	2	169	8	13	0	7	7	8	0	0	3	31	1	0	0	0	1	4	1.39602	336.0	-6.9	5.16295	139	129	-43	43.7	1.6	$4.7 \cdot 10^{-15}$	6.0
6570	07-222 06:24	1	1	145	1	10	0	15	15	0	1	0	47	31	1	0	0	0	1	4	1.39583	336.0	-6.7	5.16312	105	114	-12	11.8	11.8	$8.6 \cdot 10^{-14}$	5858.3
6571	07-222 17:12	1	1	199	1	3	0	15	15	0	1	0	5	30	1	0	0	0	1	4	1.39557	336.1	-6.4	5.16339	181	197	-68	11.8	11.8	$2.6 \cdot 10^{-14}$	5858.3
6572	07-222 20:45	1	1	70	1	10	0	15	9	0	1	0	46	28	1	0	0	0	1	4	1.39548	336.1	-6.3	5.16348	360	11	79	11.8	11.8	$8.6 \cdot 10^{-14}$	5858.3
6573	07-223 05:27	1	1	98	2	10	0	15	15	0	1	0	47	31	1	0	0	0	1	4	1.39524	336.2	-6.0	5.16376	39	93	50	11.8	11.8	$1.1 \cdot 10^{-13}$	5858.3
6574	07-223 22:44	1	1	145	3	11	0	8	15	0	1	0	47	31	1	0	0	0	1	4	1.39478	336.3	-5.5	5.16433	105	112	-12	21.4	1.9	$2.1 \cdot 10^{-14}$	10.5
6575	07-224 03:05	1	2	179	9	7	0	7	15	15	1	0	2	31	1	0	0	0	1	4	1.39464	336.3	-5.3	5.16453	152	136	-56	34.1	1.9	$5.4 \cdot 10^{-15}$	10.5
6576	07-224 18:40	2	1	202	2	1	0	15	2	12	0	0	3	26	1	0	0	0	1	4	1.39431	336.4	-4.8	5.16505	185	207	-71	11.8	11.8	$2.4 \cdot 10^{-14}$	5858.3
6577	07-224 19:25	2	2	179	11	20	0	7	7	6	0	0	40	0	1	0	0	0	1	4	1.39431	336.4	-4.8	5.16505	152	134	-56	34.1	1.9	$4.4 \cdot 10^{-14}$	10.5
6578	07-224 21:20	2	1	133	3	7	0	8	7	9	0	0	3	31	1	0	0	0	1	4	1.39425	336.4	-4.7	5.16515	87	107	4	34.6	1.6	$1.9 \cdot 10^{-15}$	6.0
6579	07-225 01:58	3	4	80	24	29	3	8	6	6	0	1	47	0	1	0	0	0	1	4	1.39419	336.5	-4.6	5.16526	13	73	75	19.5	1.6	$9.0 \cdot 10^{-12}$	6.0
6580	07-225 11:42	2	2	70	10	14	2	10	15	15	1	1	60	31	1	0	0	0	1	4	1.39401	336.5	-4.4	5.16558	358	359	83	4.9	1.7	$9.6 \cdot 10^{-12}$	7.7
6581	07-225 15:12	1	1	24	7	8	0	9	15	15	1	0	45	30	1	0	0	0	1	4	1.39391	336.5	-4.2	5.16580	294	281	24	14.1	1.9	$1.1 \cdot 10^{-13}$	10.5
6582	07-225 15:20	2	2	69	10	10	7	8	15	0	1	1	6	30	1	0	0	0	1	4	1.39391	336.5	-4.2	5.16580	357	346	83	21.4	1.9	$5.6 \cdot 10^{-14}$	10.5
6583	07-225 15:25	1	1	93	3	10	0	9	15	15	1	0	47	31	1	0	0	0	1	4	1.39391	336.5	-4.2	5.16580	31	92	59	14.1	1.9	$8.0 \cdot 10^{-14}$	10.5
6584	07-225 21:24	1	1	159	2	11	0	15	15	0	1	0	47	31	1	0	0	0	1	4	1.39380	336.6	-4.0	5.16603	123	114	-30	11.8	11.8	$1.2 \cdot 10^{-13}$	5858.3
6585	07-226 07:40	2	6	79	59	28	31	4	0	4	1	1	31	0	1	0	0	0	1	4	1.39366	336.6	-3.7	5.16637	10	75	78	43.5	1.9	$8.1 \cdot 10^{-12}$	10.5
6586	07-226 07:42	1	1	84	5	6	0	6	15	15	1	0	63	31	1	0	0	0	1	4	1.39366	336.6	-3.7	5.16637	17	85	72	43.5	1.9	$8.5 \cdot 10^{-16}$	10.5
6587	07-226 22:39	1	1	110	3	10	0	9	15	15	1	0	19	30	1	0	0	0	1	4	1.39345	336.7	-3.3	5.16696	54	100	37	14.1	1.9	$8.0 \cdot 10^{-14}$	10.5
6588	07-227 07:52	2	2	100	13	11	13	10	15	0	1	1	2	26	1	0	0	0	1	4	1.39334	336.8	-3.0	5.16732	39	98	51	10.4	1.9	$1.0 \cdot 10^{-12}$	10.5
6589	07-227 15:16	3	4	8	26	1	28	11	15	6	0	1	22	0	1	0	0	0	1	4	1.39325	336.8	-2.7	5.16769	269	275	0	2.5	1.9	$1.1 \cdot 10^{-10}$	10.5
6590	07-227 19:25	1	1	180	2	9	0	15	15	15	1	0	19	30	1	0	0	0	1	4	1.39322	336.9	-2.6	5.16782	151	122	-57	11.8	11.8	$8.8 \cdot 10^{-14}$	5858.3
6591	07-227 22:51	2	1	215	7	11	0	7	7	6	0	0	2	26	1	0	0	0	1	4	1.39319	336.9	-2.5	5.16794	200	248	-65	43.7	1.6	$2.9 \cdot 10^{-15}$	6.0
6592	07-228 05:46	1	1	112	3	12	0	10	15	15	1	0	20	31	1	0	0	0	1	4	1.39314	336.9	-2.3	5.16820	55	100	35	10.4	1.9	$2.3 \cdot 10^{-13}$	10.5
6593	07-228 12:10	2	5	252	53	2	26	13	0	6	0	1	31	0	1	0	0	0	1	4	1.39307	337.0	-2.1	5.16859	251	271	-17	2.0	1.9	$1.8 \cdot 10^{-09}$	10.5
6594	07-228 19:54	3	1	212	7	12	18	7	7	6	0	1	3	26	1	0	0	0	1	4	1.39303	337.0	-1.9	5.16885	195	243	-71	43.7	1.6	$3.3 \cdot 10^{-15}$	6.0
6595	07-228 20:43	3	3	74	23	28	12	7	5	6	0	1	47	0	1	0	0	0	1	4	1.39303	337.0	-1.9	5.16885	1	52	89	28.1	1.6	$1.6 \cdot 10^{-12}$	6.0
6596	07-229 08:12	2	3	66	23	10	23	13	9	13	1	1	22	26	1	0	0	0	1	4	1.39297	337.1	-1.5	5.16939	349	275	79	2.0	1.9	$7.9 \cdot 10^{-10}$	10.5
6597	07-229 11:10	0	1	236	1	9	0	15	15	10	0	0	41	26	1	0	0	0	1	4	1.39296	337.1	-1.4	5.16952	227	267	-41	11.8	11.8	$7.3 \cdot 10^{-14}$	5858.3
6598	07-229 12:04	2	1	207	6	10	0	7	7	7	0	0	0	0	1	0	0	0	1	4	1.39295	337.1	-1.3	5.16966	186	223	-78	43.7	1.6	$2.0 \cdot 10^{-15}$	6.0
6599	07-229 14:23	2	2	65	8	13	0	7	7	7	0	0	36	0	1	0	0	0	1	4	1.39295	337.1	-1.3	5.16966	347	273	77	43.7	1.6	$4.7 \cdot 10^{-15}$	6.0
6600	07-229 17:17	3	3	61	20	26	12	7	6	6	0	1	44	0	1	0	0	0	1	4	1.39294	337.1	-1.2	5.16980	341	273	71	22.7	1.6	$1.5 \cdot 10^{-12}$	6.0

No.	IMP. DATE	CLN	AR	SEC	IA	EA	CA	IT	ET	EIT	EIC	IIC	PA	PET	EVD	ICP	ECP	CCP	PCP	HV	R	LON	LAT	D_{Jup}	ROT	S_{LON}	S_{LAT}	V	VEF	M	MEF
6601	07-229 20:42	1	1	91	5	12	0	6	15	15	1	0	47	31	1	0	0	0	1	4	1.39294	337.2	-1.1	5.16994	23	102	67	43.5	1.9	$2.4 \cdot 10^{-15}$	10.5
6602	07-229 22:32	1	1	105	2	11	0	15	15	15	1	0	46	31	1	0	0	0	1	4	1.39293	337.2	-1.0	5.17008	42	101	48	11.8	11.8	$1.2 \cdot 10^{-13}$	5858.3
6603	07-229 23:43	1	1	154	3	2	0	10	15	15	1	0	43	30	1	0	0	0	1	4	1.39293	337.2	-1.0	5.17008	111	104	-20	10.4	1.9	$4.4 \cdot 10^{-14}$	10.5
6604	07-230 22:00	1	1	209	1	10	0	15	14	15	1	0	46	31	1	0	0	0	1	4	1.39294	337.3	-0.3	5.17123	186	232	-80	11.8	11.8	$8.6 \cdot 10^{-14}$	5858.3
6605	07-231 01:40	1	1	103	4	3	0	9	15	15	1	0	45	30	1	0	0	0	1	4	1.39295	337.3	-0.2	5.17138	37	103	53	14.1	1.9	$2.8 \cdot 10^{-14}$	10.5
6606	07-231 11:29	3	2	72	13	21	3	7	7	6	0	1	40	0	1	0	0	0	1	4	1.39298	337.4	0.1	5.17183	352	242	81	34.1	1.9	$7.1 \cdot 10^{-14}$	10.5
6607	07-231 12:51	2	1	94	2	7	0	15	7	11	0	0	0	0	1	0	0	0	1	4	1.39299	337.4	0.2	5.17198	23	109	66	56.0	2.0	$2.2 \cdot 10^{-16}$	12.5
6608	07-232 05:46	1	1	15	4	2	0	8	15	15	1	0	4	26	1	0	0	0	1	4	1.39308	337.5	0.6	5.17276	270	270	0	21.4	1.9	$5.4 \cdot 10^{-15}$	10.5
6609	07-232 23:46	2	1	54	7	7	5	10	15	15	1	1	0	0	1	0	0	0	1	4	1.39322	337.6	1.2	5.17371	322	261	51	10.4	1.9	$1.9 \cdot 10^{-13}$	10.5
6610	07-233 05:45	1	1	60	2	10	0	15	14	15	1	0	23	30	1	0	0	0	1	4	1.39329	337.7	1.4	5.17404	330	257	59	11.8	11.8	$1.1 \cdot 10^{-13}$	5858.3
6611	07-233 08:18	1	1	135	2	10	0	15	15	15	1	0	19	31	1	0	0	0	1	4	1.39332	337.7	1.5	5.17420	75	99	14	11.8	11.8	$1.1 \cdot 10^{-13}$	5858.3
6612	07-233 18:33	3	5	53	55	50	30	13	6	5	0	1	63	0	1	0	0	0	1	4	1.39346	337.8	1.8	5.17487	318	259	46	2.0	1.9	$4.1 \cdot 10^{-07}$	10.5
6613	07-234 02:33	1	1	148	2	13	0	4	15	15	1	0	63	31	1	0	0	0	1	4	1.39354	337.8	2.0	5.17521	90	97	0	11.8	11.8	$1.7 \cdot 10^{-13}$	5858.3
6614	07-234 04:49	2	2	44	13	24	6	10	7	15	0	1	27	0	1	0	0	0	1	4	1.39359	337.8	2.1	5.17538	303	262	32	10.4	1.9	$5.5 \cdot 10^{-12}$	10.5
6615	07-234 11:22	2	2	66	10	19	0	7	7	7	0	0	36	0	1	0	0	0	1	4	1.39367	337.8	2.3	5.17572	333	248	61	34.1	1.9	$2.9 \cdot 10^{-14}$	10.5
6616	07-234 18:50	3	3	84	19	24	10	6	6	6	0	1	43	0	1	0	0	0	1	4	1.39382	337.9	2.6	5.17624	357	195	76	28.0	1.6	$3.8 \cdot 10^{-13}$	6.0
6617	07-236 00:41	2	1	166	4	8	0	8	7	8	0	0	6	26	1	0	0	0	1	4	1.39439	338.1	3.5	5.17804	105	91	-15	34.6	1.6	$2.7 \cdot 10^{-15}$	6.0
6618	07-236 01:26	1	1	124	2	8	0	15	15	15	1	0	47	31	1	0	0	0	1	4	1.39439	338.1	3.5	5.17804	46	106	41	2.3	2.0	$1.3 \cdot 10^{-11}$	12.5
6619	07-236 14:31	1	1	103	2	10	0	11	15	15	1	0	47	31	1	0	0	0	1	4	1.39466	338.2	3.9	5.17879	14	139	68	11.8	11.8	$1.1 \cdot 10^{-13}$	5858.3
6620	07-237 03:07	2	3	80	23	8	3	7	15	15	1	1	47	30	1	0	0	0	1	4	1.39502	338.3	4.3	5.17974	338	228	61	14.1	1.9	$1.1 \cdot 10^{-12}$	10.5
6621	07-237 04:44	1	1	153	1	9	0	15	15	15	1	0	19	31	1	0	0	0	1	4	1.39502	338.3	4.3	5.17974	80	95	8	11.8	11.8	$7.3 \cdot 10^{-14}$	5858.3
6622	07-237 12:37	2	5	30	49	49	30	9	9	15	1	1	24	10	1	0	0	0	1	4	1.39526	338.3	4.6	5.18032	265	263	-5	11.8	11.8	$3.4 \cdot 10^{-10}$	5858.3
6623	07-238 04:37	1	1	156	3	11	0	9	15	15	1	0	47	31	1	0	0	0	1	4	1.39568	338.4	5.1	5.18130	78	94	10	14.1	1.9	$9.5 \cdot 10^{-14}$	10.5
6624	07-238 13:55	2	1	130	3	7	0	9	9	10	0	0	0	0	1	0	0	0	1	4	1.39595	338.5	5.4	5.18191	39	112	46	21.0	1.6	$1.1 \cdot 10^{-14}$	6.0
6625	07-239 02:06	1	2	84	12	10	0	14	13	15	1	0	63	30	1	0	0	0	1	4	1.39633	338.5	5.7	5.18272	330	228	52	2.0	1.9	$1.7 \cdot 10^{-10}$	10.5
6626	07-239 04:23	0	1	80	4	10	0	8	8	13	1	0	59	26	1	0	0	0	1	4	1.39643	338.6	5.8	5.18293	324	234	47	28.0	1.6	$7.4 \cdot 10^{-15}$	6.0
6627	07-239 07:31	2	2	93	11	13	12	10	15	15	1	1	7	30	1	0	0	0	1	4	1.39653	338.6	5.9	5.18314	341	213	59	4.9	1.7	$9.4 \cdot 10^{-12}$	7.7
6628	07-239 10:53	1	2	146	10	11	0	9	15	15	1	0	1	30	1	0	0	0	1	4	1.39663	338.6	6.0	5.18335	55	102	31	14.1	1.9	$3.0 \cdot 10^{-13}$	10.5
6629	07-239 20:37	1	1	119	2	9	0	10	15	15	1	0	47	31	1	0	0	0	1	4	1.39694	338.7	6.3	5.18397	13	145	61	11.8	11.8	$8.8 \cdot 10^{-14}$	5858.3
6630	07-241 05:19	3	2	89	12	20	9	7	8	6	0	1	39	0	1	0	0	0	1	4	1.39819	338.9	7.3	5.18636	321	228	42	34.1	1.9	$5.2 \cdot 10^{-14}$	10.5
6631	07-242 12:36	0	1	42	3	6	0	8	5	9	1	0	46	20	1	0	0	0	1	4	1.39961	339.1	8.3	5.18884	244	266	-24	38.7	1.6	$1.0 \cdot 10^{-15}$	6.0
6632	07-242 19:32	3	3	127	21	27	15	5	5	6	0	1	46	0	0	0	0	0	1	4	1.39988	339.1	8.5	5.18931	2	163	57	43.7	1.6	$1.9 \cdot 10^{-13}$	6.0
6633	07-243 00:09	2	4	93	28	22	18	11	9	15	1	1	24	30	1	0	0	0	1	4	1.40017	339.1	8.7	5.18978	312	228	33	2.5	1.9	$3.2 \cdot 10^{-09}$	10.5
6634	07-243 01:22	2	2	122	8	12	0	7	7	6	0	0	4	31	1	0	0	0	1	4	1.40017	339.1	8.7	5.18978	353	179	55	43.7	1.6	$4.0 \cdot 10^{-15}$	6.0
6635	07-243 09:57	2	3	104	20	10	14	14	14	15	1	1	25	31	1	0	0	0	1	4	1.40060	339.2	8.9	5.19049	325	215	42	2.0	1.9	$4.8 \cdot 10^{-10}$	10.5
6636	07-243 10:37	3	3	159	22	27	6	7	5	6	0	1	47	0	1	0	0	0	1	4	1.40060	339.2	8.9	5.19049	43	109	36	28.1	1.6	$1.1 \cdot 10^{-12}$	6.0
6637	07-243 23:21	1	1	244	2	13	0	15	15	15	1	0	46	31	1	0	0	0	1	4	1.40119	339.3	9.3	5.19144	159	26	-57	11.8	11.8	$1.7 \cdot 10^{-13}$	5858.3
6638	07-245 00:09	3	3	106	20	27	8	8	5	6	0	1	46	0	1	0	0	0	1	4	1.40261	339.4	10.1	5.19365	318	217	35	10.4	1.9	$2.2 \cdot 10^{-11}$	10.5
6639	07-245 03:06	2	3	155	17	9	2	15	15	15	1	1	47	30	1	0	0	0	1	4	1.40278	339.5	10.2	5.19390	26	124	44	2.0	1.9	$2.2 \cdot 10^{-10}$	10.5
6640	07-245 07:18	3	3	111	19	24	8	8	6	6	0	1	43	0	1	0	0	0	1	4	1.40294	339.5	10.3	5.19415	324	211	38	19.5	1.6	$1.5 \cdot 10^{-12}$	6.0
6641	07-245 11:02	2	2	159	12	14	13	11	11	15	1	1	36	9	1	0	0	0	1	4	1.40311	339.5	10.4	5.19440	31	119	41	12.6	1.6	$8.9 \cdot 10^{-13}$	6.0
6642	07-245 18:19	3	1	107	4	9	4	7	7	8	0	1	0	0	1	0	0	0	1	4	1.40362	339.6	10.7	5.19516	315	217	32	43.7	1.6	$1.2 \cdot 10^{-15}$	6.0
6643	07-246 12:56	1	1	145	1	11	0	15	14	15	1	0	47	31	1	0	0	0	1	4	1.40468	339.7	11.2	5.19671	5	153	48	11.8	11.8	$1.0 \cdot 10^{-13}$	5858.3
6644	07-247 07:06	2	1	211	7	12	0	7	7	8	0	0	35	0	1	0	0	0	1	4	1.40578	339.8	11.8	5.19829	94	70	-5	43.7	1.6	$3.3 \cdot 10^{-15}$	6.0
6645	07-247 09:04	1	2	188	9	2	0	13	15	15	1	0	44	30	1	0	0	0	1	4	1.40597	339.8	11.9	5.19855	61	91	19	2.5	1.9	$1.1 \cdot 10^{-11}$	10.5
6646	07-247 09:21	3	3	170	22	25	6	7	7	6	0	1	47	0	1	0	0	0	1	4	1.40597	339.8	11.9	5.19855	36	112	36	21.0	1.6	$2.4 \cdot 10^{-12}$	6.0
6647	07-247 12:54	3	4	124	30	49	28	8	6	5	0	1	47	0	1	0	0	0	1	4	1.40616	339.8	11.9	5.19882	330	197	39	10.4	1.9	$3.0 \cdot 10^{-10}$	10.5
6648	07-248 03:21	2	2	19	8	14	0	7	7	7	0	0	37	0	1	0	0	0	1	4	1.40713	339.9	12.4	5.20017	180	337	-55	43.7	1.6	$5.5 \cdot 10^{-15}$	6.0
6649	07-248 05:03	2	2	81	9	19	0	7	6	6	0	0	37	0	1	0	0	0	1	4	1.40713	339.9	12.4	5.20017	267	244	-5	34.1	1.9	$2.4 \cdot 10^{-14}$	10.5
6650	07-248 13:18	2	1	128	3	7	0	9	8	10	0	0	5	31	1	0	0	0	1	4	1.40773	340.0	12.7	5.20099	331	193	38	22.7	1.6	$7.8 \cdot 10^{-15}$	6.0
6651	07-249 02:23	3	3	111	20	27	11	8	5	6	0	1	46	0	1	0	0	0	1	4	1.40855	340.1	13.0	5.20209	306	216	22	10.4	1.9	$2.2 \cdot 10^{-11}$	10.5
6652	07-250 08:54	2	1	116	6	11	0	7	7	7	0	0	0	0	1	0	0	0	1	4	1.41068	340.2	13.9	5.20492	307	211	23	43.7	1.6	$2.3 \cdot 10^{-15}$	6.0
6653	07-251 08:13	2	1	148	4	10	0	8	7	8	0	0	2	26	1	0	0	0	1	4	1.41249	340.4	14.7	5.20725	349	165	40	34.6	1.6	$3.8 \cdot 10^{-15}$	6.0
6654	07-252 05:29	1	1	182	5	11	0	9	15	15	1	0	47	31	1	0	0	0	1	4	1.41413	340.5	15.3	5.20933	33	108	32	5.7	2.1	$1.6 \cdot 10^{-12}$	15.7
6655	07-253 08:25	3	1	143	4	9	12	7	7	7	0	1	2	26	1	0	0	0	1	4	1.41635	340.7	16.1	5.21208	335	177	34	43.7	1.6	$1.2 \cdot 10^{-15}$	6.0

No.	IMP. DATE	CLN	AR	SEC	IA	EA	CA	IT	ET	EIT	EIC	IIC	PA	PET	EVD	ICP	ECP	CCP	PCP	HV	R	LON	LAT	D_{Jup}	ROT	S_{LON}	S_{LAT}	V	VEF	M	MEF
6656	07-254 04:44	2	1	148	2	7	0	15	7	10	0	0	2	26	1	0	0	0	1	4	1.41814	340.8	16.7	5.21426	339	170	34	56.0	2.0	$2.2 \cdot 10^{-16}$	12.5
6657	07-254 06:33	1	1	157	1	1	0	15	15	15	1	0	2	31	1	0	0	0	1	4	1.41840	340.9	16.8	5.21458	351	155	37	11.8	11.8	$1.9 \cdot 10^{-14}$	5858.3
6658	07-254 08:21	2	3	178	18	13	7	10	15	15	1	1	47	30	1	0	0	0	1	4	1.41840	340.9	16.8	5.21458	21	118	34	5.0	1.9	$1.7 \cdot 10^{-11}$	10.5
6659	07-254 11:05	2	1	163	5	10	0	7	7	8	0	0	2	26	1	0	0	0	1	4	1.41866	340.9	16.9	5.21489	359	144	37	43.7	1.6	$1.7 \cdot 10^{-15}$	6.0
6660	07-254 22:47	2	1	152	1	6	0	15	8	11	0	0	2	26	1	0	0	0	1	4	1.41973	341.0	17.3	5.21617	342	164	35	36.7	2.0	$8.9 \cdot 10^{-16}$	12.5
6661	07-255 08:39	2	1	134	4	9	0	7	7	8	0	0	2	26	1	0	0	0	1	4	1.42054	341.0	17.5	5.21713	316	191	24	43.7	1.6	$1.2 \cdot 10^{-15}$	6.0
6662	07-255 12:32	3	1	185	5	9	1	7	7	7	0	1	2	31	1	0	0	0	1	4	1.42109	341.1	17.7	5.21778	27	109	31	43.7	1.6	$1.4 \cdot 10^{-15}$	6.0
6663	07-255 14:05	2	1	179	1	7	0	15	9	11	0	0	2	26	1	0	0	0	1	4	1.42109	341.1	17.7	5.21778	18	119	34	31.3	2.0	$1.8 \cdot 10^{-15}$	12.5
6664	07-255 15:28	3	3	201	23	26	6	7	7	6	0	1	47	0	1	0	0	0	1	4	1.42136	341.1	17.8	5.21811	49	87	21	21.0	1.6	$3.4 \cdot 10^{-12}$	6.0
6665	07-255 19:41	3	1	106	5	8	7	7	8	8	0	1	2	26	1	0	0	0	1	4	1.42164	341.1	17.9	5.21843	275	224	0	35.4	1.6	$2.9 \cdot 10^{-15}$	6.0
6666	07-255 20:04	2	1	161	4	9	0	8	7	8	0	0	3	26	1	0	0	0	1	4	1.42164	341.1	17.9	5.21843	352	150	36	34.6	1.6	$3.2 \cdot 10^{-15}$	6.0
6667	07-255 20:39	2	1	119	1	5	0	15	9	10	0	0	2	26	1	0	0	0	1	4	1.42164	341.1	17.9	5.21843	293	210	11	31.3	2.0	$1.3 \cdot 10^{-15}$	12.5
6668	07-256 11:43	2	2	189	8	8	7	9	15	15	1	1	35	30	1	0	0	0	1	4	1.42304	341.2	18.3	5.22008	30	105	30	14.1	1.9	$1.3 \cdot 10^{-13}$	10.5
6669	07-257 00:34	2	2	111	8	13	0	7	7	7	0	0	36	0	1	0	0	0	1	4	1.42448	341.3	18.8	5.22175	278	219	2	43.7	1.6	$4.7 \cdot 10^{-15}$	6.0
6670	07-258 09:31	2	2	62	8	12	0	8	7	6	0	0	2	26	1	0	0	0	1	4	1.42775	341.5	19.7	5.22549	206	282	-38	34.6	1.6	$1.1 \cdot 10^{-14}$	6.0
6671	07-261 08:19	1	2	117	8	8	0	12	15	0	1	0	12	30	1	0	0	0	1	4	1.43507	342.0	21.7	5.23367	276	213	0	5.0	1.9	$2.4 \cdot 10^{-12}$	10.5
6672	07-261 18:01	1	1	160	2	1	0	15	15	15	1	0	3	31	1	0	0	0	1	4	1.43641	342.1	22.1	5.23514	335	159	29	11.8	11.8	$2.4 \cdot 10^{-14}$	5858.3
6673	07-262 13:16	2	3	145	23	20	13	7	15	15	1	1	63	29	1	0	0	0	1	4	1.43846	342.2	22.6	5.23737	312	181	20	14.1	1.9	$5.6 \cdot 10^{-12}$	10.5
6674	07-262 14:14	3	4	142	30	51	29	6	13	5	0	1	47	0	1	0	0	0	1	4	1.43846	342.2	22.6	5.23737	308	184	18	21.4	1.9	$5.0 \cdot 10^{-11}$	10.5
6675	07-265 04:43	2	1	7	2	1	0	9	15	11	0	0	2	25	1	0	0	0	1	4	1.44596	342.6	24.4	5.24542	113	20	-16	11.8	11.8	$2.4 \cdot 10^{-14}$	5858.3
6676	07-265 12:09	1	1	73	4	1	0	8	15	0	1	0	3	31	1	0	0	0	1	4	1.44707	342.7	24.7	5.24660	205	273	-36	21.4	1.9	$4.5 \cdot 10^{-15}$	10.5
6677	07-265 12:21	2	3	170	23	14	11	12	14	15	1	1	11	31	1	0	0	0	1	4	1.44707	342.7	24.7	5.24660	342	147	29	2.0	1.9	$1.5 \cdot 10^{-09}$	10.5
6678	07-266 13:56	2	1	129	5	9	0	7	7	7	0	0	3	31	1	0	0	0	1	4	1.45009	342.8	25.4	5.24979	282	201	3	43.7	1.6	$1.4 \cdot 10^{-15}$	6.0
6679	07-267 22:27	2	2	109	15	15	10	10	0	0	1	1	47	30	1	0	0	0	1	4	1.45437	343.1	26.3	5.25426	251	225	-14	10.4	1.9	$2.3 \cdot 10^{-12}$	10.5
6680	07-268 05:28	2	3	209	19	5	4	3	2	3	1	1	46	0	1	0	0	0	1	4	1.45517	343.1	26.5	5.25508	31	87	25	70.0	1.9	$6.9 \cdot 10^{-16}$	10.5
6681	07-268 05:52	1	1	236	7	2	0	10	14	0	1	0	18	29	1	0	0	0	1	4	1.45517	343.1	26.5	5.25508	69	52	8	10.4	1.9	$8.6 \cdot 10^{-14}$	10.5
6682	07-268 07:16	1	1	152	2	7	0	15	15	15	1	0	15	31	1	0	0	0	1	4	1.45556	343.1	26.6	5.25550	311	174	18	2.3	2.0	$1.1 \cdot 10^{-11}$	12.5
6683	07-268 09:29	2	1	153	1	4	1	15	15	0	1	1	9	30	1	0	0	0	1	4	1.45596	343.2	26.6	5.25591	312	173	18	11.8	11.8	$3.0 \cdot 10^{-14}$	5858.3
6684	07-268 13:09	2	1	162	4	7	0	8	7	8	0	0	3	31	1	0	0	0	1	4	1.45636	343.2	26.7	5.25633	325	161	24	34.6	1.6	$2.2 \cdot 10^{-15}$	6.0
6685	07-270 15:52	1	1	107	5	10	0	5	10	0	1	0	47	31	1	0	0	0	1	4	1.46334	343.6	28.1	5.26351	244	229	-18	43.1	1.6	$1.8 \cdot 10^{-15}$	6.0
6686	07-272 22:38	1	2	174	8	5	0	10	15	0	1	0	40	30	1	0	0	0	1	4	1.47108	343.9	29.6	5.27138	334	147	26	10.4	1.9	$1.6 \cdot 10^{-13}$	10.5
6687	07-274 07:27	2	1	122	1	4	0	15	8	12	0	0	3	31	1	0	0	0	1	4	1.47598	344.2	30.5	5.27632	259	213	-9	11.8	11.8	$3.0 \cdot 10^{-14}$	5858.3
6688	07-276 04:27	1	1	176	4	4	0	13	15	0	1	0	45	30	1	0	0	0	1	4	1.48287	344.5	31.8	5.28322	332	146	25	2.5	1.9	$6.1 \cdot 10^{-12}$	10.5
6689	07-277 17:34	2	1	120	2	7	0	15	8	10	0	0	2	31	1	0	0	0	1	4	1.48855	344.8	32.7	5.28887	251	217	-14	36.7	2.0	$1.3 \cdot 10^{-15}$	12.5
6690	07-277 18:10	1	1	128	4	3	0	8	15	0	1	0	3	31	1	0	0	0	1	4	1.48903	344.8	32.8	5.28935	263	207	-7	21.4	1.9	$6.1 \cdot 10^{-15}$	10.5
6691	07-277 22:33	1	1	109	2	1	0	15	14	0	1	0	3	25	1	0	0	0	1	4	1.48951	344.9	32.9	5.28983	236	231	-22	11.8	11.8	$2.4 \cdot 10^{-14}$	5858.3
6692	07-278 14:31	2	1	190	3	5	0	12	3	9	0	0	17	1	1	0	0	0	1	4	1.49194	345.0	33.3	5.29222	349	127	29	18.7	4.1	$1.3 \cdot 10^{-14}$	151.2
6693	07-279 14:27	2	1	167	3	6	0	8	9	8	0	0	4	31	1	0	0	0	1	4	1.49586	345.2	33.9	5.29610	315	161	19	25.9	1.6	$4.1 \cdot 10^{-15}$	6.0
6694	07-280 00:46	2	1	198	2	1	0	15	4	12	0	0	3	31	1	0	0	0	1	4	1.49785	345.2	34.3	5.29806	358	115	29	11.8	11.8	$2.4 \cdot 10^{-14}$	5858.3
6695	07-281 00:14	3	4	172	26	49	14	7	5	5	0	1	47	0	1	0	0	0	1	4	1.50187	345.4	34.9	5.30201	320	155	21	14.1	1.9	$7.7 \cdot 10^{-11}$	10.5
6696	07-282 23:46	2	1	146	5	4	0	8	1	9	0	0	8	1	1	0	0	0	1	4	1.50958	345.8	36.1	5.30955	281	189	2	21.4	1.9	$8.3 \cdot 10^{-15}$	10.5
6697	07-283 00:22	3	3	190	21	27	11	6	5	5	0	1	46	0	1	0	0	0	1	4	1.51010	345.8	36.1	5.31006	343	130	28	34.6	1.6	$5.0 \cdot 10^{-13}$	6.0
6698	07-284 09:41	1	1	67	3	1	0	8	15	0	1	0	3	31	1	0	0	0	1	4	1.51590	346.1	37.0	5.31571	169	305	-37	21.4	1.9	$3.9 \cdot 10^{-15}$	10.5
6699	07-288 08:40	3	3	171	22	28	28	6	5	6	0	1	34	31	1	0	0	0	1	4	1.53283	346.9	39.4	5.33213	311	162	17	34.6	1.6	$7.0 \cdot 10^{-13}$	6.0
6700	07-288 14:40	1	1	190	3	9	0	10	15	0	1	0	47	31	1	0	0	0	1	4	1.53395	346.9	39.5	5.33322	337	135	26	4.9	1.7	$1.3 \cdot 10^{-12}$	7.7
6701	07-288 22:33	2	1	13	3	7	0	8	8	9	0	0	2	25	1	0	0	0	1	4	1.53564	347.0	39.7	5.33485	88	24	-2	28.0	1.6	$3.7 \cdot 10^{-15}$	6.0
6702	07-294 09:24	1	1	229	5	11	0	11	15	0	1	0	46	31	1	0	0	0	1	4	1.56130	348.2	43.0	5.35953	26	79	25	4.2	1.6	$4.0 \cdot 10^{-12}$	6.0
6703	07-295 14:24	2	1	86	5	9	0	7	7	7	0	0	3	31	1	0	0	0	1	4	1.56674	348.4	43.6	5.36475	184	283	-38	43.7	1.6	$1.4 \cdot 10^{-15}$	6.0
6704	07-296 21:39	3	4	189	28	49	29	7	6	5	0	1	47	0	1	0	0	0	1	4	1.57348	348.7	44.4	5.37121	328	144	24	14.1	1.9	$1.0 \cdot 10^{-10}$	10.5
6705	07-296 22:12	2	1	110	4	9	0	7	7	8	0	0	3	31	1	0	0	0	1	4	1.57348	348.7	44.4	5.37121	216	244	-30	43.7	1.6	$1.2 \cdot 10^{-15}$	6.0
6706	07-297 14:14	2	1	36	1	1	0	15	0	12	0	0	3	31	1	0	0	0	1	4	1.57657	348.9	44.8	5.37417	112	3	-15	11.8	11.8	$1.9 \cdot 10^{-14}$	5858.3
6707	07-304 14:04	3	3	154	21	27	3	6	5	5	0	1	47	0	1	0	0	0	1	4	1.61245	350.6	48.7	5.40849	272	194	-2	34.6	1.6	$5.0 \cdot 10^{-13}$	6.0
6708	07-306 00:29	2	1	119	4	8	0	7	7	7	0	0	3	31	1	0	0	0	1	4	1.62039	351.0	49.5	5.41612	222	239	-28	43.7	1.6	$1.0 \cdot 10^{-15}$	6.0
6709	07-306 02:32	2	2	167	8	7	4	9	15	0	1	1	2	31	1	0	0	0	1	4	1.62039	351.0	49.5	5.41612	289	180	6	14.1	1.9	$1.1 \cdot 10^{-13}$	10.5
6710	07-308 08:48	2	1	122	2	5	0	15	10	10	0	0	3	31	1	0	0	0	1	4	1.63251	351.6	50.6	5.42772	224	237	-27	26.5	2.0	$2.7 \cdot 10^{-15}$	12.5

No.	IMP. DATE	CLN	AR	SEC	IA	EA	CA	IT	ET	EIT	EIC	IIC	PA	PET	EVD	ICP	ECP	CCP	PCP	HV	R	LON	LAT	D_{Jup}	ROT	S_{LON}	S_{LAT}	V	VEF	M	MEF
6711	07-308 19:03	3	4	191	24	28	10	8	6	5	0	1	47	0	1	0	0	0	1	4	1.63524	351.7	50.9	5.43033	321	151	21	19.5	1.6	$7.6 \cdot 10^{-12}$	6.0
6712	07-309 11:53	3	3	196	23	29	29	6	5	5	0	1	47	0	1	0	0	0	1	4	1.63865	351.9	51.2	5.43360	327	145	23	34.6	1.6	$9.8 \cdot 10^{-13}$	6.0
6713	07-309 22:37	2	2	149	10	19	0	8	6	6	0	0	38	0	1	0	0	0	1	4	1.64140	352.0	51.5	5.43622	261	204	-8	21.4	1.9	$1.5 \cdot 10^{-13}$	10.5
6714	07-313 19:02	2	1	238	1	1	0	15	15	12	0	0	2	31	1	0	0	0	1	4	1.66299	353.1	53.5	5.45691	23	84	26	11.8	11.8	$1.9 \cdot 10^{-14}$	5858.3
6715	07-315 23:14	2	1	62	7	11	0	8	7	7	0	0	3	31	1	0	0	0	1	4	1.67505	353.8	54.5	5.46850	134	344	-26	34.6	1.6	$7.6 \cdot 10^{-15}$	6.0
6716	07-322 23:06	1	1	152	4	3	0	9	15	0	1	0	2	24	1	0	0	0	1	4	1.71586	356.0	57.9	5.50781	255	211	-11	14.1	1.9	$2.8 \cdot 10^{-14}$	10.5
6717	07-327 11:18	1	1	181	5	7	0	9	15	0	1	0	2	24	1	0	0	0	1	4	1.74286	357.7	59.9	5.53397	293	181	8	5.7	2.1	$7.9 \cdot 10^{-13}$	15.7
6718	07-327 23:30	1	1	150	2	9	0	9	15	0	1	0	37	31	1	0	0	0	1	4	1.74589	357.8	60.1	5.53692	249	218	-14	11.8	11.8	$8.8 \cdot 10^{-14}$	5858.3
6719	07-334 08:17	2	3	151	19	7	1	7	15	0	1	1	46	31	1	0	0	0	1	4	1.78513	0.4	62.9	5.57519	246	223	-16	14.1	1.9	$4.3 \cdot 10^{-13}$	10.5

Figures

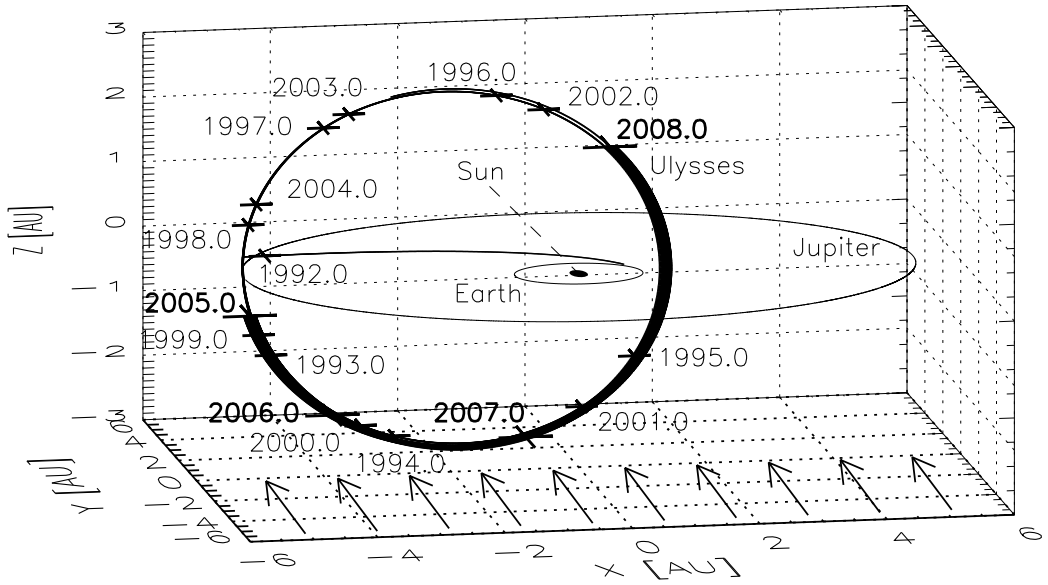

Figure 1: The trajectory of Ulysses in ecliptic coordinates with the Sun at the centre. The orbits of Earth and Jupiter indicate the ecliptic plane, and the initial trajectory of Ulysses was in this plane. Since Jupiter flyby in early 1992 the orbit has been almost perpendicular to the ecliptic plane (79° inclination). Crosses mark the spacecraft position at the beginning of each year. The 2005 to 2007 part of the trajectory is shown as a thick line. Vernal equinox is to the right (positive x axis). Arrows indicate the undisturbed interstellar dust flow direction which is within the measurement accuracy co-aligned with the direction of the interstellar helium gas flow. It is almost perpendicular to the orbital plane of Ulysses.

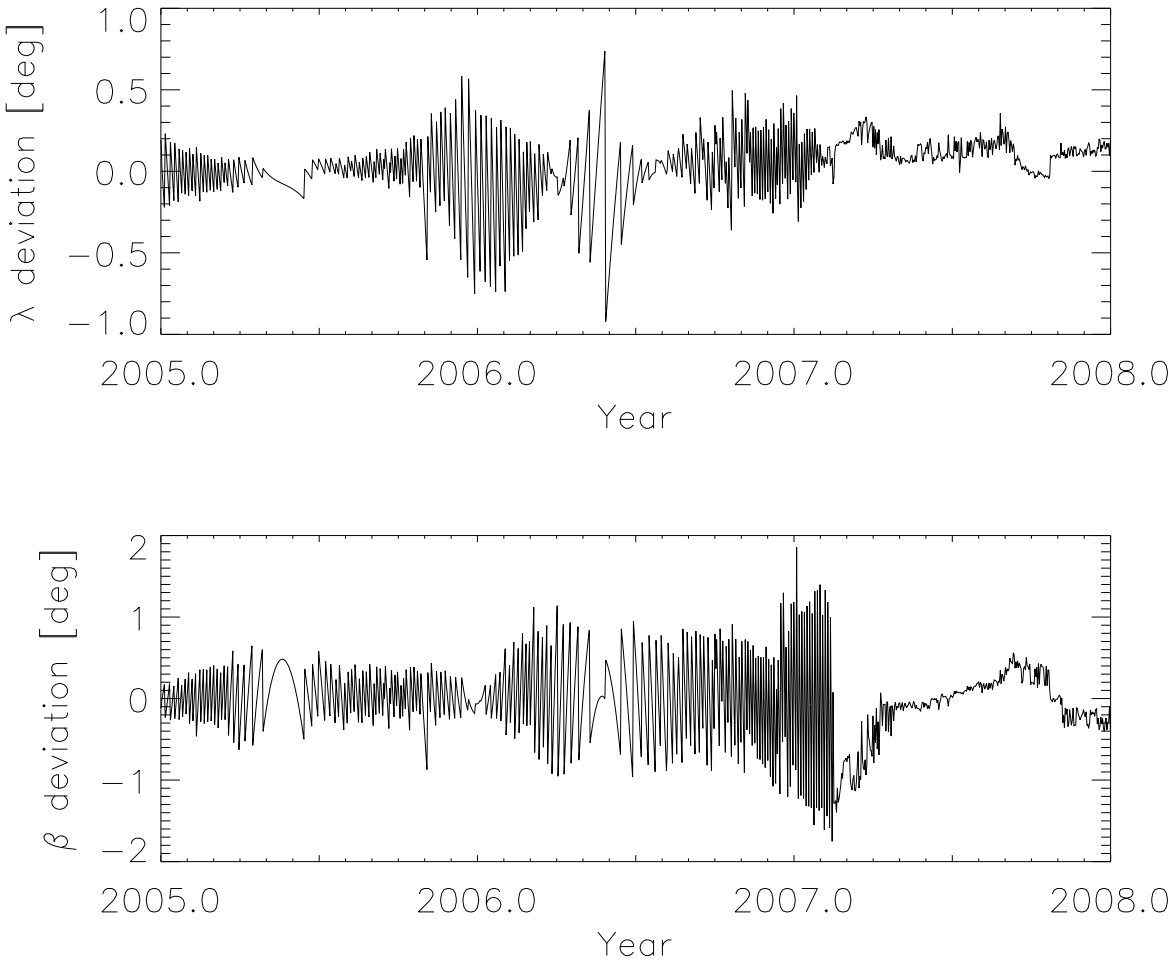

Figure 2: Spacecraft attitude: deviation of the antenna pointing direction (i.e. positive spin axis) from the nominal Earth direction. The angles are given in ecliptic longitude (top) and latitude (bottom, equinox 1950.0).

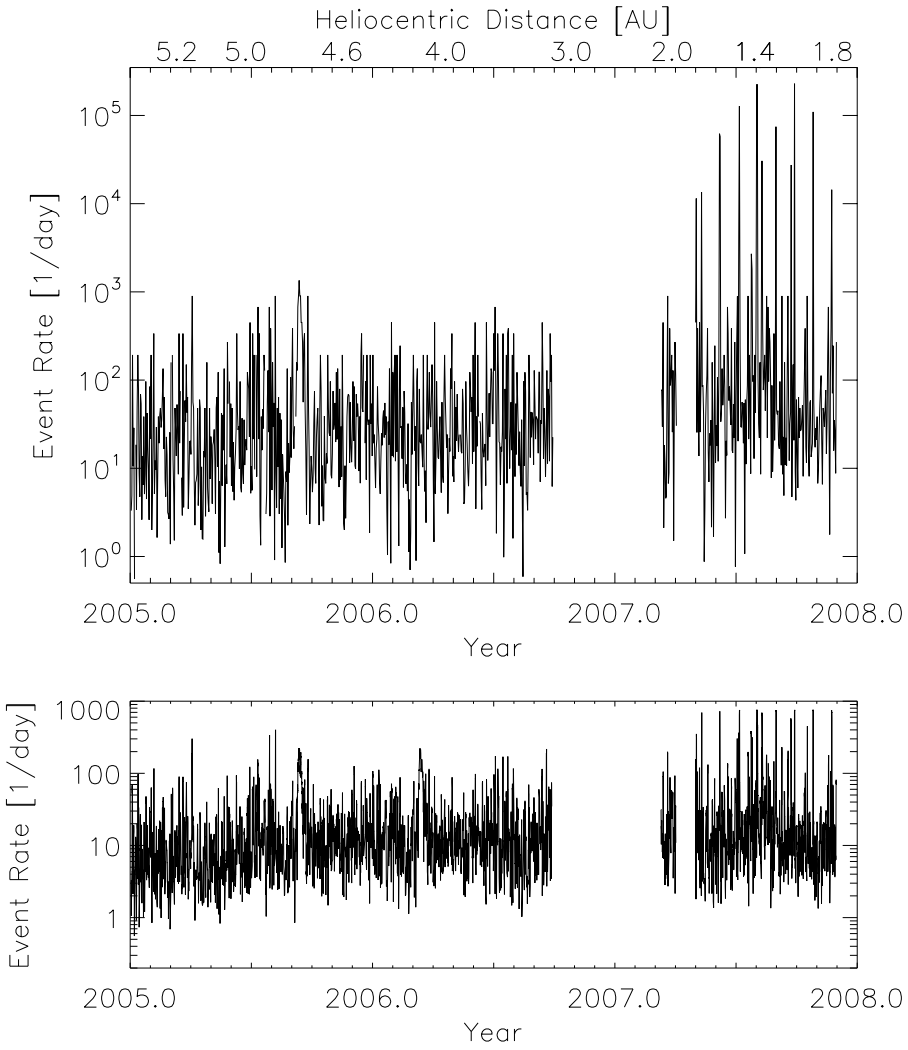

Figure 3: Noise rate (class 0 events) detected with the dust instrument. The heliocentric distance of Ulysses is indicated at the top. Upper panel: Daily maxima in the noise rate (determined from the AC01 accumulator). Sharp spikes which are strongest after May 2008 when Ulysses was in the inner solar system are caused by periodic noise tests. Lower panel: One-day average of the noise rate calculated from the number of AC01 events for which the complete information was transmitted to Earth.

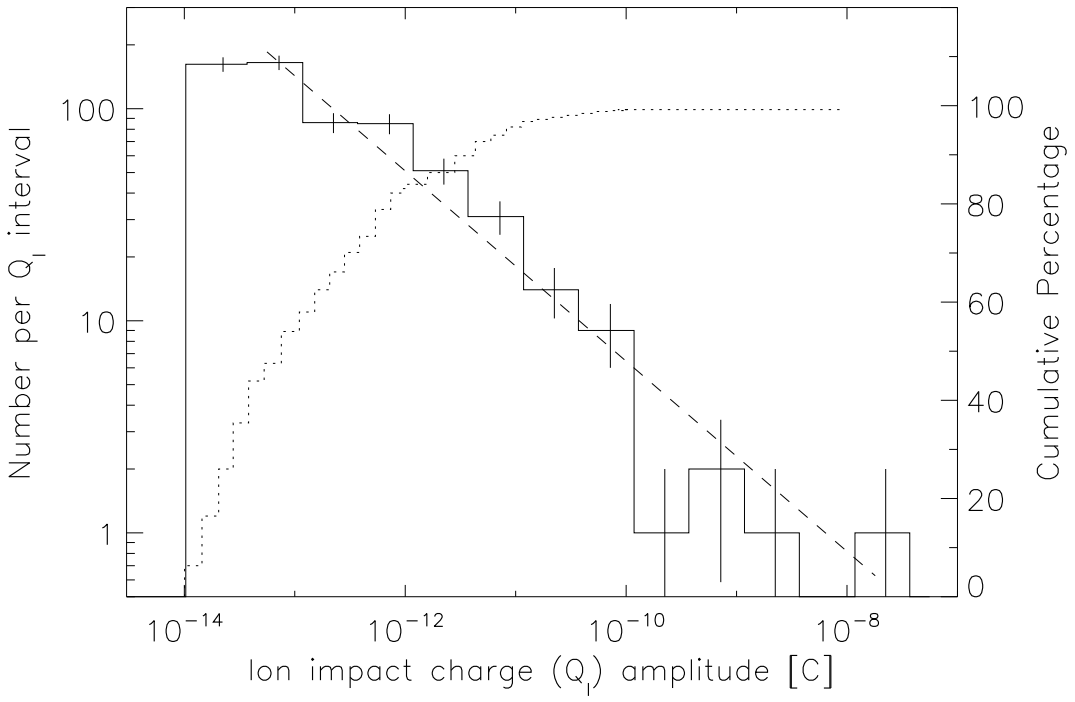

Figure 4: Distribution of the impact charge amplitude Q_{I} for all dust particles detected from 2005 to 2007. The solid line indicates the number of impacts per charge interval, and the dotted line shows the cumulative percentage. Vertical bars indicate the $\sqrt{n}$ statistical fluctuation. A power law fit to the data with $Q_{\mathrm{I}} > 3 \cdot 10^{-14}\,\mathrm{C}$ is shown as a dashed line (Number $N \sim Q_{\mathrm{I}}^{-0.45}$).

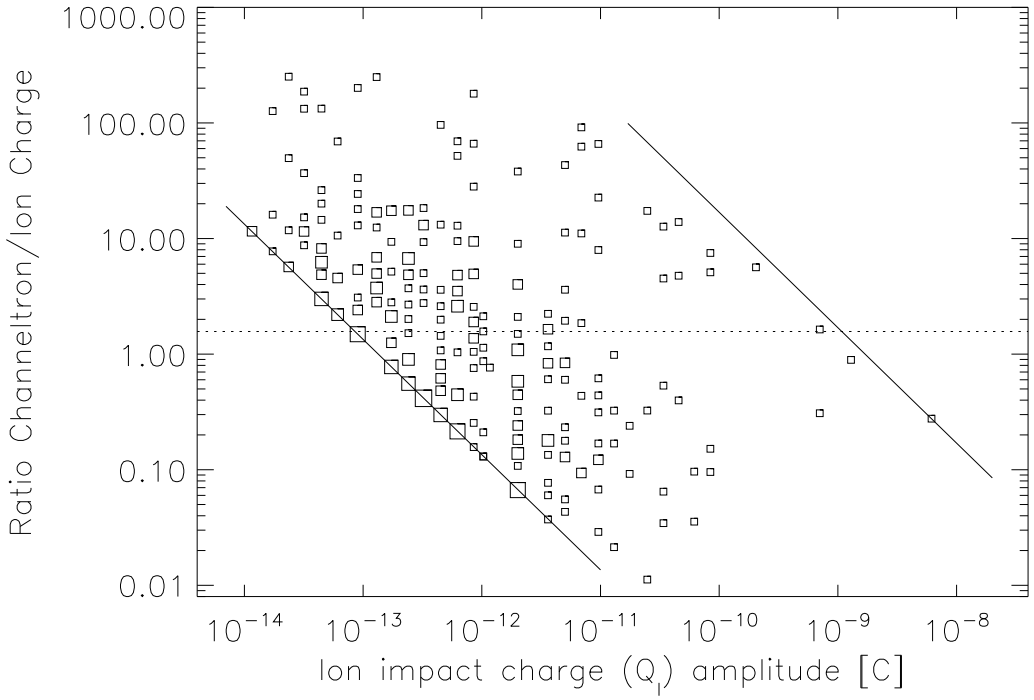

Figure 5: Channeltron amplification factor $A = Q_C/Q_I$ as a function of impact charge Q_I for all dust impacts detected between 2005 and 2007 with channeltron voltage set to HV = 4. The solid lines denote the sensitivity threshold (lower left) and the saturation limit (upper right) of the channeltron. Squares indicate dust particle impacts. The area of each square is proportional to the number of events included (the scaling of the squares is not the same as in earlier papers). The dotted horizontal line shows the mean value of the channeltron amplification A = 1.57 for ion impact charges 10^{-12} C $< Q_I < 10^{-11}$ C (82 particles).

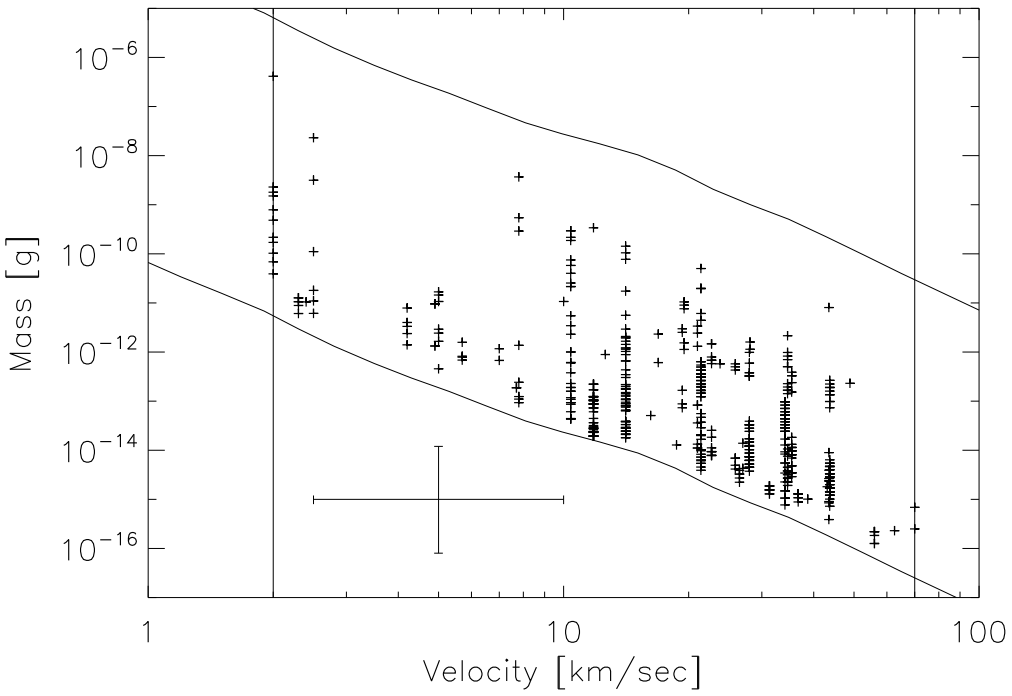

Figure 6: Masses and impact velocities of all impacts recorded with the Ulysses sensor from 2005 to 2007. The lower and upper solid lines indicate the threshold and the saturation limit of the detector, respectively, and the vertical lines indicate the calibrated velocity range. A sample error bar is shown that indicates a factor of 2 uncertainty for the velocity and a factor of 10 for the mass determination.

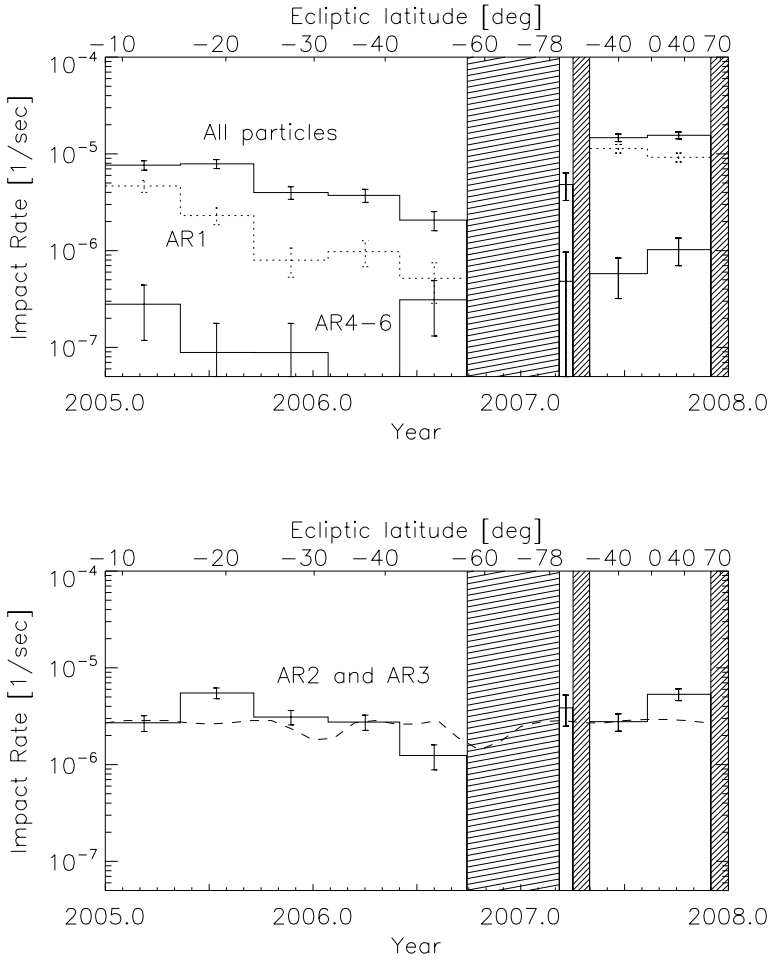

Figure 7: Impact rate of dust particles detected with the Ulysses dust sensor as a function of time. The ecliptic latitude of the spacecraft is indicated at the top. Shaded areas indicate periods when the dust instrument was switched off. Upper panel: total impact rate (upper solid histogram), impact rate of small particles (AR1, dotted histogram), and impact rate of big particles (AR4 – AR6, lower solid histogram). Note that a rate of about 10^{-7} impacts per second is caused by a single dust impact in the averaging interval of about 130 days. An averaging interval of only 24 days had to be used for March 2007 because the instrument was switched off before and after this period. Lower panel: impact rate of intermediate size particles (AR2 and AR3, solid histogram). A model for the rate of interstellar particles assuming a constant flux was fit to the data and is superimposed as a dashed line. Vertical bars indicate the $\sqrt{n}$ statistical fluctuation.

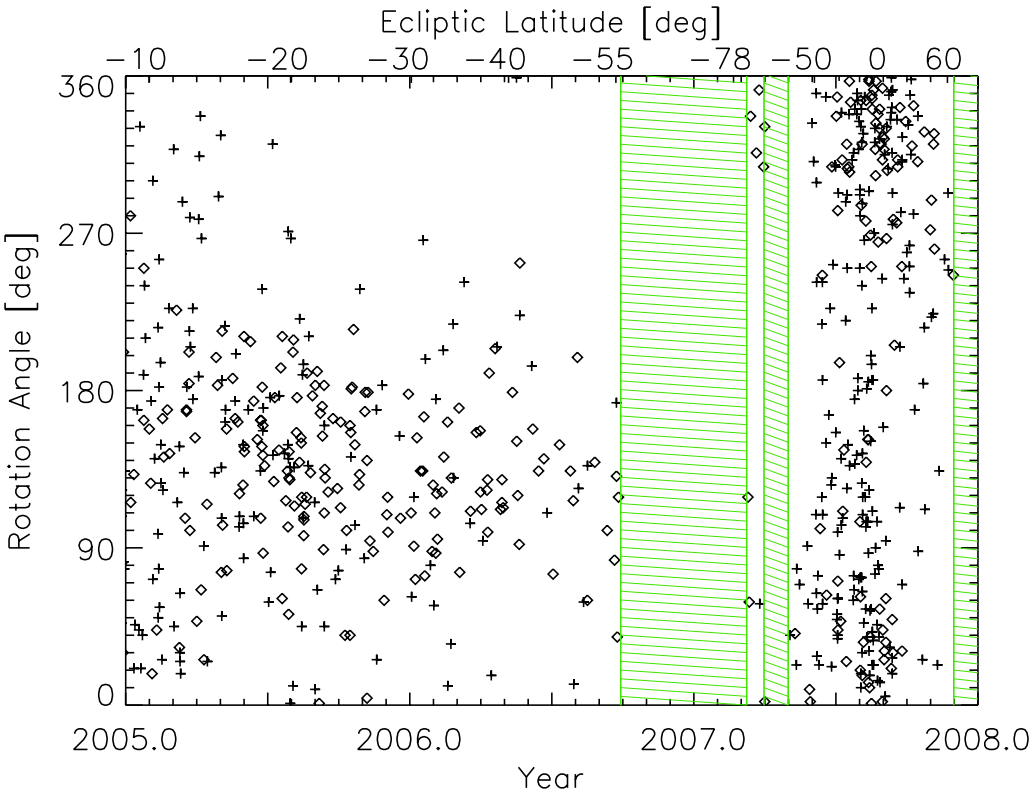

Figure 8: Rotation angle vs. time for all particles detected in the 2005-07 interval. Plus signs indicate particles with impact charge $Q_{\rm I} < 10^{-13}$ C (AR1), diamonds those with $Q_{\rm I} > 10^{-13}$ C (AR2 to AR6). Ulysses' ecliptic latitude is indicated at the top.

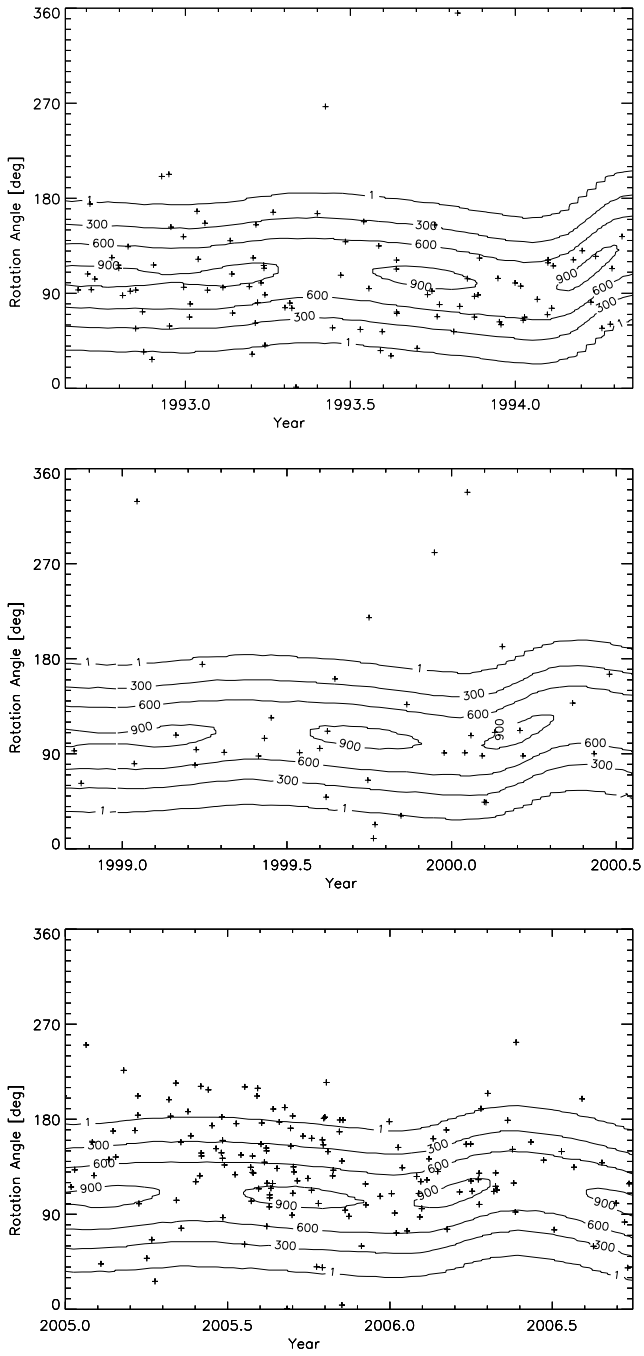

Figure 9: Rotation angle vs. time for dust impacts detected during three time intervals when Ulysses was traversing the same portion of its trajectory between $-8.5°$ and $-56°$ ecliptic latitude. Contour lines show the effective sensor area for dust particles approaching from the upstream direction of interstellar helium (Witte, 2004; Witte et al., 2004). Here we show particles with impact charges $1.5 \cdot 10^{-13}$ C $< Q_I < 10^{-11}$ C which approximately coincides with AR2-3.

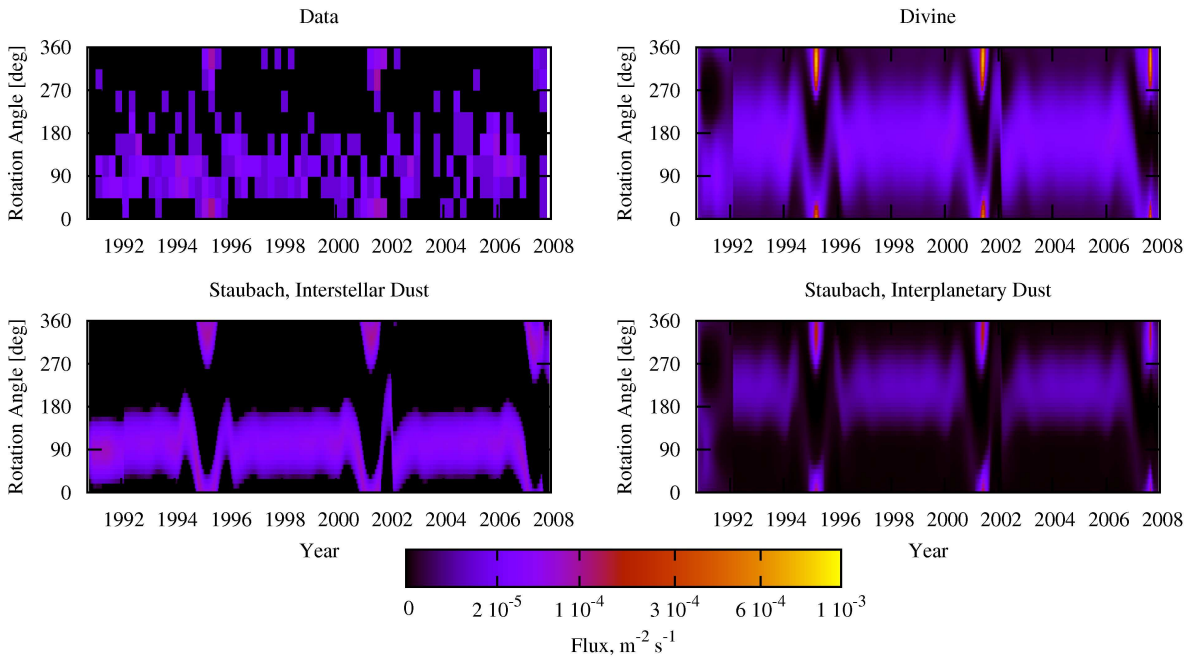

Figure 10: Particle fluxes onto the Ulysses dust detector as seen in the data (AR3 to AR6) and predicted by the meteoroid environment models by Divine (1993) and Staubach et al. (1997). The Jupiter encounter in 1992 is best seen on the model plots as a sharp swing in directionality of impacts caused by the rotation of spacecraft velocity relative to the giant planet. The ecliptic plane crossings near the perihelia in 1995, 2001 and 2007 are marked by the high impact rates due to the number density of dust increase near the Sun and high speed of Ulysses relative to this dust. As the spacecraft moved north at the times of the crossings, the meteoroids came from the ecliptic north as well (rotation angle 0).